Cross-Layer Design and Optimization of Heterogeneous Cellular Mobile Networks

Shojaeifard, Arman

Awarding institution:
King's College London

Cross-Layer Design and Optimization of Heterogeneous Cellular Mobile Networks

Arman Shojaeifard

Institute of Telecommunications (IOT)

King's College London

A DISSERTATION PRESENTED TO THE GRADUATE SCHOOL OF KING'S COLLEGE LONDON, IN PARTIAL FULFILMENT OF THE REQUIREMENTS FOR THE DEGREE OF

Doctor of Philosophy

January 2013

The world and the universe is an extremely beautiful place,
and the more we understand about it the more beautiful does it appear.

Richard Dawkins

Abstract

The rapid growth of wireless communication and access, in conjunction with increasing demand and sophistication of wireless applications, supplicate intelligent and reliable systems to support the exchange of large classes of traffic with rising quality of service (QoS) requirements. In addition, co-operation among cellular systems that incorporate different radio access technologies is notably important as the current third generation (3G) universal mobile telecommunication systems (UMTS) are expected to co-exist with the emerging fourth generation (4G) long term evolution (LTE) technologies for years to come. To these ends, radio resource management (RRM) techniques across different network layers, conjointly with spectrum sharing strategies, are vital in achieving desirable performance in heterogeneous networks.

In this thesis, novel cross-layer design strategies, for jointly optimizing the physical (PHY)-layer and data link layer (DLL) parameters, are proposed in the contexts of code division multiple access (CDMA) and shared-spectrum heterogeneous orthogonal frequency division multiplexing (OFDM)/CDMA networks. These strategies facilitate dynamic radio resource allocation by exploiting the random variations of channel and network activity. Transmit power and QoS constraints are imposed on systems to maintain communication costs, effectiveness and quality.

This thesis makes four main contributions. Firstly, in the proposed cross-layer techniques, based on automatic repeat request (ARQ) delay limits and prescribed maximum packet loss rates in the DLL, the optimum outer-loop power control (OLPC) SNR-targets and the corresponding adaptive spreading factors are derived in the PHY-layer, as functions of the number of active users in the cell. The optimality is, in this sense, maximization of cell effective throughput. Secondly, the performance of the proposed interference-based resource allocation schemes are evaluated over Nakagami-m frequency -flat and -selective fading channels. In particular, frequency-selective channels with maximum ratio combining (MRC) RAKE receiver are considered. Thirdly, I consider the uplink in multi-user cellular communication systems with single- and multi- service traffic scenarios, which are respectively modeled with one- and multi- dimensional discrete Markov chains. Finally, a dynamic cross-layer resource allocation algorithm in the context of shared-spectrum heterogeneous OFDM/CDMA networks is proposed. Opportunistic spectrum access (OSA) is employed to utilize the idle parts of the primary spectrum, effectively minimizing the interference levels, to maximize the total deliverable secondary throughput.

Throughput performance of the optimized schemes and the achieved improvements, relative to the non-optimized and state-of-the-art schemes, are demonstrated with theoretical and simulation results for various settings of system parameters.

Table of Contents

Author's Publications

[1] **A. Shojeifard**, F. Zarringhalam and M. Shikh-Bahaei, "Joint Physical Layer and Data Link Layer Optimization of CDMA-Based Networks," *Wireless Communications, IEEE Transactions on*, vol. 10, no. 10, pp. 3278-3287, Oct. 2011.

[2] **A. Shojeifard**, F. Zarringhalam and M. Shikh-Bahaei, "Packet Error Rate (PER)-Based Cross-Layer Optimization of CDMA Networks," *Global Telecommunications Conference (GLOBECOM 2011), 2011 IEEE*, pp. 1-6, Dec. 2011.

[3] **A. Shojeifard** and M. Shikh-Bahaei, "Cross-Layer Design and Optimization of CDMA Networks in Frequency-Selective Fading Channels," *Wireless Communications Letters, IEEE*, vol. 1, no. 6, pp. 605-608, Dec. 2012.

[4] **A. Shojaeifard**, F. Zarringhalam, M. Shikh-Bahaei, "Throughput-Optimal Cross-Layer Resource Allocation in DS-CDMA Systems with Nakagami Multipath Fading," *Personal Indoor and Mobile Radio Communications (PIMRC 2011)*, pp. 1526-1530, Sep. 2011.

[5] **A. Shojeifard** and M. Shikh-Bahaei, "Joint Physical Layer and Data Link Layer Optimization of Multi-Service Networks," *Wireless Communications Letters, IEEE, submission under 2^{nd} round of review*, pp. 1-4, Sep. 2012.

[6] **A. Shojeifard** and M. Shikh-Bahaei, "Cross-Layer Design and Optimization of Multi-Service CDMA Networks," *VTC, 2013 Proceedings IEEE, submission under review*, pp. 1-7, Aug. 2012.

[7] **A. Shojeifard**, M. M. Mahyari and M. Shikh-Bahaei, "Cross-Layer Design with Dynamic Resource Allocation in Heterogeneous Cognitive Radio Networks," *ICC, 2013 Proceedings IEEE, submission under review*, pp. 1-5, Sep. 2012.

[8] **A. Shojeifard** and M. Shikh-Bahaei, "Cross-Layer Design and Optimization of Shared-Spectrum Heterogeneous Networks," *Wireless Communications, IEEE Transactions on, to be submitted in Jan. 2013.*

[9] M. M. Mahyari, **A. Shojeifard** and M. Shikh-Bahaei, "Probabilistic Optimization of Shared-Spectrum Wireless Communication Systems," *Wireless Communications Letters, IEEE, submission under review*, pp. 1-4, Jan. 2013.

List of Figures

Acronyms

AL	Access-limited
AMC	Adaptive modulation and coding
AMPS	Advanced mobile phone service
ARQ	Automatic repeat request
AWGN	Additive white Gaussian noise
BER	Bit error rate
BLER	Block error rate
BPSK	Binary phase shift keying
BS	Base station
CDMA	Code division multiple access
CDI	Channel distribution information
CNR	Carrier-to-noise ratio
CSI	Channel state information
CP	Cyclic prefix
CR	Cognitive radio
CRC	Cyclic redundancy check
CU	Cognitive user
DLL	Data link layer
DS-CDMA	Direct sequence code division multiple access
FCC	Federal communications commission
FDM	Frequency division multiplexing
FDMA	Frequency division multiple access
FEC	Forward error correction
FER	Frame error rate
FFT	Fast Fourier transform
GSM	Global system for mobile communications

HARQ	Hybrid automatic repeat request
HSPA	High speed packet access
IFFT	Inverse fast Fourier transform
i.i.d.	Independent and identically distributed
IL	Interference-limited
ILPC	Inner-loop power control
IP	Internet protocol
ISI	Inter-symbol interference
KT	Kuhn-Tucker
LAN	Local area network
LTE	Long term evolution
MAC	Medium access control
MC	Multi-carrier
MC-CDMA	Multi-carrier code division multiple access
MC-DS-CDMA	Multi-carrier direct sequence code division multiple access
MIMO	Multiple-input multiple-output
MIP	Multipath intensity profile
MRC	Maximum ratio combining
OFDM	Orthogonal frequency division multiplexing
OFDMA	Orthogonal frequency division multiple access
OLPC	Outer-loop power control
OSA	Opportunistic spectrum access
OSI	Open systems interconnection
PAPR	Peak-to-average-power ratio
pdf	Probability density function
PDP	Power delay profile
PER	Packet error rate
PHY	Physical

PSD	Power spectral density
QoE	Quality of experience
QoS	Quality of service
QPSK	Quadrature phase-shift keying
OSI	Open systems interconnection
RAN	Radio access network
RRM	Radio resource management
RTD	Round-trip delay time
SC-FDMA	Single-carrier frequency division multiple access
SIR	Signal-to-interference ratio
SINR	Signal-to-interference-and-noise ratio
SMS	Short messaging services
SNR	Signal-to-noise ratio
SP	Secondary-primary
SS	Secondary-secondary
TCP	Transport control protocol
TDM	Time division multiplexing
TDMA	Time division multiple access
UE	User equipment
UMTS	Universal mobile telecommunications system
WAN	Wide are network
WCDMA	Wideband code division multiple access
WLAN	Wireless local area network
WWAN	Wireless wide area network
2G	2^{nd} generation
3G	3^{rd} generation
3GPP	3^{rd} generation partnership project
4G	4^{th} generation

The wireless telegraph is not difficult to understand. The ordinary telegraph is like a very long cat. You pull the tail in New York, and it meows in Los Angeles. The wireless is the same, only without the cat.

Albert Einstein

Chapter 1

Introduction and Overview

1.1 Birth of Radio to the Modern Era of Wireless Communications

In 1867, James Clark Maxwell, a professor of Natural Philosophy at King's College London (1860-1865), predicted the existence of electromagnetic (EM) waves travelling at the speed of light. Twenty years later, in 1887, Heinrich Hertz proved the existence of EM waves, which together with the works of Édouard Branly and Guglielmo led to the birth of radio and hence wireless communication. From then on, by a considerable margin, the most successful application of the communication industry has been the cellular telephone system. The roots of these systems began in 1910s, when for the first time a wireless voice over radio transmission was established between New York and San Francisco. Following the works of researchers at AT&T Laboratories, the first commercial cellular mobile telephony was developed and introduced in the early 1980s, with the release of first generation (1G) of cellular communication systems by Nippon Telegraph and Telephone (NTT) in Japan. In the USA, the first 1G network was launched in 1983 by Ameritech Corporation. Here in the UK, Vodafone, and shortly after Cellnet, released the first 1G network in 1985. The Cellnet network consisted of a single base station located at the BT Tower which provided coverage for Greater London county. In the first year $25,000$ customers joined this network. By 1994, Cellnet had over one million subscribers.

Over the last decade, wireless communications, in particular, cellular systems, have experienced extensive research, development and proliferation. Emergence of second- and third- generation (2G and 3G) of wireless communication systems provided users with new modes of communication, which ultimately transformed every day lives. Rapidly evolving from the initial focus on voice services, wireless technologies nowadays offer multimedia communication from any part of the world using a mobile device, i.e. mobility. Success of 2G and 3G technologies, particularly, Universal Mobile Telecommunication System (UMTS) standards such as Wideband Code Division Multiple Access (WCDMA) and High-Speed Packet Access (HSPA), has seized the interest and imagination of the population. As a result, there has been an exponential demand for cellular mobile technologies; according to ICT Facts and Figures in 2011, the global penetration reached 87%, with almost 6 billion cellular mobile subscriptions in the world, more than double the number in 2006. Rapid increase in the number of mobile users, together with the demand for faster and more reliable wireless technologies in a growing number of mobile devices, such as smartphones and tablets, highlights the significance and vision of wireless communication over the next coming decades.

1.2 Wireless Vision: Technical Challenges

Current and emerging future wireless communication technologies, are encompassed with difficult but fascinating technical challenges, that span over all aspects of the system design. To achieve fast and reliable communication, wireless systems must combat the adverse characteristics of wireless channels, such as time-variant fluctuations, multipath propagation and interference from neighbouring transmitting cells. Moreover, an increasingly severe challenge is the scarcity of available radio resources, in particular transmit power and bandwidth. As a result of the rapid developments in digital signal processing and microelectronic circuits, nowadays the problems associated with transmission over wireless channels are mostly resolved. Particularly, state-of-the-art developments such as space diversity combining, adaptive antennas, digital modulation schemes, spread spectrum transmission, multiple-input multiple-

output (MIMO) and multi-carrier (MC) modulation, have overcome the channel impairments and have therefore played a major role in growth of cellular technologies. Consequently, nowadays and most probably in the future, the focus has shifted towards overcoming the scarcity of power and spectrum. In his speech, *Spectrum Policy in the Dynamic Age* at ECTA Regulatory Conference 2011, the Office of Communications (Ofcom) chief executive, Ed Richards, states:

> *I want to suggest today that the rapidly increasing rate of change in spectrum use - the dynamism in innovation, technology and in market demand - has injected a new urgency into the need to manage spectrum effectively.*

To these ends, the following are some of the important techniques towards tackling the challenges associated with limited energy and crowded spectrum. To achieve desirable performance, it is essential to design effective and efficient *adaptive* resource allocation algorithms. Adaptive resource allocation methods have been widely studied in the last decade. These algorithms exploit the time-varying nature of communication channels in order to manage resources optimally, yielding better throughput. Further, contrary to the traditional rigorous non-shared regulation of frequency bands, *cognitive radio* techniques are nowadays favourable to overcome the spectrum shortage problem. Shared-spectrum schemes, enable unlicensed (i.e. secondary) users to opportunistically communicate over unused and under-utilized parts of a primary spectrum without imposing quality of service (QoS) degradation to the primary service. In addition, conceivably the most significant design challenge in wireless networks, is the stringent division of the protocols associated with different layers in the network, e.g. Open Systems Interconnection (OSI) protocol model. Such rigorous network architectures, where layers of the network perform independent operations and are therefore isolated, are not effective in the context of present-day wireless communication networks. Therefore, designing interconnected layered network protocols and joint optimization of parameters across layers, i.e. *cross-layer* design and optimization, are vital tools for enhancing performance and guaranteeing the QoS requirements in different layers of modern wireless systems.

In the rest of this chapter, I highlight the fundamental concepts of current and future emerging cellular mobile systems and provide a more detailed prospective on the technical challenges that these networks are faced with. In the last section of this chapter, the research questions of interest are listed and an outline of the aims and contributions of this thesis is provided.

1.3 Fundamentals

1.3.1 Telecommunication Networks

A telecommunication network, for example a data network [1–3], represent a flow system of connected devices or nodes, in which a certain commodity, e.g. message, is moved from one point to another over one or several finite-capacity communication channels. To support successful exchange of information (in the form of numbers, texts, pictures, audio and video) between devices, telecommunication networks incorporate a certain set of rules, i.e. protocol, using a combination of hardware and software components. In order to facilitate reliable communication, messages, typically consisting of long stream of bits, are divided into shorter bit streams called 'packets'. Each corresponding packet, conferred as an individual entry, is then directed to the communication part of the network, called subnetwork or subnet. The subnetwork aim is to receive the packets from outside nodes, then transmit them over the communication link paths and finally deliver them reliably and speedily to the receiver. At the receiver end, packets are reconstructed into the original messages. The transaction in which interchange of messages between two or more terminals takes place is called a session.

Modern telecommunication networks are generally divided into wide area network (WAN) and local area network (LAN) categories [1, 4, 5]. WANs, providing long-distance data communication, correspond to the networks that cover large geographical areas, for example covering a country, a continent or an entire planet. In particular, wireless wide area networks (WWAN), such as cellular mobile networks, provide radio communication by employing radio access technologies. A LAN pro-

vides connection between devices in a small geographical area such as a home or an office. Specifically, wireless local area networks (WLAN) link two or more computers or mobile devices in limited areas by employing modulation schemes such as spread spectrum and/or Orthogonal Frequency Division Multiplexing (OFDM).

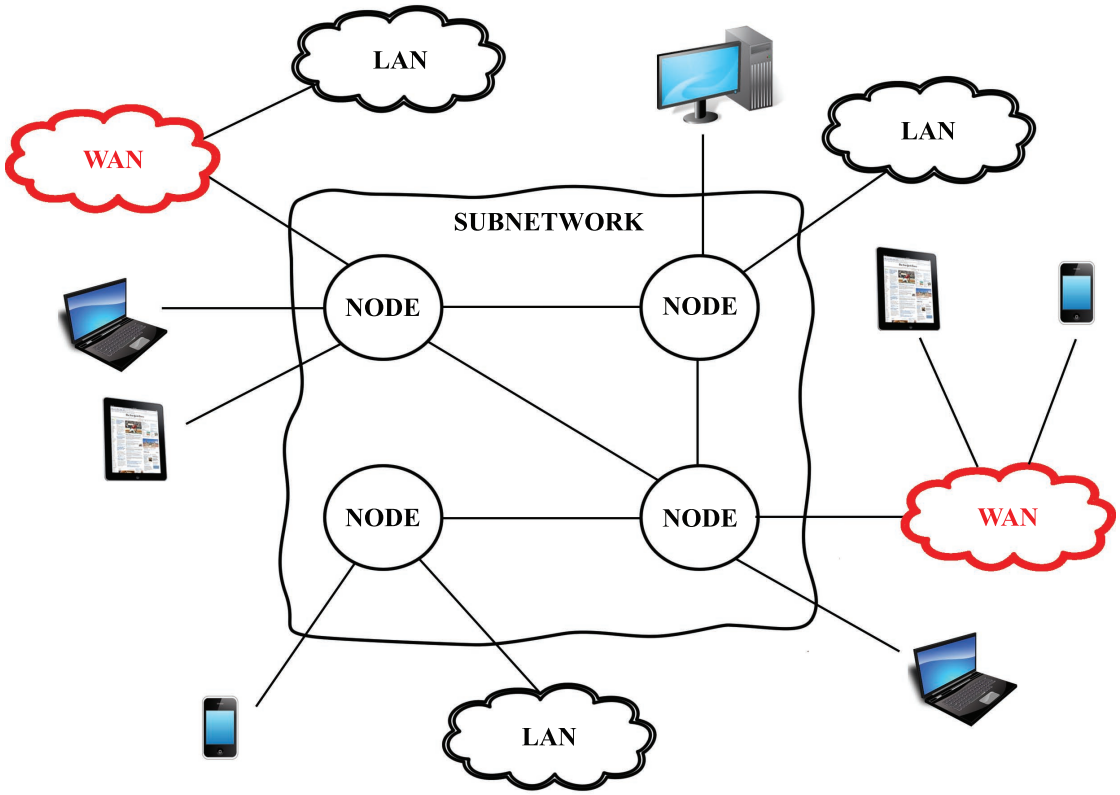

Figure 1.1: Interconnected wide and local area (WAN/LAN) networks.

The growing demand for high-speed connectivity necessitate heterogeneous networks that can communicate reliably with one another. As a result, nowadays, more and more networks are linked together through gateways, allowing the users of a network to virtually connect to any other device on the planet. Fig. 1.1 illustrates an interconnected network, facilitating communication between WANs, LANs, terminals and personal devices. The two dominant interconnected networks in operation worldwide, are the Internet and the public switched telephone network (PSTN). The modern Internet, is a hierarchical structure composed of many WANs and LANs, linked with an increasingly large number of computers, mobile devices and stations. These networks are implemented based on the Transport Control Protocol/Internet

Protocol (TCP/IP) and OSI layered networking models. The focus of this work is on current and future emerging wide area cellular mobile networks.

1.3.1.1 Cellular Mobile Networks

Cellular mobile networks provide wireless communication of data, voice and video between hand-held mobile devices with coverage in various network environments such as urban, suburban and rural [6]. Generally, a cellular network consists of spatially-separated cells, conventionally hexagonally shaped, where operation within cells is restricted to certain radio frequency spectrum (i.e. distinct set of wireless channels). In each cell, a base station (BS), typically located at centre, controls the operation of mobile users present in the cell. Cellular systems facilitate reuse of the same radio frequency spectrum by limiting the operation of each BS to a singular cell. Cellular mobile users communicate with one another through the BSs which are connected to each other via Mobile Telephone Switching Office (MTSO). MTSO, the primary controller in cellular networks, allocates the wireless channels to cells and accommodates handovers when users go across a cell border. Moreover, MTSO connects the cellular network to the PSTN and the Internet.

Fig. 1.2 illustrates a conventional cellular mobile network architecture, consisting of hexagonal cells, base stations, cellular mobile users, MSTO, the PSTN and the Internet. In the event of a new active mobile user in the cell, a call request over a control channel is sent to the BS. The request is diverted to the MTSO which examines the availability of a channel in that cell and responds to the active user accordingly. In case that a channel is available the call is accepted, otherwise, the call request is denied. A handover is initiated when the BS or the cellular user detects that the active user's received signal power is approaching a certain threshold. The MTSO then makes an enquiry to the neighbouring base stations to verify if one of these BSs senses the cellular user's activity. If the corresponding BS's cell has available channels, the handover between the original BS and the new BS is commenced. In case of unavailability of channels, handover is aborted and the call request is dropped [7].

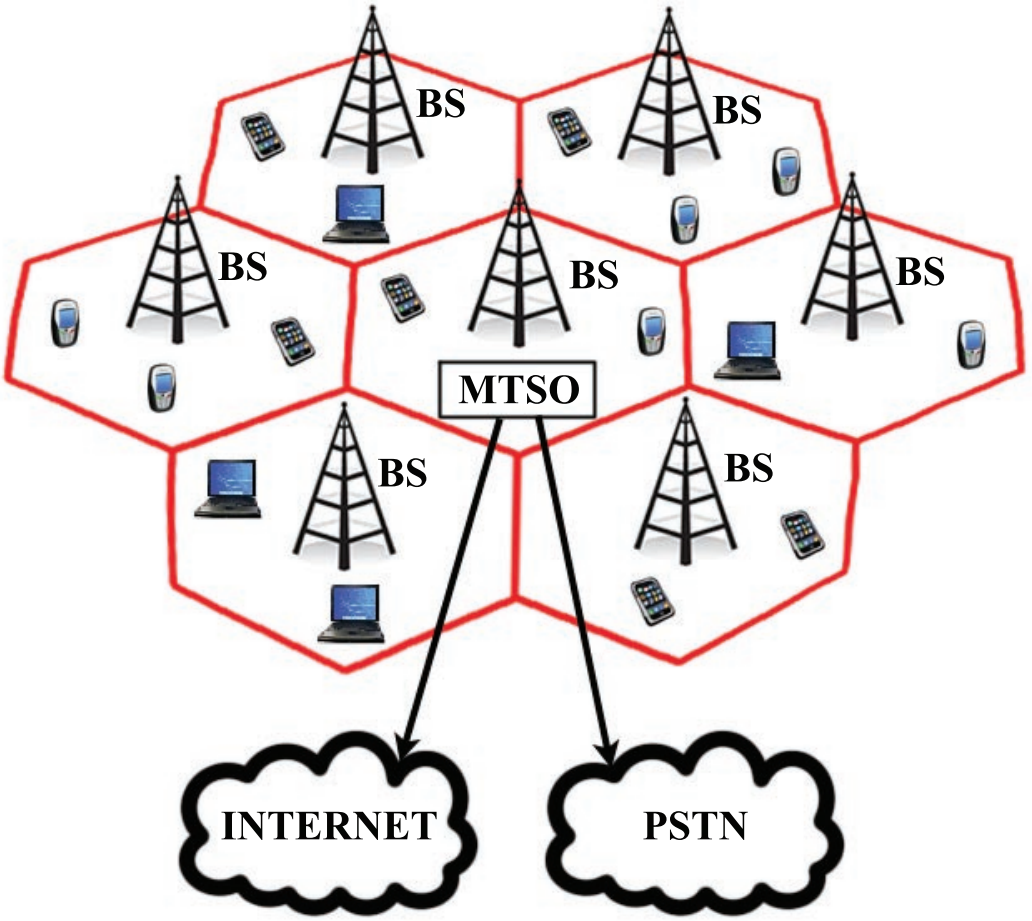

Figure 1.2: Conventional cellular mobile network.

1.3.1.2 Layered Network Architecture

Layered architecture (also called layering), a hierarchy structure of hardware and software modules, is the dominant network-design approach in today's telecommunications systems. The traditional layering design approach, divides the overall networking task into a stack of isolated and transparent protocol layers, where each layer is assigned with a hierarchy of distinct functionalities. Each layer functionality is to provide certain services to the higher layers, without revealing how the services were implemented. The main motivation behind the layered network design is the advantages in the sense of modularity, such as simpler implementation, reduced complexity and expandability.

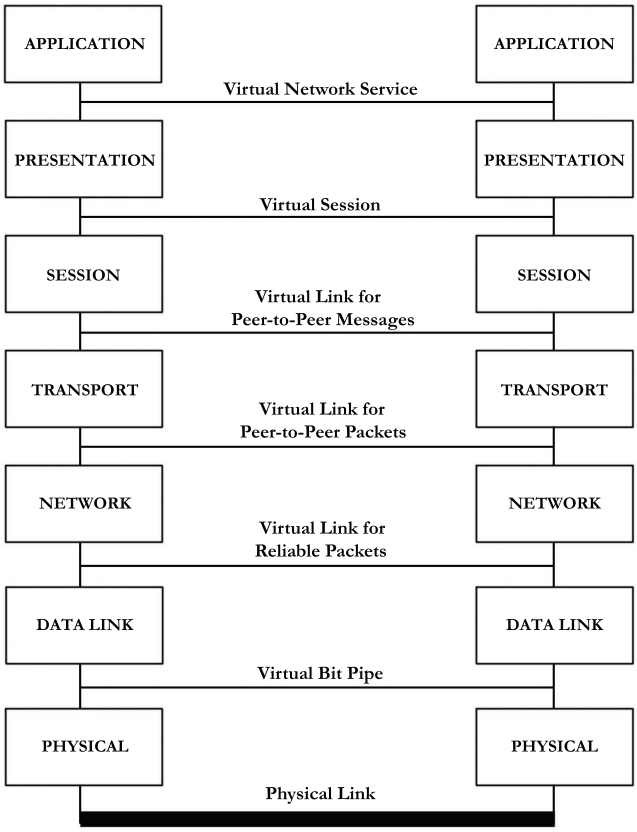

Figure 1.3: Open Systems Interconnection (OSI) seven-layer network architecture. Each layer corresponds to a virtual communication link and facilitates distinct functionalities to the next-higher layer.

OSI, introduced in 1947 by the International Standards Organization (ISO), is the standard model for data communication networks. The OSI model serves as a theoretical framework which facilitates the interchange of information between different systems without any requisite changes in the networks underlying hardware or software modules. OSI model consists of seven distinct yet related layers, where each layer performs a well-defined part of the overall networking task. Specifically, the OSI model, organized from bottom to top, consists of physical (PHY)-layer, data link layer (DLL), and, network, transport, session, presentation and application layers. Fig. 1.3 depicts the different layers of OSI model involved in moving information between two devices.

The three bottom layers of the OSI model, physical, data link and network layers, are responsible for implementing the physical aspects involved in information interchange between two nodes, and hence are regarded as the network support layers. Specifically, the PHY-layer corresponds to a virtual link, called virtual bit pipe, for carrying a stream of bits between two nodes over a physical communication channel. Generally, the PHY-layer enables transmission to occur, by specifying the appropriate mechanical and electrical functions that the devices and the physical channel must implement. Moreover, PHY-layer is involved in link configuration, encoding of bit streams, defining the bit duration (i.e. data rate), clock synchronization between devices, link placement (i.e. physical topology) and defining the mode of transmission. The unreliable bit pipe from PHY-layer is then converted into a reliable link for transmitting packets by the data link layer. The DLL is also responsible for dividing the bit streams (i.e. packets) into frames, error control and correction and link access control. In the case of multiple access communication, an intermediate layer called Medium Access Control (MAC) is needed in the DLL, to avoid interference imposed on the reference transmitting node by other nodes. Subsequently, through the DLL, the raw PHY-layer bit streams appear as error-free packets to the network layer. The network layer delivers the packets from the source to the destination over the network links. It is important to note that the delivery of a packet between two nodes on the same link is provided by the DLL, and the network layer is responsible for connecting devices across different networks. Moreover, network layer is responsible for logical addressing and routing of packets. In this contribution, the main focus is on the network support layers, in particular the PHY-layer and the DLL.

Generally, the upper layers in the OSI protocol stack, session, presentation and application layers, are regarded as the user support layers. Transport layer, the fourth layer in OSI model, serves as a link between the network and user support layers. Specifically, the transport layer is involved in delivery of messages, i.e. breaking of messages into packets at the transmitter side and reassembling the packets into messages at the receiver end. Detailed information on the functionalities of the higher layers of the OSI mode can be found in the literature [1, 3, 8–10].

Unlike the OSI network model that was never fully implemented, the TCP/IP protocol suite has been extensively tested and employed in the Internet. The original network architecture of TCP/IP model consisted of five layers, namely physical, data link, internetwork, transport and application layers. To compare these with the layers in the OSI model, the first four layers of the TCP/IP are equivalent to those of the OSI model. However, the upper layer of the TCP/IP protocol suite, application layer, represents the upper three layers of the OSI model, i.e. session, presentation and application layers. The main difference between the OSI model and the TCP/IP protocol suite, is that the layers in the former facilitate distinct yet interdependent protocols, whereas in the latter this is not necessary the case. Specifically, the TCP/IP protocol suite layers consist of independent protocols that can be moved around depending on the network current tasks. Extensive description of TCP/IP networking model architecture and protocols can be found in the literature, e.g. [3, 11, 12].

As highlighted, the traditional layering approach provides advantages mostly in the sense of modularity. However, with the rapid evolution of wireless networks, the strict layered architecture has proved to be inefficient. This has given rise to the notion of cross-layer design, one of the main focuses of this contribution, to remedy the shortcomings of the layered network architecture. I will elaborate on this notion in Section 1.5 and the subsequent chapters of this thesis.

1.3.2 Radio Access Technologies

1.3.2.1 Multiple Access and Spread Spectrum

The rapid increase in the number of cellular mobile users implies that cellular systems must concurrently accommodate multiple users. Multiple access techniques have therefore been widely employed to share the available radio resources among multiple users and ensure reliable and high-rate wireless transmission. Generally, there are two common types of multi-user communication systems [13]. A first type of multiple access cellular systems, is one in which a single transmitter communicates with multiple receivers, e.g. downlinks in satellite communication systems. The sec-

ond type is where several transmitters transmit to a single receiver, e.g. uplinks in mobile communication systems. Several multiple access techniques are widely employed to enable multiple users communicate through the wireless channel to the receiver. Multiple access techniques, typically divide the available radio resources along frequency, time or code space dimensions, and therefore are essential tools for design of uplink and downlink channels to compensate for scarce and expensive bandwidth [14].

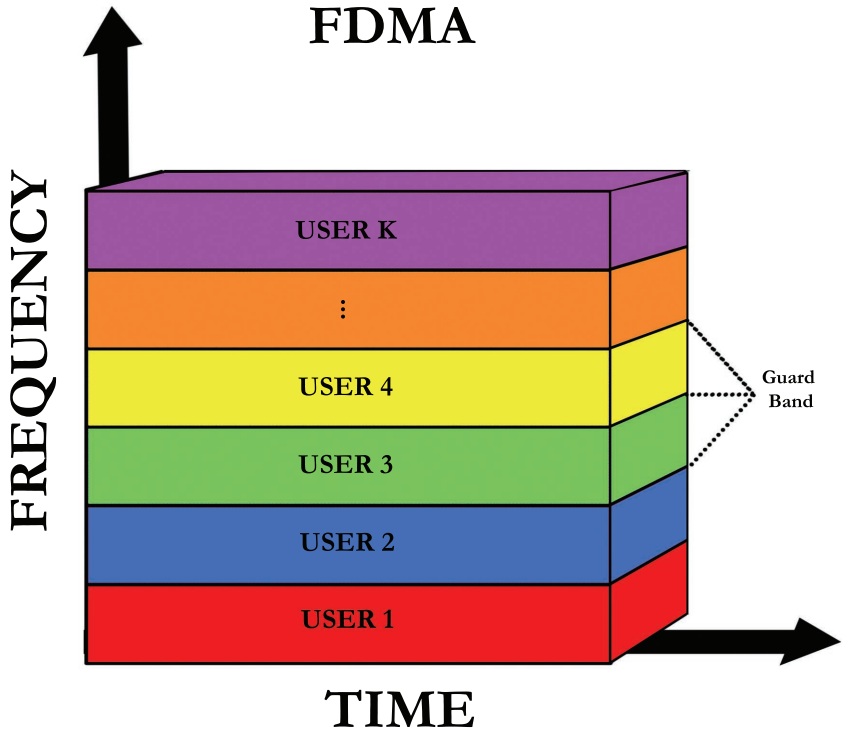

Figure 1.4: Frequency Division Multiple Access (FDMA).

The first generation of mobile cellular networks, such as Advanced Mobile Phone Service (AMPS) and Extended Total Access Communications System (ETACS) in the US, implemented Frequency Division Multiple Access (FDMA) and analog Frequency Modulation (FM) technologies [15]. The bandwidth allocated to these systems by the Federal Communications Commission (FCC), was divided into a number of non-overlapping sub-channels, and thus upon request, each user was assigned with a sub-channel for transmission of information. In order to minimize the adjacent

channels interference and as a remedy for imperfect filters and Doppler spreading, guard bands were placed between sub-channels. Fig. 1.4 illustrates the FDMA technique for sharing of resources among a number of users. FDMA techniques benefit from invulnerability to timing problems, low transmit power requirements and simple channel equalization. However, main disadvantages of FDMA such as complex filtering criteria and inefficient allocation of bandwidth (i.e. spectrum is divided into non-shared frequency bands), limit their achievable performance. 1G voice-only cellular systems offered a maximum data rate of 56 Kbits/second. Multi-carrier FDMA transmission schemes, known as Orthogonal Frequency Division Multiple Access (OFDMA), are employed in multiple access fourth generation (4G) OFDM systems. Detailed descriptions of OFDM and OFDMA are included in Section 1.3.2.2.

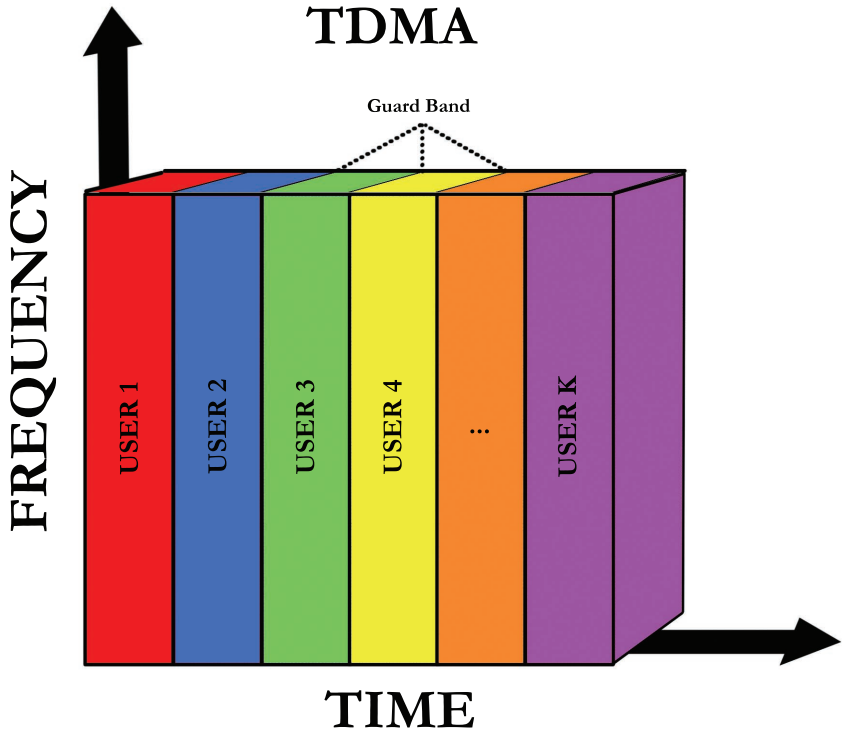

Figure 1.5: Time Division Multiple Access (TDMA).

Second generation cellular standards, with focus on transition from analog to digital modulation, were based on a combination of Time Division Multiple Access (TDMA) and FDMA techniques. In 2G standards such as Global System for

Mobile Communications (GSM), the frame duration is divided into a number of non-overlapping time intervals, and hence each user is assigned a single time slot and a frequency band for transmission of data. The radio channel is therefore shared between users with no interference. 2G systems greatly improved cell capacity, providing data rates of up to 100 Kbits/second through the General Packet Radio Service (GPRS) enhancement. Moreover, GPRS systems enabled wireless data services, known as Short Message Service (SMS), which has become the most widely used data application worldwide. The performance of 2G systems was further improved, with the introduction of adaptive Enhanced Data Services for GSM Evolution (EDGE). The disadvantages of TDMA techniques, in particular the significant overhead due to complex synchronization requirements between users, limit the capacity achieved by these techniques.

Third generation wireless mobile systems implement Code Division Multiple Access (CDMA) and spread spectrum techniques [16, 17]. CDMA integrates all data rates on a single carrier and therefore allows users to share a common channel, i.e. overlapping in both time and bandwidth as illustrated in Fig. 1.6, for transmission of information to corresponding receivers. As a result of users simultaneously occupying time and frequency, CDMA-based radio access technologies are highly sensitive to mutual interference caused by active cellular users, commonly known as multiple access interference (MAI) [18]. Spread spectrum modulation schemes are therefore employed in the PHY-layer, to minimize the inter- and intra- cell interference and hence enhance the performance of CDMA systems. Using this method, each user's signal is spread in the channel by a unique pseudo-random code signature sequence. As a result, unique spreading codes, enable the receiver to distinguish between the signals transmitted by several users with minimized interference. Further, spread spectrum techniques are greatly effective in combating or suppressing detrimental interference caused by jammers, for this reason these systems were originally targeted for military applications. This high level of security is achieved by implementing pseudo-random coded spread messages that are hidden with background noise at lower power, where only the intended receiver has the information, i.e. the keys, required to decode these random patterns.

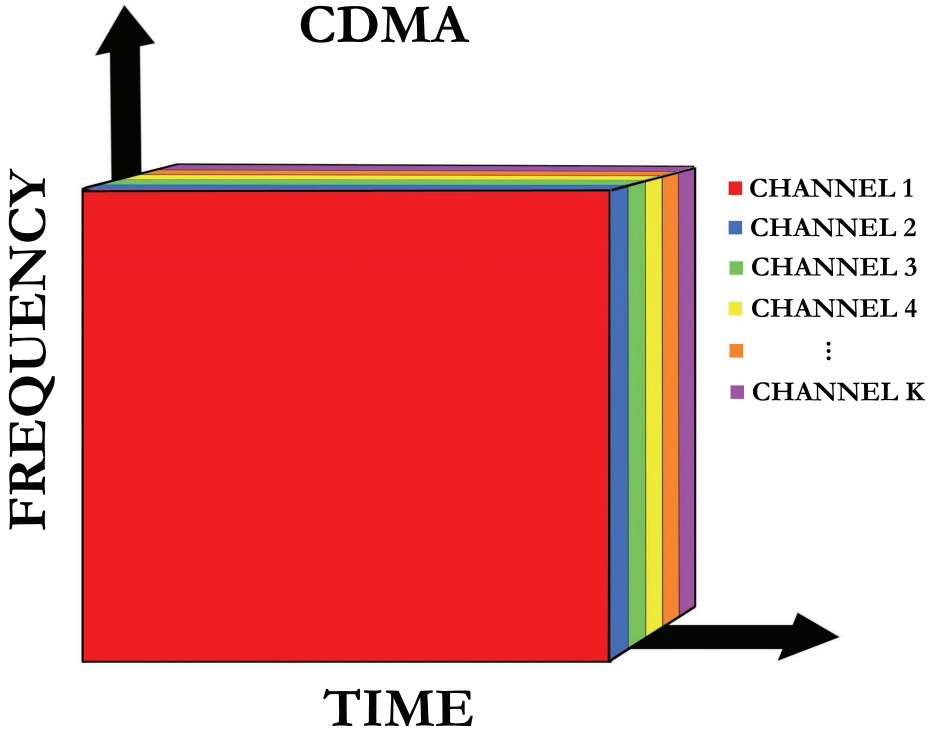

Figure 1.6: Code Division Multiple Access (CDMA).

Emergence of 3G UMTS standards, in particular WCDMA digital cellular standard, enabled multimedia communication of data, voice and video at data rates of up to 2 Mbits/second and 384 Kbits/second for local area access and wide area access, respectively. Direct-sequence (DS) and frequency-hopping (FH), are two of the most distinct spread spectrum techniques implemented in UMTS standards [19]. DS-CDMA systems are divided into wideband (e.g. WCDMA) and narrowband (e.g. narrow DS-CDMA) standards. In DS spread spectrum modulation techniques, a user signal is spread over the frequency band by multiplying the signal data by a pseudo-random sequence, i.e. chips. In case of binary phase shift keying (BPSK) modulation, the spreading factor, an integer value in practical systems, is given by:

$$N = \frac{T_b}{T_c} \tag{1.1}$$

where T_b and T_c denote bit duration and chip duration, respectively. The transmitted spread signal is then despread at the receiver using the same spreading code, in order

to recover the original sequence. The basic operation of spreading and despreading in a BPSK DS-CDMA system, assuming perfectly synchronised codes, is demonstrated in Fig. 1.7.

Current cellular networks implement two types of DS-CDMA systems: wideband (e.g. WCDMA) and narrowband (e.g. narrow DS-CDMA) standards. The chip rate of 3G DS-CDMA standards is 3.84 Mchips/s, with carrier bandwidths of ∼5 MHz for wideband and ∼1.25 MHz for narrowband [20]. Within any given channel bandwidth, to achieve high data rates, lower spreading factors are required, the higher the bandwidth expansion factors, the lower the user data bit rates are. To achieve the maximum data rate of 2Mbits/second in UMTS, the required theoretical spreading factor can therefore be calculated using (1.2):

$$N = \frac{T_b}{T_c} = \frac{3.84 \text{ Mchips/second}}{2 \text{ Mbits/second}} = 1.92 \text{ chips/bit} \tag{1.2}$$

however, such low spreading factors degrade the robustness to interference.

As a result of technological advantages, such as high data rates, flexibility of PHY-layer to support multi-class traffic, and improved multipath fading (i.e. self-interference) resilience through space diversity, Wideband DS-CDMA has become the dominant air interface technology in 3G cellular systems. However, CDMA systems, in particular on the uplink, necessitate dynamic power control policies due to presence of MAI and near-far effect. The near far effect occurs when received signal-to-noise ratios (SNRs) of the transmitters at the receiver are different, and therefore the lower-power signals may be overpowered. Specifically, assuming users with equal transmit power, the signals generated by users further away from the BS, are surpassed by the users closer to the access point. Multi-carrier versions of CDMA, such as MC-CDMA and MC-Direct-Sequence-CDMA (MC-DS-CDMA), simultaneously transmit chips of spread data over several sub-carriers. This is further discussed in the next subsection of this thesis.

The principal focus of this thesis is on the uplink of CDMA-based systems, with the aim of achieving optimal performance by employing Radio Resource Management (RRM), cross-layer design and optimization, and spectrum sharing strategies.

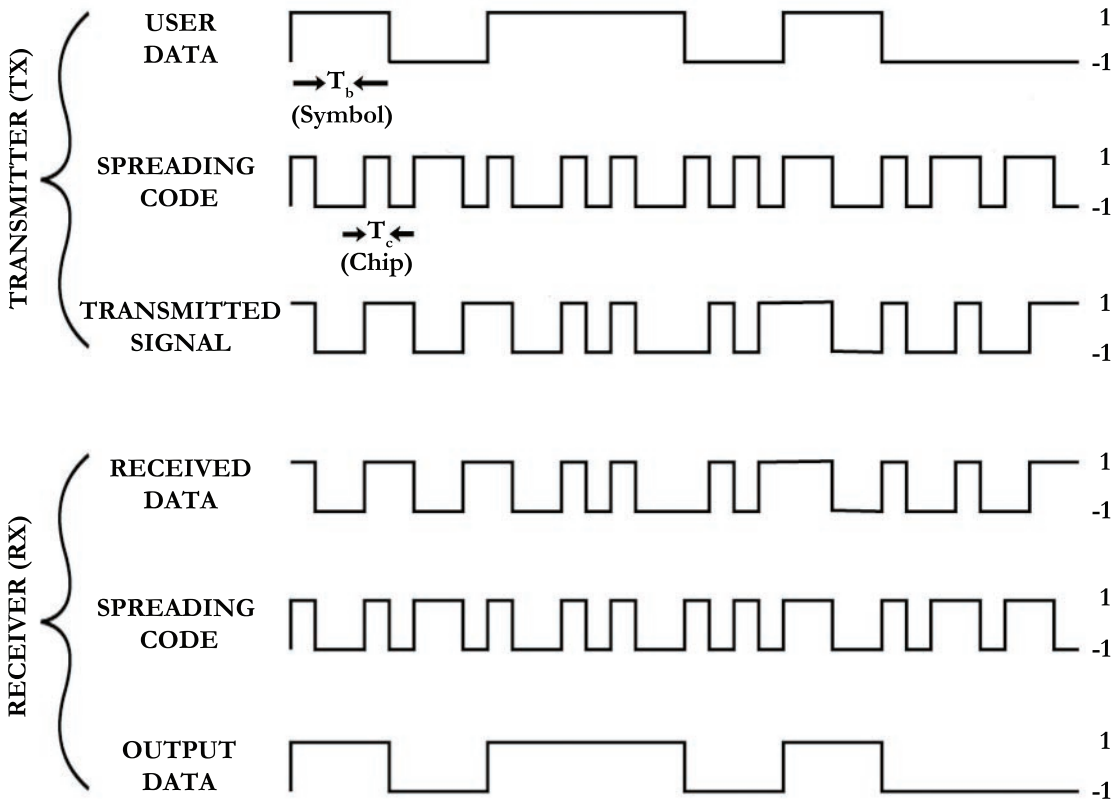

Figure 1.7: Spreading and despreading in Direct-Sequence (DS)-CDMA.

1.3.2.2 Multi-Carrier Communications

One of the main obstacles of data transmission over the wireless medium is the inter-symbol-interference (ISI), which is caused by the frequency-selective nature of communication channels. MC techniques are therefore widely employed in wireless systems to enhance performance by tackling ISI [21], [22]. MC schemes divide the high data rate streams into a number of low data rate sub-streams which require smaller frequency bands for transmission. The low data rates are then mapped onto a set of independent sub-carriers, which are then transmitted at considerably lower symbol rates, over several different sub-channels. These narrowband signals are particularly more resilient to multipath fading and require simpler equalization in comparison to the original wideband signal. Although MC modulation was introduced in the late 1950s, only sometime in the past decade the advancements in electronic hardware technology enabled practical use of MC methods, mostly in

terms of OFDM. To prevent ISI, it is essential to achieve no overlapping in the spectrum, since each sub-carrier conveys independent data from other sub-carriers. OFDM modulation scheme incorporates this principal, therefore sub-carriers are typically selected in a way that they are orthogonal to each other. Orthogonality between sub-carriers indicate that for each sub-carrier there is a null at the centre frequency of all other sub-carriers. In the earlier MC Frequency Division Multiplexing (FDM) techniques, guardbands were placed between sub-carriers in order to avoid overlap in spectrum, therefore more bandwidth is required to transmit the same amount of information compared to OFDM. Consequently, the orthogonality property means that OFDM systems can achieve much higher spectral efficiencies compared to FDM schemes as demonstrated in Fig. 1.8, and therefore are considered as the main modulation technique candidate in PHY-layer of emerging and future 4G technologies [21], [22].

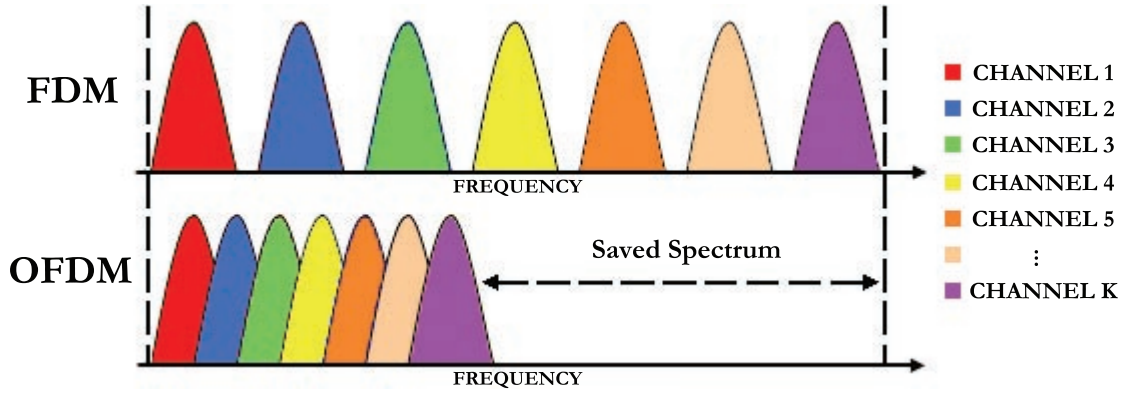

Figure 1.8: Spectrum efficiency comparison of conventional FDM versus OFDM.

Practical OFDM systems are implemented using Fast Fourier Transform (FFT) and Inverse Fast Fourier Transform (IFFT) algorithms. Specifically, IFFT at the transmitter is used to map the data sub-streams onto unique sub-carriers, typically OFDM divides bandwidth into 64 upto 256 sub-carriers [23]. The original data stream is then reconstructed at the receiver using FFT. FFT operations offer an efficient and cost-effective discrete domain solution towards implementations of OFDM systems, particularly as a result of exponential advancements in digital signal processing. Moreover, the receiver side of OFDM is significantly simplified, since it

does not require an equalizer and only compensates for channel amplitude and phase impact of individual sub-carriers. There are several drawbacks in practical implementation of OFDM systems. Firstly the notion of orthogonal sub-carriers may be degraded due to high sensitivity to Dopler shift, therefore guard intervals in terms of Cyclic-Prefix (CP) are typically required which lowers the achievable spectral efficiency. Moreover, MC signals posses high peak-to-average-power ratio (PAPR), therefore high linear amplifiers are required to avoid performance degradation.

Currently, there are several multiple access OFDM candidates for the next generation Long Term Evolution (LTE) cellular radio access technologies. In particular, OFDMA and MC-CDMA, have increasingly attracted attention [24]. In case of OFDMA, one or several sub-groups of sub-carriers are allocated to each user. Each sub-group of sub-carriers is called a sub-channel. It should be noted that the sub-carriers forming a sub-channel are not required to be adjacent. In practice, guardbands in terms of CP are required to combat ISI in OFDMA systems, which effectively reduce the achievable spectral efficiency. The main advantage of OFDMA, particularly in comparison to DS-CDMA where transmission spectrum is independent of information's bandwidth, is the frequency diversity by spreading the sub-carriers for a given sub-channel over the entire available spectrum, as demonstrated in Fig. 1.9. Moreover, at the receiver side, OFDMA is less complex than CDMA as intra-cell interference is avoided. OFDMA implementation in mobile applications is especially desired due to decrease in power consumption and resilience towards long echoes, which is achieved as a result of the large number of available sub-carriers (typically varied from 256 upto 2048 sub-carriers) [23]. Moreover, OFDMA, in comparison to OFDM with the same data rate, requires a lower number of guardbands and therefore overall coverage is improved. It should be noted that OFDMA is mostly considered for downlink, due to undesirable high PAPR, however, an extension of OFDMA, known as Single-Carrier Frequency Division Multiple Access (SC-FDMA) is one of the main radio access technology candidates in LTE uplink. However, there are several drawbacks in implementing OFDMA systems, such as high sensitivity to frequency offsets which may degrade orthogonality of sub-carriers and therefore severely affect performance. Moreover, in comparison to

DS-CDMA, OFDMA imposes more complex design challenges for combating channel interference from neighbouring cells. Adaptive sub-carrier assignment based on fast feedback channel is also more complex to implement compared to the fast power control strategies in CDMA systems.

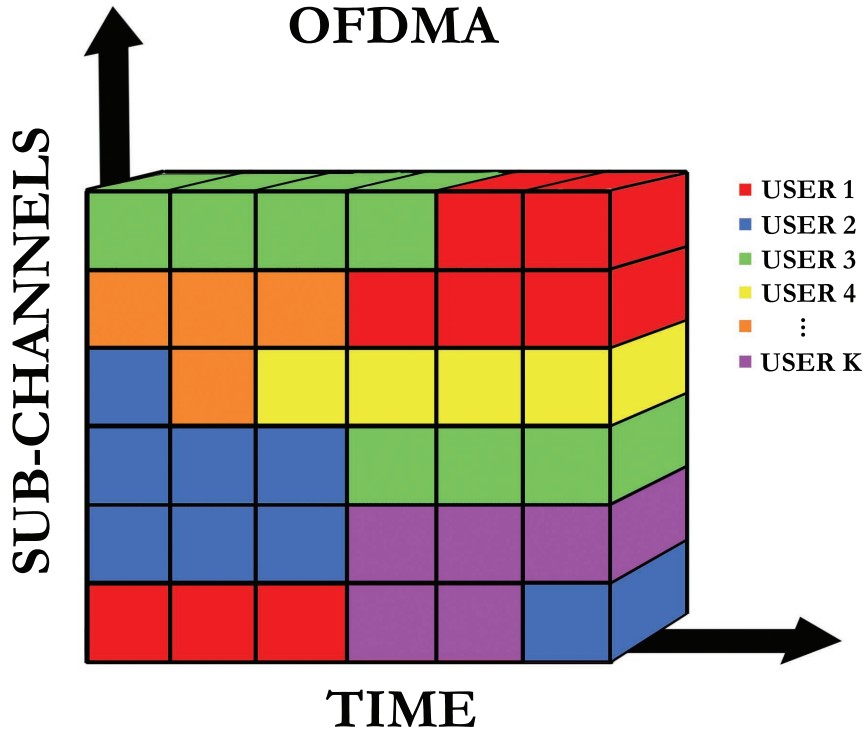

Figure 1.9: Orthogonal Frequency Division Multiple Access (OFDMA).

MC-CDMA, a combination of multi-carrier OFDM modulation and spread spectrum technique, is another interesting implementation concept for the next generation multiple access cellular technologies [25], [26]. In MC-CDMA, data is spread in terms of direct-sequence chips, where each chip is mapped onto a separate OFDM sub-carrier. The chips are therefore transmitted in parallel over a number of sub-carriers. In other words, MC-CDMA employs spread spectrum techniques in the frequency domain, rather than spreading in the time domain in case of DS-CDMA. MAI in MC-CDMA is tackled by using orthogonal spreading sequences, such as Walsh Hadamard codes. The main difference between MC-CDMA and OFDMA therefore arises from the fact that in OFDMA users are assigned with unique set

of sub-carriers, whereas in MC-CDMA all users simultaneously employ all the sub-carriers. The main advantage of MC-CDMA is the frequency diversity capabilities, which correspondingly enables transmission of high data rates in highly hostile wireless situations. MC-CDMA is particularly suitable for implementation in downlink of 4G systems, as a result of high spectral efficiency performance and low receiver complexity. However, MC-CDMA is mainly a considered for downlink, because of the difficult task of synchronisation between users in the uplink. Consequently, an extension of MC-CDMA, known as MC Direct-Sequence CDMA (MC-DS-CDMA), where spreading is achieved in the time domain, is introduced which is highly desirable for asynchronous uplink implementation of 4G cellular networks as a result of lower number of sub-carriers and low PAPR. MC-CDMA systems, however, necessitate complex equalization techniques, particularly as orthogonality of sub-carriers may be degraded due to code distortion in frequency selective channels.

In a part of Chapter 4, we consider the uplink of a primary OFDM network which employs SC-FDMA for uplink MAC scheduling.

1.3.3 Performance Analysis of Cellular Mobile Networks

The ultimate goal of radio access technologies is to provide high-rate and reliable wireless services for a large number of users in wide coverage areas. Consequently, the performance of cellular mobile systems is broadly evaluated in terms of capacity, quality, efficiency, versatility, and capital and operational expenditures. The term 'channel capacity', pioneered by Claude Shannon in the late 1940s, defines the maximum data rates that can be transmitted over physical links at arbitrary low probability of errors. Consequently, Shannon capacity is regarded as an optimistic upper-bound in the achievable practical rate of data transmission, and a benchmark comparison tool to evaluate the spectral efficiency and throughput performance of radio access technologies.

In this part of the thesis, I first look at the achievable capacity of a single user, with single antenna transmitter and receiver, over a time-invariant Additive White Gaussian Noise (AWGN) channel. I then study the capacity of the single user over frequency-flat and frequency-selective fading channels. Subsequently, I introduce

and define the terms delay, spectral efficiency and throughput, which are commonly used to analyse the performance of cellular networks.

1.3.3.1 Capacity over AWGN Channels

The Shannon capacity of an AWGN channel is arguably the most revolutionary result in the field of Information Theory [27]. Before Shannon's contributions, basic error-correcting codes such as Repetition Coding were known to be the only solutions towards achieving reliable performance over noisy channels. Shannon, through his intelligent approach towards coding of information, proved that communication at strictly positive rates with low probability of errors is achievable. Capacity over AWGN is widely used as a building block for analysing capacity over fading channels. Consider the following discrete-time AWGN channel:

$$y[t] = x[t] + n[t] \tag{1.3}$$

where $x[t]$, $y[t]$ and $n[t]$ are respectively used to denote the input, output and zero-mean additive white Gaussian noise, $n \sim \mathcal{N}(0, \sigma^2)$, at time t. With a channel bandwidth of B Hz and a constant transmit power of $\overline{S}$ watts, under AWGN with a power spectral density of N_0, the capacity is given by [28]:

$$C_{\text{AWGN}}(\overline{S}, B) = B \log_2 \left(1 + \frac{\overline{S}}{N_0 B}\right) \quad \text{bits/second.} \tag{1.4}$$

It should be noted that the constant received SNR over the AWGN channel is obtained as follows:

$$\gamma = \frac{\overline{S}}{N_0 B}. \tag{1.5}$$

The Shannon capacity expression is particularly significant as it highlights the impact of basic channel resources, in terms of bandwidth and power, on the performance of communication schemes. Dividing the capacity expression in (1.4) with the available bandwidth B, results in an expression for the maximum achievable

spectral efficiency over the AWGN channel:

$$\frac{C_{\text{AWGN}}}{B} = \log_2(1+\gamma) \quad \text{bits/second/Hz.} \tag{1.6}$$

1.3.3.2 Capacity over Fading Channels

Signals transmitted over wireless channels experience random power fluctuations, a phenomenon called fading. Fading occurs as a result of time- and frequency- varying channel conditions, and multipath components, which significantly attenuate the signals' power at the receiver. The latter, multipath, is generally considered as the main cause of fading [28]. It arises from the fact that there may be multiple propagation paths at the receiver, due to the presence of reflecting obstacles and the non-uniformity of propagation medium. The multipath components, also referred to as echoes, reach the receiver at different times and with different attenuations. Consequently, the reconstructed version of the signal at the receiver is a distorted variation of the original transmitted signal. In severe fading conditions, signals may exhibit something called a deep fade, where the low instantaneous received SNR or carrier-to-noise ratio (CNR) may result in the failure of transmission. Generally, channel gain, causing fading, possesses time- and frequency- selective characteristics.

Time-varying conditions refer to variation of channel characteristics as a function of time, which are mainly caused as a result of the changes in the propagation medium and the movement of the transmitter and/or receiver. More specifically, transmitted signals may experience rapid fluctuations over short durations or fade away over a long period. The latter is called slow-fading and the former is known as fast-fading. The time-selectiveness of a fading channel can be determined according to its coherence time, $T_{\text{coherence}}$, also called 'Doppler spread', which represents the time period in which the channel impulse response remains stationary. Consequently the channel is said to be slow-fading if the bit duration of the transmitted signal is shorter than the channel coherence time, and fast-fading if the bit duration exceeds the coherence time. A transmitted signal may avoid fast-fading conditions if its bandwidth is restricted to be smaller than $1/T_{\text{coherence}}$ Hz.

High frequency-varying nature of the wireless channels result from different delays and attenuations of multipath components. Consequently, different propagation components may be more distorted than others. Distinguishing between high and low attenuated components is highly difficult and uniformly boosting the overall signal power still results in propagation components with different attenuation levels. This has given rise to the implementation of equalizers at the receiver end of communication systems. With given information on the channel behaviour, an equalizer aims to amplify the parts of the signal spectrum that are fluctuated more. If fading on a transmitted signal is such that all its frequency components experience the same attenuation, the channel is said to be flat-fading. The range of frequencies in which the channel impulse response remains smooth is called the coherence bandwidth of the channel, $B_{\text{coherence}}$. If a signal bandwidth is larger than the coherence bandwidth of the channel then it is experiencing frequency-selective fading.

In the following parts of this subsection, I study the achievable capacity over time-varying frequency-flat and frequency-selective fading channels.

Frequency-Flat Fading Channels

The capacity analysis over AWGN channels in the previous section can be used to study the transmission limitations over wireless fading channels. Assume a discrete-time channel with stationary and ergodic time-varying channel gain $g[t]$, $0 \leq g[t]$, AWGN $n[t]$ with two-sided noise power spectral density of $N_0/2$ and channel bandwidth B. The channel gain follows a random distribution with a corresponding probability density function (pdf), $p(g)$. For example in the case of Rayleigh-distributed channel response envelope, the squared magnitude, $|g[t]|^2$, also called power gain, is Exponentially-distributed. Channel gain is assumed to be independent of channel input and the former can change at each time t [14]. Denoting the average transmit signal power with $\overline{S}$, the instantaneous received SNR for a constant transmit power is given by:

$$\gamma[t] = \frac{|g[t]|^2 \, \overline{S}}{N_0 B}. \tag{1.7}$$

The capacity of the fading channel depends on how much information, in terms of instantaneous value and the distribution, is known about $g[t]$ at the transmitter and

receiver. In the practical sense, the following are the three possible scenarios [14], [28]:

1. Channel Distribution Information (CDI): Transmitter and receiver have information regarding the distribution of $g[t]$. Deriving the capacity expression under CDI is very challenging, in fact it remains an open problem for almost all channel distributions apart from i.i.d. Rayleigh fading channels and finite state Markov channels [14], [29].

2. Receiver Channel Side Information (CSI): Transmitter and receiver have information regarding the distribution of $g[t]$ and receiver knows the instantaneous value of $g[t]$. In this case, the Shannon capacity of the frequency-flat fading channel with receiver CSI is given by [28]:

$$C_{\text{Receiver-CSI}} = \int_0^\infty B \log_2(1+\gamma) p(\gamma)\, d\gamma \quad \text{bits/second.} \tag{1.8}$$

Another performance criteria, called outage probability, P_{outage}, is typically associated with fading channels, particularly in slow-fading channels, to incorporate the probability of a transmission failure, in other terms possibility of a deep fade. It is typically defined as the probability that the received SNR falls below a certain predefined threshold, or the probability that the instantaneous probability of error exceeds a specific target. For a given SNR threshold, γ_{thresh}, set by the transmitter, the outage probability is obtained as follows [30]:

$$P_{\text{outage}} = P(\gamma < \gamma_{\text{thresh}}) = \int_0^{\gamma_{\text{thresh}}} p(\gamma)\, d\gamma. \tag{1.9}$$

The Shannon capacity of the frequency-flat fading channel with receiver CSI and an outage probability of P_{outage} can therefore be expressed as [14]:

$$C_{\text{outage}} = (1 - P_{\text{outage}}) B \log_2(1+\gamma_{\text{thresh}}) \quad \text{bits/second.} \tag{1.10}$$

A more lenient QoS requirement here, i.e. higher non-outage probability, results in higher capacity, however, this increases the probability of error at the receiver.

3. Transmitter and Receiver CSI: Both transmitter and receiver have information

regarding the distribution and instantaneous value of $g[t]$. In this total CSI case, by incorporating a feedback channel, the transmitter can adapt its instantaneous signal power as a function of the received SNR. Power adaptation in practical systems is subject to average and peak constraints, to incorporate the resource limitations of these systems and to avoid excessive interference.

With an adaptive transmit power of $S(\gamma)$, and denoting the average transmit power with $\overline{S}$, the following average power constraint is considered for the transmitter and receiver CSI case [31], [32]:

$$\int_0^\infty S(\gamma)p(\gamma)\,d\gamma \leq \overline{S}. \tag{1.11}$$

Hence, the following optimization problem for the Shannon capacity of the transmitter and receiver CSI is formulated:

$$\underset{S(\gamma)}{\text{maximize}} \qquad C_{\text{T\&R-CSI}} = \int_0^\infty B\log_2(1+\frac{S(\gamma)}{\overline{S}}\,\gamma)p(\gamma)\,d\gamma \tag{1.12a}$$

$$\text{subject to} \qquad \int_0^\infty S(\gamma)p(\gamma)\,d\gamma \leq \overline{S}. \tag{1.12b}$$

Solving the optimization problem yields the following water-filling optimal power adaptation policy:

$$\frac{S(\gamma)}{\overline{S}} = \begin{cases} \frac{1}{\gamma_0} - \frac{1}{\gamma} & \gamma \geq \gamma_0 \\ 0 & \gamma < \gamma_0 \end{cases} \tag{1.13}$$

where γ_0 represents the cut-off SNR threshold. Using (1.17), the optimal Shannon capacity of transmitter and receiver CSI is derived:

$$C_{\text{T\&R-CSI}} = \int_{\gamma_0}^\infty B\log_2(\frac{\gamma}{\gamma_0})p(\gamma)\,d\gamma \quad \text{bits/second.} \tag{1.14}$$

Apart from the optimal water-filling transmitter adaptation scheme, there are sub-optimal power adaptation policies that utilize transmitter and receiver CSI to maintain a constant received power. Due to presence of near-far effect, such channel inversion policies are particularly important in uplink of 3G CDMA systems where power control is required so that the cellular mobile users' SNRs remain equal at

the BS [20], [33]. To incorporate this adaptation idea, total and truncated channel inversion policies, where channel fading is inverted, are widely employed in literature [34–36]. The general total channel inversion policy is expressed as:

$$\frac{S(\gamma)}{\overline{S}} = \frac{\sigma}{\gamma} \tag{1.15}$$

where the constant SNR-target, σ, is given by:

$$\sigma = \frac{1}{E[\frac{1}{\gamma}]} = \frac{1}{\int_0^\infty \frac{1}{\gamma} p(\gamma)\, d\gamma}. \tag{1.16}$$

The total channel inversion policy requires large transmit powers during deep fades, hence, truncated channel inversion policy is the preferred choice for implementing practical power adaptation schemes:

$$\frac{S(\gamma)}{\overline{S}} = \begin{cases} \frac{\sigma_{\text{trunc}}}{\gamma} & \gamma \geq \gamma_0 \\ 0 & \gamma < \gamma_0 \end{cases} \tag{1.17}$$

where σ_{trunc} and γ_0 are the constant SNR-target and the cut-off SNR threshold, respectively. The corresponding outage probability is given by: $P_{\text{outage}} = p(\gamma < \gamma_0)$. For truncated channel inversion policy, σ_{trunc} is expressed as:

$$\sigma_{\text{trunc}} = \frac{1}{E[\frac{1}{\gamma}]_{\gamma_0}} = \frac{1}{\int_{\gamma_0}^\infty \frac{1}{\gamma} p(\gamma)\, d\gamma}. \tag{1.18}$$

Compared to optimal water-filling power policies, sub-optimal channel inversion strategies are less power efficient, as large amounts of power is consumed in order to invert the fade level when quality of channel is low. However, it should be noted that total and truncated channel inversion policies do not require statistical information of fading, as a result, they are delay-independent over channel variations and therefore are less complex to implement.

Frequency-Selective Fading Channels

In this part, I study the Shannon capacity over time-varying frequency-selective channels with transmitter and receiver CSI. Dividing the channel bandwidth B

into a number of time-varying frequency-flat fading sub-channels, the size of the coherence bandwidth of the channel, $B_{\text{coherence}}$, the instantaneous received SNR of sub-channel-j at time t is given by:

$$\gamma_j[t] = \frac{|H_j[t]|^2 \, \overline{S}}{N_0 B_{\text{coherence}}} \tag{1.19}$$

where $H_j[t]$ and $\overline{S_j}$ denote the channel gain and average transmit power of sub-channel-j at time t, respectively. I denote the average total allocated power in the channel with $\overline{S}$. The following average power constraint is therefore considered over all sub-channels [37]:

$$\sum_j \int_0^\infty S_j(\gamma_j) p(\gamma_j) \, d\gamma_j \leq \overline{S}. \tag{1.20}$$

Hence, the following optimization problem for the Shannon capacity of the frequency-selective channel with transmitter and receiver CSI is formulated:

$$\underset{S_j(\gamma_j)}{\text{maximize}} \qquad C_{\text{T\&R-CSI}} = \sum_j \int_0^\infty B_{\text{coherence}} \log_2(1 + \frac{S_j(\gamma_j)}{\overline{S}} \, \gamma_j) p(\gamma_j) \, d\gamma_j \tag{1.21a}$$

$$\text{subject to} \qquad \sum_j \int_0^\infty S_j(\gamma_j) p(\gamma_j) \, d\gamma_j \leq \overline{S}. \tag{1.21b}$$

Solving the optimization problem yields the water-filling optimal power adaptation policy for the frequency-flat case in (1.17). Hence, the upper-bound Shannon capacity of the frequency-selective channel with transmitter and receiver CSI is derived as follows [14]:

$$C_{\text{T\&R-CSI}} = \sum_j \int_{\gamma_0}^\infty B_{\text{coherence}} \log_2(\frac{\gamma_j}{\gamma_0}) p(\gamma_j) \, d\gamma_j \quad \text{bits/second.} \tag{1.22}$$

1.3.3.3 Statistical Models for Fading Channels

In order to tackle the adverse effects of fading, statistical models, derived from the field of Probability Theory and Stochastic Processes, are of great importance towards implementing effective receivers and consequently devising efficient wireless communication systems. Although exact mathematical description of propagation in wireless channels is too complex to derive, statistical models are necessary to, at

least approximately, characterise the behaviour of fading channels. Based on the nature of the wireless propagation environment and the underlying communication scenario, distinct statistical models are used. In this subsection, I briefly outline some of the most well-known fading distributions, modeling small-scale indoor and outdoor propagation environments, that are used in cellular communication systems. Information regarding statistical models, in particular Log-Normal distribution for shadowing, for large-scale propagation environments, where distance between transmitter and receiver is large, can be found in the literature [7, 38–40].

Rayleigh Fading Channel

For asymptotically large number of scatterers over the fading channel, such as signal propagation in ionosphere and troposphere layers of the earth's atmosphere [41, 42], central limit theorem can be invoked to show that the channel impulse response follows a Gaussian distribution [43, 44]. In the event that there is no direct LOS path, the Gaussian distribution can be modelled with a zero mean. In this case, the envelope of channel response is said to be Rayleigh-distributed [45, 46]. Hence, the instantaneous received SNR, γ, over the Rayleigh fading channel, is Exponentially-distributed with the following pdf:

$$p(\gamma) = \frac{1}{E[\gamma]} \exp(\frac{-\gamma}{E[\gamma]}) \tag{1.23}$$

where $E[\gamma]$ denotes the average received SNR.

Rayleigh distribution imposes severe amplitude fluctuations, as a result, it is most suitable for modeling macro-cell (i.e. wide radius cells) propagation environments, and more generally in cases where there is no direct LOS path between transmitter and receiver.

Ricean Fading Channel

In propagation scenarios, where there are randomly moving and fixed number of scatterers, the envelope of channel response follows a Ricean distribution. Ricean fading channel, also called Nakagami-n, typically consists of a direct LOS path and multiple lower-power multipath components. Denoting the average SNR with $E[\gamma]$,

the instantaneous received SNR, γ, is distributed with the following chi-square pdf:

$$p(\gamma) = \frac{(1+n^2)e^{-n^2}}{E[\gamma]} \exp(\frac{-(1+n^2)\gamma}{E[\gamma]}) \ , \ \ n \geq 0 \tag{1.24}$$

where n denotes the Nakagami-n fading parameter. Moreover, Ricean parameter K $(= n^2)$, corresponds to the ratio of the LOS path strength over the average power of the scattered multipath components. Hence, K serves as an indicator of the Ricean-distributed channel quality [47, 48]. The Ricean distribution is equivalent to Rayleigh fading where $n = 0$, whereas it converges to a non-fading distribution in the limit as $n \longrightarrow \infty$.

Ricean fade levels are more benign compared to Rayleigh fading, as a result Ricean-distributed channel models are typically employed for micro-cellular (i.e. relatively small coverage cells) fading environments, such as indoor, urban and sub-urban areas [49–51].

Nakagami-m Fading Channel

The Nakagami-m distribution, where m denotes the Nakagami-m fading parameter, provides a wide range of fading distributions [52]. Specifically. it incorporates the Gaussian, Rayleigh, Ricean and many more fading distributions through the parameter m. The instantaneous received SNR, γ, over Nakagami-m fading, is Gamma-distributed with the following pdf:

$$p(\gamma) = \frac{1}{\Gamma(m)} \left(\frac{m}{E[\gamma]}\right)^m \gamma^{(m-1)} \exp(\frac{-m\gamma}{E[\gamma]}) \ , \ \ m \geq \frac{1}{2} \tag{1.25}$$

where

$$\Gamma(m) = \int_0^\infty t^{m-1} e^{-t} dt. \tag{1.26}$$

For higher values of m the severity of fading decreases, as illustrated in Fig. 1.10. The worst fade levels are experienced where $m = \frac{1}{2}$, which corresponds to one-sided Gaussian fading distribution, whereas in the limit as $m \longrightarrow \infty$, the Nakagami-m converges to a non-fading distribution. Moreover, $m = 1$ corresponds to a Rayleigh distribution, and $m = 2$ is approximately equivalent to Rayleigh distribution with

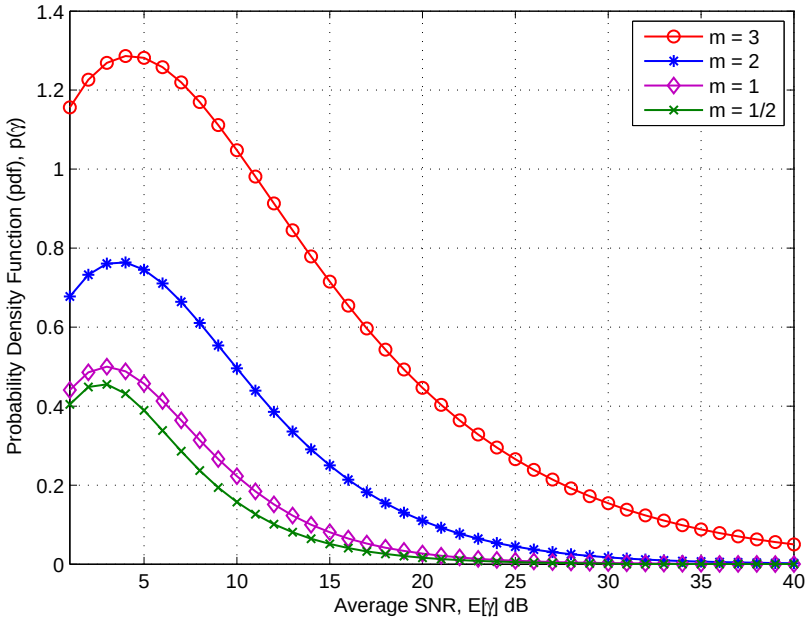

Figure 1.10: Gamma-distributed probability density function for various values of the Nakagami parameter m.

two-antenna diversity. Further, for $m \geq 1$, the Nakagami-m distribution closely approximates the Ricean distribution with the following Ricean parameter:

$$K = \frac{\sqrt{m^2 - m}}{m - \sqrt{m^2 - m}} \quad , \quad m \geq 1. \tag{1.27}$$

As a result of the Nakagami-m advantages over other statistical models, such as spanning a wide range of fading distributions and its closed-form analytical convenience [53–55], it fits best with empirical indoor, sub-urban, urban and ionospheric environments [52, 56, 57]. Hence, in this thesis I have extensively incorporated the general Nakagami-m distribution as the main statistical fading model for evaluating the performance of our proposed schemes.

1.3.3.4 Diversity Combining

Diversity is a general term used to describe a family of techniques that reduce the effects of fading [13, 54, 58]. Even though fading is considered as a destructive phe-

nomena in wireless communications, multipath components can be used constructively by employing diversity combining techniques. The technique for combining multipath components is also called 'path diversity'. There are typically two important diversity methods. The simpler method, called Selection Combining (SC), only selects the path with the highest received SNR (i.e. maximum amplitude) at the receiver. In the other method, called Maximum Ratio Combining (MRC), all the received paths, after delay compensation, are summed based on their revived SNRs. In order to improve performance over frequency-selective channels, RAKE (i.e. bank of correlators, for example matched filters) receivers with MRC are widely studied and employed in current- and future- generation wireless communication systems. MRC RAKE receiver achieves this by reducing the effects of fading fluctuations and improving the average SNR, without increasing the transmit power [28]. A basic system model for a single-transmitter with an L_p-path MRC RAKE receiver is presented in Fig. 1.11.

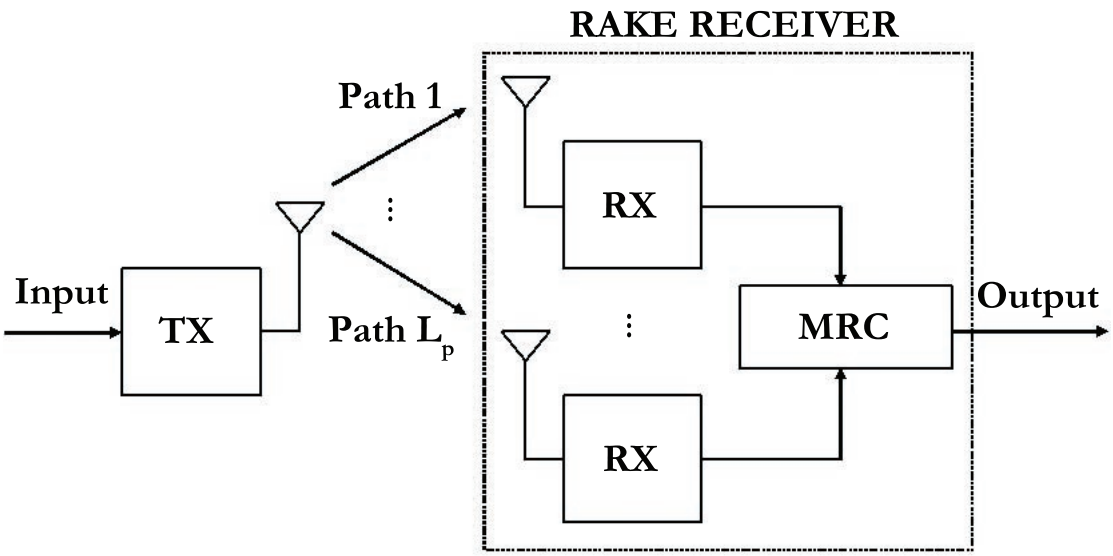

Figure 1.11: Maximum Ratio Combining (MRC) RAKE receiver.

To study the MRC RAKE receiver, consider a single-user transmission over an L_p path time-varying frequency-selective fading channel with stationary power gains $H_j(t),\ j = 1, ..., L_p$ at time t. Given that AWGN with two sided power spectral density of $N_0/2$ is present in the channel, the instantaneous received SNR of the

reference user over the j-th path is expressed as:

$$\gamma_j(t) = \frac{|H_j(t)|^2 \overline{S_j}}{N_0 B}. \tag{1.28}$$

where $\overline{S_j}$ denotes the average transmit power over path-j and B is the bandwidth of the channel. The instantaneous respective SNR of the reference user at the output of the MRC combiner at time t is given by:

$$\gamma(t) = \sum_{j=1}^{L_p} \gamma_j(t). \tag{1.29}$$

It is important to note that, the multipaths typically do not experience the same amount of fading, since higher delay results in decreased power and therefore less resilience to fade levels. As a result, the first arriving path from the reference user, which may also be the LOS path, exhibits the least amount of fading and the last arriving path experiences the highest fade levels [59, 60]. The term multipath intensity profile (MIP), also called power delay profile (PDP), is used to describe the decay in power relative to the delay. Given the average SNR of the reference (i.e. first) path is denoted with $\overline{\gamma_r}$, and assuming equally spaced delays equal to symbol time T_s, the average SNR of the j-path is given by:

$$\overline{\gamma_j} = \overline{\gamma_r} e^{-\delta(j-r)}. \tag{1.30}$$

where δ denotes the rate of Exponentially-decaying MIP. For almost all fading statistics, MRC is generally considered as the optimum diversity combining technique, however, it's implementation is complex in comparison to other combining methods, as it requires knowledge of all channel fading parameters [61].

1.3.3.5 Delay and Queueing Models

One of the most important performance evaluation measures in cellular mobile networks, is delay (also called latency). It defines the amount of time required to deliver an entire packet from the source to the destination. Delay specifications highly affect the performance and limitations of networks. As a result, understanding the

nature of latency is of great importance to network designers. Queuing theory is the framework for understanding and modeling latency in telecommunication networks.

Generally, there are four main latency components, namely propagation, processing, queuing and transmission delays [62, 63]. However, in the case of multi-access communications, such as radio networks, one must also incorporate the probability of retransmission, in case of erroneous packets, when modeling delay. The propagation delay is generally computed as the ratio of distance between the source and the destination over the propagation speed. The processing delay is a measure of the amount of time required for a packet to be processed and assigned to the transmitting node. As a result, propagation and processing components of delay, are independent of the amount of traffic congestion in the network. Moreover, queuing delay, is a measure of the time a packet waits in the buffer queue before it can be processed. Queuing delay is highly dependent on the network traffic load. Further, processing delay, a measure of the amount of time required to transmit all the bits of a packet, depends on the packet length and the channel data rate. Incorporating all the practical aspects of delay in the network design is an extremely complex task. Therefore, assumptions are typically made for simplicity's sake. Throughout this work, I consider the limitations of the buffer size and the tolerable delay, by capping the number of ARQ retransmissions. This is further elaborated in Section 1.5.

Mobile communication systems, can be described as queuing systems with finite number of transmission links, where cellular users arrive at random times, requesting service. Queueing systems incorporate parameters representing packets arrival, departure, waiting and servicing times. The process of a packet arrival is typically independent of other packets arrival and is random in time. As a result, Poisson distribution may be employed as a basic but essential design tool to model these stochastic processes. Consequently, for Poisson distributed user arrivals, mutually independent service times are Exponentially-distributed. The relationship between Poisson and Exponential processes, emanate memoryless characteristics, meaning the probabilities of arrival and service times occurring in the future are independent of present users' arrival and service times. One of the main goals of this thesis, is to devise dynamic resource allocation algorithms, according to the number of present

active users in the cell. Hence, based on these assumptions, I exploit Markovian distributions to model the number of users. In particular, I employ one- and multi-dimensional discrete-time Markov chains to obtain blocking probabilities of the cellular networks under consideration.

M/M/m/m Queuing System

Throughout this contribution, I adopt M/M/m/m queuing birth-death discrete-time Markovian distributions to model the number of active users in radio communication cells. The first and second letters in the name of this model, 'M' and 'M', correspond to a memoryless queueing system with Poisson-distributed user arrivals and Exponentially-distributed service times, respectively. Hence, I assume a Poisson-distributed user arrival rate with mean λ and Exponentially-distributed service times with an average of $1/\mu$ seconds. The third letter, 'm', denotes the number of servers or transmission line channels. The fourth letter, 'm', denotes the maximum number of users supported by the network. Moreover, birth-death, a property of Markov processes, corresponds to the condition that a change in the state only occurs between 'neighbouring' states.

To obtain the equilibrium solution of steady-state probabilities of the discrete-time Markov chain, we need to write down the birth-death coefficients of the queueing system. Denoting the number of active users with k and maximum allowed number of users with K, the birth (λ_k) and death (μ_k) coefficients are expressed as:

$$\lambda_k \Delta T = \begin{cases} \lambda & k < K \\ 0 & k \geq K \end{cases} \tag{1.31}$$

$$\mu_k \Delta T = k\mu \quad , \quad k = 1, 2, ..., K \tag{1.32}$$

where λ and μ are the transition probabilities occurring in a small time ΔT. Equation (1.31) adopts the condition for a maximum number of users by suspending transmission of newly arrived users when $k = K$. The corresponding state-transition-diagram of the M/M/m/m discrete-time Markov chain is presented in Fig. 1.12. The steady-state probabilities in equilibrium, i.e. when rate of inward and outward flow in the system are equal, result in the following *global balance equation*:

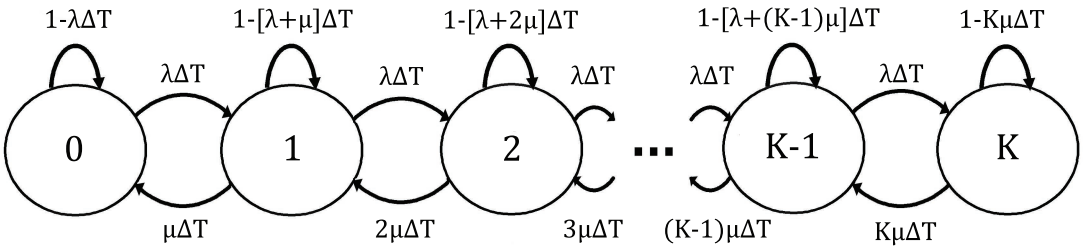

Figure 1.12: M/M/m/m queuing discrete-time Markov chain.

$$\lambda P(k-1) = k\mu P(k) \quad , \quad k = 1, 2, ..., K \tag{1.33}$$

where $P(k)$ and $P(k-1)$ are used to denote the probabilities of any two neighbouring states, where there are 'k' and '$k-1$' active users, respectively. Equation (1.33) together with the probability condition for all states, $\sum_{k=0}^{K} P(k) = 1$, can be used to derive an expression for probability of having k active users (*Erlang formula*) in the radio network under consideration here:

$$P(k) = \frac{\frac{(\lambda/\mu)^k}{k!}}{\sum_{n=0}^{K} \frac{(\lambda/\mu)^n}{n!}}. \tag{1.34}$$

Analysis for deriving the joint equilibrium probability expression in a multi-dimensional discrete Markov chain with two truncated M/M/m/m queues, is provided in Chapter 4.

1.3.3.6 Spectral Efficiency and Throughput

As previously discussed, the primary goal of radio access technologies is to accommodate the demand for high data rates in a given scarce spectrum, while minimizing costs, satisfying QoS constraints of the supported services and satisfying predefined complexity criteria. Hence, wireless technology developers must find the appropriate trade-off between these various competing requirements by incorporating a combination of modulation, coding and diversity techniques, in order to design effective and efficient radio access networks. Developers typically make design decisions by

evaluating the quantitative performance of these conjoined schemes over wireless fading channels. Particular emphasis is placed on performance measures in terms of received SNR, bit/packet error rate (BER/PER), transmission delay, outage probability, dropping probability, capacity, spectral efficiency and throughput.

The term, spectral efficiency, is defined to demonstrate the ability of a cellular network to accommodate data transmission in a given spectrum. Specifically, spectral efficiency, measured in bits/second/Hz or bits/second/Hz/cell, is given by the maximum possible data rate per unit of bandwidth. Spectral efficiency is an especially important performance metric, as it illustrates the joint performance of various design aspects such as the multiple access technology, digital communication scheme, diversity technique and channel resource reuse. Spectral efficiency performance is directly associated with the requisite amount of bandwidth, required number of base stations and cells, and customer pricing.

Another metric for evaluating the performance of radio access technologies is throughput. It is defined as the total number of bits successfully delivered to the receiver within a unit time. The network effective throughput, also called sum-throughput, is the aggregate data throughput of all users in the system, measured in bits/second. Throughput performance is directly linked with the ratio of the number of erroneous bits/packets over the total number of transmitted bits/packets, measured in terms of BER/PER, respectively. To compare spectral efficiency with throughput, the former provides a potential measure of the channel capacity, whereas the latter is an actual indication of how fast the data can be transmitted via the channel. Throughput performance versus delay is an essential design aspect in wireless networks. Typically increasing throughput results in more delay, as a result there is a trade-off between achievable data rates and traffic congestion.

In this development, one of the main goals is to maximize the effective cell throughput, defined as the total number of successfully transmitted packets by all supported mobile users in the cell within a unity-duration time interval over the total channel packet rate. In the following sections of this chapter, dynamic design strategies towards achieving this goal are proposed.

1.4 Radio Resource Management

The scarcity of radio resources, mostly defined in terms of bandwidth, power and time, stress the ever increasing importance of effective and efficient use of available resources. The rapid demand for simultaneously supporting more and more services with different data rates and QoS requirements, highlights the significance of *Radio Resource Management* algorithms.

In the context of radio access networks, RRM strategies, facilitating efficient utilisation of air interface resources, are essential for meeting the distinct QoS demands of services and achieving optimal throughput. Consequently, extensive research has been carried out over the last decade on devising RRM algorithms that optimize the performance of 3G and emerging 4G systems. Research studies over the years have led to a broad range of RRM functionalities, such as power control, rate control, hand-off control, packet scheduling and traffic control. Here I outline some of the most important RRM mechanisms devised towards enhancing the performance of 3G systems with a brief reference to evolving 4G technologies.

1.4.1 Adaptive Modulation and Coding

A fundamental concept of RRM, known as Adaptive Modulation and Coding (AMC), is to exploit the time-varying nature of physical channels in order to manage resource optimally. This idea was first proposed in [64], where channel information was fed to the transmitter through a feedback channel in order to modify transmission power. Contrary to the non-adaptive modulation and coding schemes that necessitate fixed link margins to ensure reliable transmission, AMC schemes adapt the transmission to channel characteristics and hence are robust to poor channel conditions. Furthermore, employing AMC can significantly improve the throughput performance, reduce the average transmit power and decrease the average probability of error. It is important to note that adaptive modulation schemes necessitate a feedback channel between transmitter and receiver which exhibits a delay, which may be infeasible in certain practical scenarios. In particular, in case of fast-fading wireless channels, the channel gain may be changing at a faster pace than the delay of the

feedback channel and hence AMC schemes may perform poorly. Further, how rapid rate and/or power can be varied, is subject to certain hardware and software constraints imposed on the underlying system which effectively edict the achievable gain of adaptive modulation schemes. Although many parameters can be adapted to the channel gain, throughout this contribution, we have specifically combined *interference-based* adaptive power and rate techniques with automatic repeat request (ARQ) retransmission in order to enhance the performance of radio access networks under consideration.

1.4.2 Power Control

In Subsection 1.3.3.2, we analytically demonstrated the maximum achievable capacity of wireless channels under presence of AWGN and fading, by employing optimal water-filling and sub-optimal total and truncated channel inversion policies. In this part, we focus on practically feasible power adaptation techniques in the presence of fading and *interference*. The interference imposed on a cellular mobile user could be the result of a number of factors, namely co-channel interference, adjacent channel interference, inter- and intra- cell interference, fading and finally thermal noise. The co-channel interference arises from the frequency-reuse phenomenon, where different cells, given they are located sufficiently apart, may be allocated the same spectrum for transmission, and hence could deteriorate performance of one another on the receiver side. In case of insufficient separation between operating frequencies of neighbouring cells, adjacent channel interference refers to the interference imposed on the reference cell by the neighbouring cells. As previously discussed, inter- and intra- cell interference correspond to interfering signals generated by users, in the same cell and in the neighbouring cells, respectively. As we will discuss in detail throughout this contribution, intra-cell MAI is the main phenomenon in limiting the performance of CDMA systems, where as, in multi-carrier OFDM systems intra-cell self-interference, in terms of ISI and inter-carrier-interference (ICI), is per se the main cause of performance degradation. Naturally, apart from interference, fading and noise levels limit the performance of wireless channels. Detailed information on fading and thermal noise, typically modeled as AWGN, were given in Section 1.3.3.

As previously mentioned, CDMA-based radio access technologies, particularly WCDMA, are the dominant air interface in current 3G UMTS standards. WCDMA employs spread spectrum modulation schemes, which aim to minimize the MAI by spreading the signals that are overlapping in both time and frequency over the entire bandwidth. MAI limits the maximum number of supported users in a CDMA cell, and the achievable capacity, i.e. *soft capacity*. Moreover, CDMA systems are highly vulnerable to the near-far phenomenon, where users that are closer to the BS may overshadow the signals transmitted by users that are located farther from the BS. Hence, UMTS-specific RRM algorithms, in particular dynamic power control, are immensely important towards achieving desirable performance in both uplink and downlink of CDMA-based networks. In the uplink, power control is the established mechanism in UMTS for tackling the MAI and the near-far phenomena, in addition to minimizing the energy consumption of cellular users (e.g. battery power). Power control is less significant in UMTS downlink, and is mainly responsible for tackling near-far problem by adjusting the transmit power accordingly.

One of the main concerns of this thesis, is the uplink power control mechanism in CDMA-based networks. Power control in UMTS is a combination of open-loop power control and closed inner- and outer- loop power control (ILPC/OLPC). The OLPC sets the required transmission quality that would meet the requisite QoS constraints of all users. The ILPC then aims to attain the OLPC transmission quality target by accordingly adjusting the instantaneous transmit power. The combination of OLPC and ILPC essentially minimizes the interference and tackles the near-far effect by maintaining equal received signal-to-interference-and-noise ratio (SINR/SNR) for all users at the BS. The open-loop power control is only responsible for setting the initial uplink and downlink transmission powers and therefore is not considered in this work. In UMTS standards, ILPC operates at the slot level (at a frequency of 1500 Hz) and OLPC operates at the frame level (at frequencies of $10 - 100$ Hz), where the duration of one frame is 10 ms, and there are 15 slots per frame [19, 20, 65].

The OLPC defines the required transmission quality in terms of BER or frame error rate (FER), by accurately setting the target signal-to-interference-and-noise

ratio (SINR/SNR-target). The SINR-target, set to cater for QoS requirements of the services in a cell, is typically derived as a result of Cyclic Redundancy Check (CRC) carried out by the Load Control (LC) unit [20, 66, 67]. The choice of SINR-target is highly capacity sensitive, i.e. while an increase improves the probability of violating the imposed QoS constraints, in turn, costs extra power and increases interference, resulting in capacity loss. The BS frequently estimates the received SINR (SINR-estimate) of all users, and compares them with the OLPC SINR-target. If a user SINR-estimate is below/over the OLPC SINR-target, then the SINR-based ILPC increases/decreases the transmit power of the user accordingly. In UMTS, the uplink ILPC basic power step size is 1 dB, but this may be increased to 2 dB depending on the environment and hardware conditions. However, excessive power step sizes may result in interference, whereas insufficient steps in power may impose high delays towards attaining the OLPC SINR-target. For the sake of notational consistency with our published papers, throughout this thesis, we refer to the combination of 'interference and noise' as *noise*, and hence mostly use the term 'SNR' instead of SINR.

Throughout this contribution, we explicitly include the OLPC SNR-target in a cross-layer optimization problem, in order to achieve optimal throughput performance in CDMA networks while satisfying predefined QoS constraints in the presence of near-far effect, MAI and fading. Total and truncated channel inversion policies in the ILPC are employed in order to attain the SNR-target.

As discussed in Subsection 1.3.3.2, optimal water-filling power allocation policies are not practically feasible in certain systems. These polices use the favourable channel conditions and typically try to suspend transmission in poor channel conditions in order to achieve maximum capacity. However, in services with high-delay constraints, such as voice or video, these policies may severely degrade the QoS performance. In particular, in the context of single-carrier CDMA transmission, optimal power adaptation policies result in more severe near-far effect. However, these issues are much less of a problem in the context of LTE radio access technologies. In fact, with appropriate modulation and coding techniques, water-filling power adaptation policies achieve optimal performance in multi-carrier OFDM-based ra-

dio access networks without violating imposed QoS constraints of high data rate services [21, 27, 68–72].

1.4.3 Rate Control

In radio access networks, the choice for an effective data transmission rate is directly linked with the SNR levels. In the case of fixed-rate systems, the power control is responsible for meeting the requisite QoS requirements of all users by setting the required transmission quality, SINR-target, and adjusting the transmit power to attain SINR-target. However, this approach is not practical in modern multimedia networks, where different services with different data rates must be supported. In addition, the fluctuations in the wireless communication channels, dictate the use of variable-rate transmission schemes in order to utilize the available radio resources efficiently and effectively.

In the context of CDMA systems, due to the high sensitivity to interference, the trade-off between low power consumption and high data rate is an important design aspect. Achieving a higher data rates require greater transmit power, which in turn increases the MAI levels. On the other hand, transmitting at low data rates does not affect the MAI levels, however, it prolongs the duration of the MAI, which may severely degrade the performance. Consequently, it is advantageous to jointly include power control and rate control in the system design. One of the main aims of this work, is to incorporate this design approach with the goal of maximizing system throughput performance. We achieve this by devising a dynamic algorithm that assigns optimal SNR-targets and data rates to cellular mobile users subject to predefined QoS constraints.

In variable-rate modulation schemes, data rate (R) is typically adapted to the received SNR (γ), i.e $R(\gamma)$. This is achieved by either fixing the symbol rate ($R_s = 1/T_s$) and employing multiple modulation schemes or constellation sizes, or by fixing the modulation and varying the symbol rate. Throughout this work, we employ the latter, by incorporating BPSK and varying the symbol rate. Particularly, we adopt variable spreading factor (VSF) adaptation, where users' data rates are varied over a fixed chip rate sequence. This is in line with rate control mechanism in UMTS

standards, where a fixed chip rate of 3.84 Mchips/s is implemented [19,20,65,66]. In Section 1.3.2.1 of this chapter, we studied the concept of spread spectrum in UMTS using spreading factors. With a fixed chip rate, higher/lower bit rates result from lower/higher spreading factors. Maximum achievable data rate is limited by a cap in the minimum spreading factor, on the other hand, to avoid bandwidth expansion as a result of excessive spreading factors, the minimum practical bit duration is set to be equal to the chip duration.

In CDMA networks the concept of a common spreading code, is typically adopted for users of all classes in the system, as they are spread over the same bandwidth. We incorporate this methodology in parts of the thesis where a single-service scenario is considered. However, the use of multiple spreading codes for different services is considered in Chapter 4, where a multi-service system of heterogeneous data traffic is considered.

1.5 Cross-Layer Design and Optimization

As extensively discussed in Subsection 1.3.1.2, the success and proliferation of today's telecommunication networks, in particular the Internet, is based on the layering design approach. Although the traditional layered architecture, originally intended for wired networks, is desirable in the sense of modularity, standardization and expandability, its rigid design makes it inefficient to solve the problems associated with wireless networks. Particularly because in-depth understanding and possible tradeoffs in multimedia quality, implementation complexity, and spectrum utilization, that are provided by different layers in the OSI architecture, are essential towards obtaining an optimal global design solution.

In fact, one of the main challenges associated with the design of modern wireless networks is the overhaul of the reference layered design approach. As an illustration, wireless links, may exhibit poor performance, which changes, together with user connectivity and network topology, over time. As a result of link fuzzy nature, network parameters must be adaptive to link variations, in order to achieve higher throughput whilst meeting user-specified QoS demands. However, these parameters

are not limited to a specific layer of the protocol stack, for example, transmission power and data rate are PHY-layer parameters, whereas delay is a performance measure at the DLL. Degradation in performance may lead to packet loss, which may be a result of deep fluctuations in the underlying wireless channel in the PHY-layer, or due to queuing in the DLL. Thus, networks require integrated and adaptive protocols across different layers, from the PHY-layer to the application layer, in order to achieve optimal performance and guarantee the QoS constraints across all layers.

The unique challenges posed by the wireless link and the demand for opportunistic communication on the wireless medium, has given rise to the notion of *cross-layer design and optimization* [73, 74]. The term *design* corresponds to creating protocols which merge or redefine the layer boundaries, and the terms *optimization* refers to joint tuning of the parameters across different layers. Nowadays, wireless networks necessitate flexible interaction across different layers of the network architecture, to accommodate applications with rising QoS demands. Cross-layer design is widely considered as an essential tool for radio resource optimisation in future wireless communication systems. Hence, the long familiar and widely referred OSI model is an increasingly outdated concept in the modern telecommunications literature. However, in practice, cross-layer design techniques result in significant architectural complexity [73]. Specifically, cross-layer strategies aim to solve the problems that extend to a broader region, typically across several layers, instead of carrying out the analysis in parts at individual layers. This makes the process of obtaining a global solution more challenging. Hence, design of efficient and practical cross-layer protocols require interdisciplinary expertise in communications, signal processing, information theory and network design.

The principal focus of this thesis is optimal resource allocation in a joint PHY-layer and DLL cross-layer design. As explained in subsection 1.3.1.2, the LLC sub-layer, together with the MAC sub-layer, comprise the DLL. The MAC sub-layer is responsible for scheduling, i.e. allocating radio resources to users who request access to the transmission medium. On the other hand, the LLC improves the link quality using forward error correction (FEC), flow control and ARQ. FEC adds redundant bits using coding schemes for the purpose of error control, which cost extra band-

width and is only effective for small number of errors. FEC is typically employed when retransmission of lossy packets is not incorporated in the design. In addition, retransmission requests may be undesirable due to stringent delay requirements. However, in the case where retransmissions are viable, a tactical ARQ mechanism can effectively reduce error.

In the cross-layer schemes developed in this thesis, the focus is on the error control, i.e. error detection and error correction, feature of the DLL using coding and packet retransmissions. Coding techniques are generally divided into two categories: block coding and convolutional coding. Throughout this work, we concentrate on linear block coding capabilities. In Chapter 5, a brief discussion on extending the analysis using convoultional coding is made. Furthermore, we consider ARQ for error control, and consequently, throughput improvement. This is particularly beneficial in data communication, e.g. messaging, where the delay constraints are relaxed. There are several different ARQ implementations. The stop-and-wait ARQ mechanism, stops the transmission of the next packet until it receives acknowledgement from the receiver that the previous packet is correctly received. The transmission is slowed down in this case, and therefore this simple ARQ protocol is inefficient in practice. In order to improve the transmission efficiency, transmission of other packets must be allowed while the sender is awaiting confirmation. This Go-Back-N ARQ mechanism incorporates this approach by allowing several packets to be transmitted without requiring acknowledgement. The number of packets that can be transmitted without confirmation from receiver, i.e. the go-back-number, N, is pre-determined and a copy of the packets is preserved until an acknowledgement is received. In case of an erroneous received packet, all the subsequent packets as well as the reference packet must be retransmitted. Hence, this ARQ scheme may perform poorly, particularly in noisy channels or/and in case of high-speed transmissions where occurrence of erroneous packets is more likely. To implement an efficient ARQ scheme for noisy channels, the transmitter must only resend the erroneous packets. This scheme is called Selective Repeat ARQ, and is proven to be an improvement on the performance of the Go-Back-N ARQ mechanism [75, 76]. In this development, we employ a Selective Repeat truncated-ARQ scheme in the DLL,

where maximum number of retransmissions is capped, for error correction, in order to elevate the achievable throughput.

To achieve higher performance, the error control mechanism at the DLL may be adopted to physical link varying characteristics to reduce the probability of faulty received packets. To achieve this, the maximum number of retransmissions can be varied to channel current state, which also provides better control over the trade-off between the achievable throughput and the induced delay [75]. This is however, beyond the scope of this thesis and is merely suggested in Chapter 5, as a possible future work.

1.6 Spectrum Sharing and Opportunistic Communication

In the previous two sections, we highlighted the increasing importance of efficiency and reliability in wireless communication systems. On the other hand, bandwidth is an important concern with the exponential growth in access and sophistication of wireless applications. However, existing spectrum allocation policies are incapable of coping with spectrum access demand. This is because the traditional rigorous regulation of frequency bands offer little or no sharing, thus a large part of the useful spectrum remains idle. The FCC report published in November 2002, states that a large part of useful frequency bands, such as TV frequency spectrum, remains unused due to legacy command-and-control regulation. This has resulted in a shortage of available spectrum. This has given rise to the notion of *cognitive radio* [77], a prominent candidate to solve the problem of spectrum shortage.

Cognitive radio offers intelligent and efficient utilization of unused or under-utilized parts of the spectrum by providing cognitive (unlicensed) users with temporary access to a primary (licensed) spectrum band, subject to constraints on the imposed interference on the primary users. Cognitive radio networks achieve this by actively observing the activity in the spectrum and adapting their parameters accordingly. The ultimate goal of cognitive radio is to maximize the performance

of the secondary service, whilst ensuring smooth primary service operation without harmful intervention from the secondary users. In practice, the implementation of this goal is challenging and necessitate intelligent decisions on various requirements and constraints.

Generally, the functionalities of cognitive radio can be divided into the following four categories: spectrum sensing, spectrum management, spectrum mobility and spectrum sharing. Spectrum sensing is one of the main challenging concepts in cognitive radio. It involves the accurate sensing of the spectrum usage and detection of primary users in the surroundings. The sensing must be carried out across all radio dimensions, i.e. time, frequency, space and code. Spectrum sensing mechanisms are not addressed further in this thesis. More information on spectrum sensing algorithms and the associated challenges can be found in the literature [78–80]. On the other hand, spectrum management handles the task of spectrum allocation and spectrum access. Spectrum allocation involves assigning the unused or under-utilized parts of the spectrum to cognitive users subject to meeting pre-set constraints. Further, the spectrum access is responsible for adapting the PHY-layer parameters such as transmit power and rate according to the predetermined interference and QoS constraints. Moreover, the cognitive radio network must consider the probability of a change in the primary spectrum activity at any time. For example, the primary users may reoccupy the spectrum, hence, the cognitive users must redirect their operating frequency to the secondary spectrum when required, otherwise they must be dropped in order to avoid degrading the primary service. This is done through spectrum mobility techniques. Finally, the task of devising fair and efficient shared-spectrum strategies is handled by *spectrum sharing* algorithms.

Spectrum sharing algorithms can be characterized into two centralized and distributed categories. In the latter, cognitive users are permitted to handle the task of spectrum allocation and access themselves, whereas the former achieves the spectrum sharing task through a centralized unit. Moreover, spectrum sharing strategies, based on their behaviour, are divided into cooperative and non-cooperative cases. In the former, cognitive users share information with each other, whereas in the latter, no information is exchanged between secondary users.

Furthermore, spectrum sharing strategies, based on spectrum access approach, are divided into two classes: access-limited (AL) and interference-limited (IL) opportunistic spectrum access (OSA). IL-OSA allows primary spectrum access to cognitive users subject to interference threshold constraints on the primary receiver. Cognitive users in IL-OSA cannot intervene with the primary service operation, in other words they must not cross the maximum allowed interference limit. Hence, cognitive users in IL-OSA typically operate at low transmit powers, particularly when the sensing of primary users' activity is inaccurate. On the other hand, AL-OSA method provides opportunistic access only to idle parts of the primary spectrum, given these spectrum holes are accurately sensed to be inactive. Therefore, in theory, cognitive users in AL-OSA can fully exploit the spectrum holes by transmitting with high power. However, it is important to take into account the imperfectness of sensing mechanisms in practice. As a result the system must take into account the misdetection probability, i.e. detecting an occupied part of the spectrum as idle, and the false alarm probability, i.e. detecting a spectrum hole as busy. The challenges associated with opportunistic spectrum access techniques are widely considered in the literature [80–83].

It is beneficial to consider parameters from different layers of the protocol stack to devise efficient and effective spectrum sharing strategies. Particularly because parameters from different OSI network layers play an important role in carrying out the cognitive radio functionalities. In a part of Chapter 4, a shared-spectrum heterogeneous OFDM/CDMA network is considered. By employing AL-OSA, a joint PHY-layer and DLL optimization algorithm is proposed to dynamically allocate the idle parts of a primary spectrum to secondary users, based on random variations in the number of secondary and primary users. The goal is to maximize the total deliverable throughput of a secondary service by exploiting the inactive parts of the primary spectrum. Devising spectrum sharing strategies among 3G and 4G networks is of great importance, particularly because the transition of upgrading the current 3G UMTS to 4G-LTE is expected to take many years. Integration of these technologies into a common platform can go a long way towards improving connectivity and performance, whilst reducing communication costs.

1.7 Thesis Aims and Contributions

This thesis concentrates on radio resource management techniques to enhance the performance of heterogeneous cellular mobile networks over fading channels by means of cross-layer design and optimization. The primary emphasis is on the PHY-layer design, with the interaction between this layer and higher layers, specifically, the DLL. The parameters under consideration include transmission power, transmission rate, automatic repeat request and packet error rate, while constraints on average transmission power and target packet error rate are imposed. Frequency -flat and -selective fading channels with maximum ratio combining RAKE receiver are considered. Cross-layer strategies, coupling PHY-layer and DLL parameters, are proposed in the context of uplink transmission in multi-user single- and multi- service mobile communication systems. Further, a joint PHY-layer and DLL resource allocation algorithm for heterogeneous OFDM/CDMA networks with opportunistic spectrum access is proposed. One- and multi- dimensional discrete Markov chains are used to model the number of active users according to specifications of the supported services. The organization of this thesis is as follows:

In Chapter 1, a survey on the fundamental concepts of current and future emerging cellular mobile networks is conducted. I highlight the main challenges associated with the networks under consideration and provide a brief overview of the relevant techniques undertaken towards tackling these obstacles. Subsequently, research goals and methodologies are addressed.

Chapter 2 makes several contributions. Firstly, a novel cross-layer design technique, jointly optimizing closed-loop power control, transmission rate and error control, is proposed. The primary goal is to maximize the effective throughput of a multi-user CDMA-based cellular mobile network. Secondly, a closed-form expression for the optimum OLPC SNR-target is derived and joint optimization of outer-loop power control, variable spreading factors and truncated-ARQ, is facilitated. Average power and target packet error rate constraints are imposed to maintain transmission costs, quality and effectiveness. The other goal is to show through theoretical and simulation results that, using this joint optimization technique, for

a given target packet error rate, adapting the spreading factor to the optimum outer-loop SNR-target, a function of MAI, can realize a significant gain in system effective throughput. Maximum achievable throughput, and improvements achieved relative to a 'constant SNR-target' case, the 'optimized PHY-layer based variable SNR-target' scheme in [84], and the 'optimized VSF' system in [85], are demonstrated for various sets of system parameters. The research conducted in Chapter 2, led to the following publications [86, 87]:

[**86**] **A. Shojeifard**, F. Zarringhalam and M. Shikh-Bahaei, "Joint Physical Layer and Data Link Layer Optimization of CDMA-Based Networks," *Wireless Communications, IEEE Transactions on*, vol. 10, no. 10, pp. 3278-3287, Oct. 2011.

[**87**] **A. Shojeifard**, F. Zarringhalam and M. Shikh-Bahaei," "Packet Error Rate (PER)-Based Cross-Layer Optimization of CDMA Networks, *Global Telecommunications Conference (GLOBECOM 2011), 2011 IEEE*, pp. 1-6, Dec. 2011.

In Chapter 3, the proposed cross-layer optimization scheme is extended and analysed for frequency-selective channels. The objective is to derive a closed-form expression for the optimum OLPC SNR-target expression in presence of multipath fading with MRC RAKE receiver. The optimal spreading factor using the optimum OLPC SNR-target is selected at the PHY-layer, which satisfies the QoS imposed for the PER with truncated-ARQ retransmissions at the DLL. I assume random arrival times for new users within a frame, and consider discrete spreading factors as a practical case. A considerable gain in sum-throughput is achieved through joint optimization of PHY-layer and DLL variables, over multipath fading channels. The work carried out in Chapter 3, led to the following publications [88, 89]:

[**88**] **A. Shojeifard** and M. Shikh-Bahaei, "Cross-Layer Design and Optimization of CDMA Networks in Frequency-Selective Fading Channels," *Wireless Communications Letters, IEEE*, vol. 1, no. 6, pp. 605-608, Dec. 2012.

[**89**] **A. Shojaeifard**, F. Zarringhalam, M. Shikh-Bahaei, "Throughput-Optimal Cross-Layer Resource Allocation in DS-CDMA Systems with Nakagami Multipath Fading," *Personal Indoor and Mobile Radio Communications (PIMRC 2011)*, pp. 1526-1530, Sep. 2011.

In Chapter 4, firstly, the problem of maximizing the sum-throughput of a multi-service cellular mobile network, in the presence of MAI, is investigated. The goal is to extend the cross-layer analysis to a multi-service system of heterogeneous data traffic. A multi-dimensional Markov chain is used to model the number of users in each service. According to the service specifications of the classes, we derive unique optimum OLPC SNR-targets and hence optimal spreading factor expressions, as functions of the number of active users in system. Distinct DLL QoS constraints are imposed on each service, with different target packet error rates, maximum number of retransmissions and traffic loads. Sum-throughput performance and the improvements achieved, relative to the non-optimized case, are demonstrated with theoretical and simulation results for various sets of the network parameters. The idea behind this work was incorporated in the following submissions [90, 91]:

[90] A. Shojeifard and M. Shikh-Bahaei, "Joint Physical Layer and Data Link Layer Optimization of Multi-Service Networks," *Wireless Communications Letters, IEEE, submission under 2nd round of review*, pp. 1-4, Sep. 2012.

[91] A. Shojeifard and M. Shikh-Bahaei, "Cross-Layer Design and Optimization of Multi-Service CDMA Networks," *VTC, 2013 Proceedings IEEE, submission under review*, pp. 1-7, Aug. 2012.

Next in Chapter 4, a dynamic spectrum sharing algorithm with cross-layer design for multi-user heterogeneous OFDM/CDMA networks is proposed. Using access-limited opportunistic spectrum access, the unused parts of a primary OFDM spectrum are dynamically allocated to secondary CDMA users, based on random variations in the number of secondary and primary users. The main goal is to maximize the total deliverable secondary throughput, by exploiting the inactive parts of the primary spectrum, effectively minimizing MAI and hence transmitting at higher power and rate. Average power constraints on secondary-secondary and cognitive (i.e. secondary-primary) users are imposed to ensure effective and efficient performance in both primary and secondary services. The optimal achievable secondary sum-throughput expression using the dynamic cross-layer shared-spectrum algorithm, is formulated based on randomly-varying number of primary and secondary users. Distinct one-dimensional discrete Markov chains are used to model

the number of active users in the OFDM and CDMA cells. The following papers endorse the work conducted in this part of the chapter [92, 93]:

[92] A. Shojeifard, M. M. Mahyari and M. Shikh-Bahaei, "Cross-Layer Design with Dynamic Resource Allocation in Heterogeneous Cognitive Radio Networks," *ICC, 2013 Proceedings IEEE, submission under review*, pp. 1-5, Sep. 2012.

[93] A. Shojeifard and M. Shikh-Bahaei, "Cross-Layer Design and Optimization of Shared-Spectrum Heterogeneous Networks," *Wireless Communications, IEEE Transactions on, to be submitted in Jan. 2013.*

As well as the following submission, which is not included in this thesis [94]:

[94] M. M. Mahyari, **A. Shojeifard** and M. Shikh-Bahaei, "Probabilistic Optimization of Shared-Spectrum Wireless Communication Systems," *Wireless Communications Letters, IEEE, submission under review*, pp. 1-4, Jan. 2013.

Chapter 5 provides a summary of conclusions and contributions of this thesis. Finally, ample suggestions for future research are included at the end of Chapter 5.

What can be asserted without proof can be dismissed without proof.

Christopher Hitchens

Chapter 2

Joint Physical Layer and Data Link Layer Optimization of CDMA-based Networks

2.1 Introduction

Effective and efficient resource allocation strategies are vital in achieving desirable performance in DS-CDMA systems. The significance of this concept is heightened by the need for accommodating multiple classes of traffic (e.g. voice, data, and compressed video) with different QoS requirements. In particular, QoS provisioning in 3G networks with Femto-cell layers requires more efficient techniques for allocation of limited resources [95–98].

Adaptive resource allocation methods have been widely considered in the last decade. These schemes exploit the time-varying nature of wireless channel in order to manage resources optimally, yielding better throughput. Typical adaptive techniques in CDMA systems include adaptive transmitter power [99–104], adaptive rate modulation [105–108], adaptive coding [109–112], adaptive spreading factor [85,113–115], or any combination of these methods [113,116,117]. In addition, cross-layer optimization techniques have been considered in the last decade for guaranteeing QoS requirements in different layers of wireless CDMA systems [75,118–120]. Further, cross-layer design techniques enable joint optimization of transmission pa-

rameters across different layers of the communication network which can significantly improve performance.

As discussed in Chapter 1, power control is the established mechanism to combat the near-far phenomenon in CDMA systems, and helps to minimize interference in the air interface so as to provide the necessary QoS for all users [121–123]. In the uplink, the closed-loop power control mechanism is a combination of ILPC and OLPC. The fast ILPC is SNR-based, if the estimated received SNR is below/above the SNR-target, the user is commanded to increase/decrease the transmit power. OLPC determines the SNR-target used by ILPC[1]. The SNR-target is set to cater for QoS requirements in the current channel state and is commonly decided from the results of CRC. The objective of OLPC is to provide the required transmission quality, generally defined in terms of BER or block error rate (BLER), by setting the SNR-target accurately. The determination of the SNR-target is highly capacity-sensitive. For instance, increasing it diminishes the probability of violating QoS requirements, but costs extra power and increases interference, which in turns leads to capacity loss [124, 125].

By far, most of the closed-loop power control algorithms found in the literature focus on ILPC issues. They usually overlook OLPC, assuming the SNR-target is a constant [126, 127], or equivalently assuming perfect SNR estimation [128], i.e. perfectly working OLPC (without analyzing its functioning). Indeed, if the ILPC is perfect, fading and shadowing effects are completely mitigated, hence, the channel turns into an AWGN channel and there is no need for the OLPC. However, due to highly-variable nature of wireless links, the ILPC cannot track the variations in power perfectly, hence, the SNR-target must be adapted to the channel state. Different propagation conditions, power delay profiles, mobile user speeds, number of users, and etc, will need different (adaptive) SNR-target setpoints in order to satisfy the prescribed QoS. OLPC is therefore essential for dynamic minimization of the power link margins and avoiding capacity degradations induced by the ILPC systematic use of static link margins. SNR-target setting in practical systems is performed

[1]In UMTS standards, ILPC operates at the slot level and OLPC operates at the frame level where the duration of one frame is 10 ms, and there are 15 slots in each frame [19].

at frame level. At a higher frequency, at slot level, total [31, 121, 122, 129], or truncated [104, 130] channel inversion power control policies are used in the inner-loop to adjust transmit power to short-time channel variations. In [131], it was assumed that the outer-loop SNR-target can be modeled as a log-normal random variable. A number of simulation-based studies examine performance improvements achieved by optimizing OLPC, e.g. [132–137]. In practice, predefined look-up tables are used to determine the appropriate SNR-target according to the obtained BER/BLER. This BER-based method accommodates for the quality requirements of users; however, it does not achieve optimal throughput. In [108], the BER-based joint optimization of constellation size and OLPC was considered. A higher spectral efficiency was achieved relative to the SNR-based variable-rate variable-power scheme of [116]. Adaptive rate and power schemes based on imperfect estimation of BER were studied in [138]. Optimizing the OLPC SNR-target and variable spreading factor (VSF), by considering physical layer only, was studied in [84].

On the other hand, there are inevitably erroneous packets at the receiver. The truncated-ARQ error control mechanism, where the maximum number of retransmissions is capped, is employed for throughput enhancement over fading channels. Truncated-ARQ protocols have been widely employed to compensate for throughput loss and to minimize buffer sizes and delays [75, 76, 139]. The maximum number of retransmissions delay limit, a function of the tolerable packet error rate, can be analytically computed by dividing the maximum tolerable system packet error rate over the round-trip delay time (RTD) of transmitted packets. In [140], an scheme for deriving the optimum maximum number of retransmissions over wireless channels is proposed. As previously discussed in Chapter 1, there is a trade-off between the achievable throughput and delay. A small number of retransmissions generally yields higher throughput-delay gains, however, the improvement is diminished as the number of retransmissions increases. In particular, in services with high-delay constraints, such as voice or video, a large number of retransmissions may highly degrade the quality of experience (QoE).

In this chapter, OLPC is explicitly included in a cross-layer optimization process. Given an ARQ delay limit, and for a prescribed maximum packet loss rate in the

DLL, we derive the optimum OLPC SNR-target set-point and adaptive spreading factor in the PHY-layer, analytically as functions of the number of active users in the cell. This methodology is in line with practical UMTS where the LC unit controls the network traffic load, a function of the number of active users in the system [19]. The optimality is, in this sense, maximizing the system effective throughput. The number of users in the system is modeled with a discrete Markov chain.

The main contribution of this chapter is in maximizing the system effective throughput by joint optimization of OLPC and VSF in PHY-layer whilst satisfying DLL QoS constraints. In particular, to the best of author's knowledge, this is the first time to mathematically derive the optimum SNR-target in a multi-user scenario by incorporating cross-layer variables. Due to different operating and modeling assumptions, our results are different from results obtained in the preceding research.

The reminder of this chapter is as follows. Section 2.2 presents the proposed system model and operation assumptions. In Section 2.3, the analysis for throughput optimization is provided. Section 2.4 presents numerical and simulation results and highlights the advantages of the proposed scheme. In Section 2.5, concluding comments on the throughput performance of the proposed cross-layer system are presented, and finally Section 2.6 summarizes the chapter and its contributions. A summary of the notations used in this chapter is provided in Appendix A, Table I.

2.2 System Model and Operation Assumptions

This section outlines the proposed system model and describes the approach to maximizing system effective throughput, subject to satisfying pre-defined QoS constraints. System effective throughput is defined as the average rate of successfully transmitted packets over the total packet rate. The focus is on the uplink of a single-cell conventional cellular DS-CDMA communication system, and it is assumed that a single BS, situated in the centre of the cell, receives communication signals from Uniformly-distributed mobile users. Asynchronous operation is also assumed.

The block diagram shown in Fig. 2.1 illustrates the selection of parameters used for the proposed system. Each mobile user (source) generates a sequence

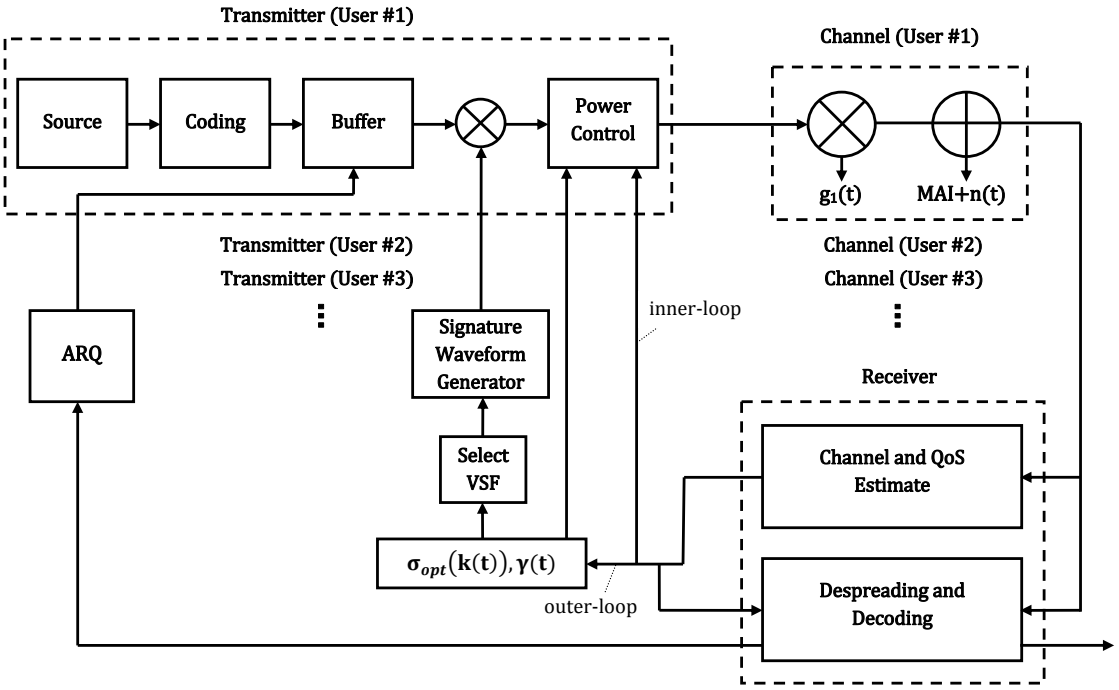

Figure 2.1: Block diagram of the proposed cross-layer optimization scheme. The diagram depicts the inner- and outer- loop power control schemes that adapt, respectively, transmit power and optimum OLPC SNR-target (hence spreading factor) to channel variations, number of users, and the requisite target packet error rate.

of fixed-length packets of length L bits, where L depends on the source. These packets enter the buffer after coding[1]. The buffer contents[2] are then converted to DS-CDMA signals using a spreading factor, $N(k(t); PER_{target})$, where $k(t)$ is the number of users at time t for a given target packet error rate (PER-target), PER_{target}. The parameter PER_{target}, is set according to the desired packet error rate quality which is required by the users in the cell. The chip rate is kept constant. The spreading is done over bandwidth B with Nyquist data pulses, $B = 1/T_c$, where, $T_c = T_b/N(k(t); PER_{target})$, is the chip duration, and T_b is the bit duration.

The channel is frequency-flat and time-varying with stationary gain $g_i(t)$ for the i-th user. During transmission, zero-mean AWGN, $n(t)$, with a two-sided power spectral density, $N_0/2$, is added to the binary phase shift keying (BPSK)-modulated signal. The only interference present in the cell is assumed to be multiple access

[1]Coding issues are not addressed in this thesis.

[2]To simplify the analysis, the probability of packet loss due to packet drop in queue is assumed to be zero. In practice, the packets arriving when the buffer is full, will be dropped from the queue.

interference, generated by other active users.

For sufficiently large number of users in the cell, central limit theorem [63] can be invoked to show that MAI at the receiver is asymptotically normal with zero mean [54, 141]. Central limit theorem for BER estimations in CDMA systems has been widely used and has been shown to provide accurate results even for small number of active users (< 10) for BER $\leq 10^{-3}$ [141, 142]. Let $S_i(\gamma_i(t), k(t))$ denote the adaptive transmit signal power of the i-th user at time t. $E[S_i]$ is the corresponding average transmit signal power of user-i, where

$$\gamma_i(t) = \frac{|g_i(t)|^2 E[S_i]}{N_0 B} \tag{2.1}$$

corresponds to the instantaneous received SNR for a constant transmit power $E[S_i]$. In Chapter 3, with appropriate adjustments, we extend the analysis for frequency-selective channels with maximum ratio combining coherent RAKE receiver.

Due to significance of near-far effect in CDMA systems, it is vital to apply an efficient power control scheme so that the users' received SNRs at the BS remain equal. Hence, here we assume that the centralized power control mechanism maintains a uniform value for $\gamma_i(t)$, for all users [143]. Moreover, the proposed system is assumed to support a single-class of services, therefore all active users are assumed to have the same SNR-target requirements. For this reason and for brevity, subscript i is hereafter removed from $\gamma_i(t)$. Also, all further time references are omitted for stationary channel conditions. As we will illustrate in Chapter 4, the single-class analysis can be extended for multiple classes of traffic, providing that unique QoS constraints of different services are satisfied.

In this work, the assumption is that the *optimum* OLPC SNR-target, $\sigma_{opt}(k)$, which maximizes the throughput under packet error rate, PER, and transmit power constraints, is set and adjusted in the outer-loop according to the number of active users. This is in line with the power control process in practical CDMA systems, where the OLPC controller uses information provided by the LC unit in order to update the SNR-target [19]. According to $\sigma_{opt}(k)$ and PER_{target}, the relevant spreading factor is selected at frame level, and the signature waveform is generated. Each

physical layer frame may contain dynamic traffic from the data link layer. We also assume that transmit power $S_i(\gamma, k)$ in the inner-loop is adapted to γ and k, at slot level with a higher frequency than outer-loop power control [33, 144], through the channel inversion power adaptation policy in order to attain $\sigma_{opt}(k)$. The total channel inversion policy[1] [31]

$$\frac{S_i(\gamma, k)}{E[S_i]} = \frac{\sigma_{opt}(k)}{\gamma} \tag{2.2}$$

requires a large transmit power during deep fades. Hence, truncated channel inversion policy [104]

$$\frac{S_i(\gamma, k)}{E[S_i]} = \begin{cases} \frac{\sigma_{opt}(k)}{\gamma} & \gamma > \gamma_0 \\ 0 & \gamma \leq \gamma_0 \end{cases} \tag{2.3}$$

is practically preferred for a given threshold value γ_0.

At the BS, the signal goes through a matched-filter detector for despreading. After despreading and decoding the received packet, the receiver may, due to erroneous bits, request a retransmission. This is done through the truncated-ARQ scheme with a maximum number of retransmissions, η [75, 76]. Perfect channel estimation is assumed at the receiver, as is an error-free feedback path between the receiver and the transmitter.

2.3 Analysis

In this section, there is firstly a formulation of the PER-target as a function of the maximum number of ARQ retransmissions allowed as well as the target packet loss rate. Next, the spreading factor is derived in terms of the SNR-target. System throughput is then defined and the optimum SNR-target to maximize it is obtained. Using this optimum SNR-target value, the optimal spreading factor can be chosen, where optimality means maximizing system effective throughput.

[1]This equation has been used in [31] for a constant received SNR. However, in our adaptive scheme we have assumed $\sigma_{opt}(k)$, an SNR-target that is adaptive to the number of active users.

2.3.1 PER and Spreading Factor Formulation

If block codes with r-bit error correction capability are used, the PER can be written as [145]:

$$PER = 1 - \sum_{\alpha=0}^{r} \left(\begin{array}{c} L \\ \alpha \end{array} \right) (BER)^{\alpha}(1 - BER)^{L-\alpha}. \tag{2.4}$$

Recall that L denotes packet length. Considering that BER is expected to be small, it was proven in [146] that the PER can be approximated by

$$PER \approx \frac{(BER)^{r+1}L!}{(r+1)!(L-r-1)!}. \tag{2.5}$$

In [16], it was shown that for Normally-distributed MAI at the receiver, under frequency-flat fading channels, SNR at the output of the matched-filter detector is given by

$$SNR = \left\{ \frac{k-1}{3N} + \frac{N_0}{2E_b\Omega} \right\}^{-1} \tag{2.6}$$

where N is the spreading factor, E_b denotes the bit energy and Ω indicates the reference user's path strength. As mentioned, Gaussian MAI is assumed due to central limit theorem for a large number of users. Hence, the preceding SNR formula is used; but, with notational revision. Firstly, $N(k; PER_{target})$ is used instead of N; secondly, as far as the multiplication $|g_i(t)|^2 E[S_i]$ in (2.1) is concerned, with appropriate scaling of $E[S_i]$ we can assume that $E[|g_i(t)|^2] = 1$ [116]. Moreover, as the parameter Ω corresponds to the second moment of $g_i(t)$, i.e. $E[|g_i(t)|^2]$, in the adaptive transmission scheme, $\frac{E_b\Omega}{N_0/2}$ is replaced by the variable optimum OLPC SNR-target, $\sigma_{opt}(k)$.

Given that the noise is a zero-mean Gaussian process, using the matched-filter detector with BPSK modulation, we have, $BER = Q(\sqrt{SNR})$ [13], where $Q(\alpha) \triangleq \frac{1}{\sqrt{2\pi}} \int_{\alpha}^{\infty} e^{-u^2/2} du$. Therefore, BER is given by

$$BER = Q\left(\sqrt{\left[\frac{k-1}{3N(k; PER_{target})} + \frac{1}{\sigma_{opt}(k)} \right]^{-1}} \right). \tag{2.7}$$

Using the above BER expression and the upper bound of

$$Q(x) \leq \frac{1}{2} e^{-x^2/2} \tag{2.8}$$

we deduce

$$BER \leq \frac{1}{2} \exp\left\{ -\frac{1}{2} \left[\frac{k-1}{3N(k; PER_{target})} + \frac{1}{\sigma_{opt}(k)} \right]^{-1} \right\}. \tag{2.9}$$

That is, the worst case of BER, $BER \cong \frac{1}{2} e^{-x^2/2}$, is used as an approximation. Furthermore, from (2.5),

$$BER \approx \left[\frac{(r+1)!(L-r-1)!}{L!} PER \right]^{\frac{1}{r+1}}. \tag{2.10}$$

Using (2.10) and approximating BER with its upper bound from (2.9), which corresponds to the worst case of BER and therefore PER, we can write:

$$\left[\frac{(r+1)!(L-r-1)!}{L!} PER \right]^{\frac{1}{r+1}} = \frac{1}{2} \exp\left\{ -\frac{1}{2} \left[\frac{k-1}{3N(k; PER_{target})} + \frac{1}{\sigma_{opt}(k)} \right]^{-1} \right\} \tag{2.11}$$

and thus PER can be approximated as

$$PER = \frac{L!}{(r+1)!(L-r-1)!} \left\{ \frac{1}{2} \exp\left\{ -\frac{1}{2} \left[\frac{k-1}{3N(k; PER_{target})} + \frac{1}{\sigma_{opt}(k)} \right]^{-1} \right\} \right\}^{r+1}. \tag{2.12}$$

Recall that the maximum number of retransmissions allowed per packet is denoted by η. If a packet is not received correctly after η retransmissions, it is dropped and assumed to be lost. The value of η in practical systems is set according to the maximum delay that can be tolerated by each packet. Suppose the target packet loss rate after η retransmissions is denoted by Λ. Therefore, in order to satisfy the packet loss QoS constraint, we have:

$$PER^{\eta+1} \leq \Lambda. \tag{2.13}$$

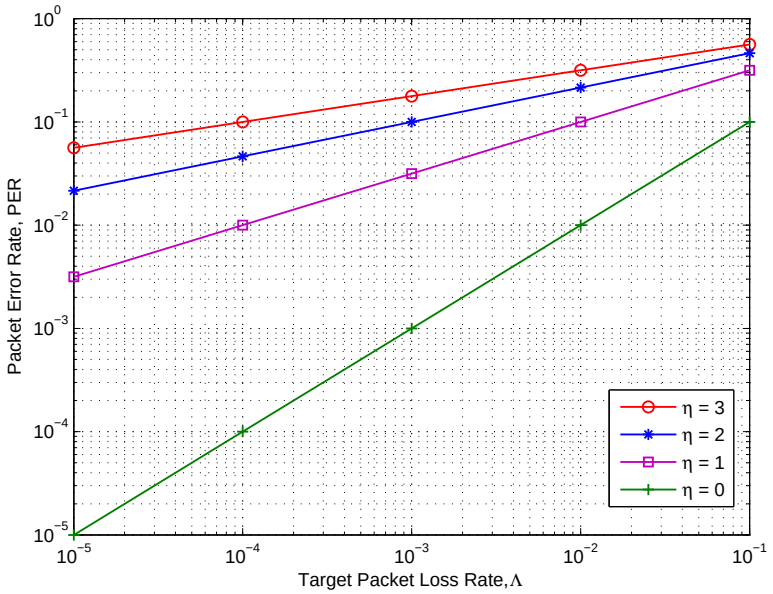

Figure 2.2: Packet error rate for various target packet loss rates, for different maximum number of ARQ retransmissions.

Hence,

$$PER \leq \Lambda^{\frac{1}{\eta+1}} := PER_{target}. \tag{2.14}$$

In Fig. 2.2, PER has been plotted versus target packet loss rate. It is observed that higher PERs are tolerable for a certain target packet loss rate when the maximum number of retransmissions is elevated. Using equations (2.12) and (2.14), we design the system for the worst case condition; where upper bound of PER is equal to PER_{target}, that is:

$$\begin{aligned} PER &= \frac{L!}{(r+1)!(L-r-1)!}\left\{\frac{1}{2}\exp\left\{-\frac{1}{2}\left[\frac{k-1}{3N(k;PER_{target})}+\frac{1}{\sigma_{opt}(k)}\right]^{-1}\right\}\right\}^{r+1} \\ &= \Lambda^{\frac{1}{\eta+1}}. \end{aligned} \tag{2.15}$$

The corresponding spreading factor can be obtained by solving (2.15) for

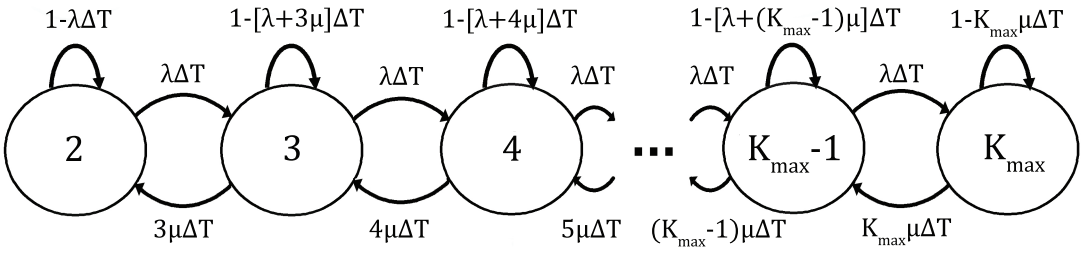

Figure 2.3: M/M/m/m queuing discrete-time Markov chain with $(K_{max}-1)$ states modeling the number of users in the single-service cell.

$N(k; PER_{target})$:

$$N(k; PER_{target}) = \frac{1}{3}\left\{ \frac{1}{\Psi} - \frac{1}{\sigma_{opt}(k)} \right\}^{-1} (k-1) \tag{2.16}$$

where

$$\Psi = -2\ln\left\{ 2\left[\frac{(r+1)!(L-r-1)!}{L!}\Lambda^{\frac{1}{\eta+1}} \right]^{\frac{1}{r+1}} \right\}. \tag{2.17}$$

It should be emphasized that the parameter PER_{target} in (2.16) and other formulas is considered as fixed and its value is given according to the desired PER for a specific service. The optimum values for spreading factor and SNR-target will be obtained, for this specific PER_{target}, as functions of the number of users k. Continuous-rate spreading factor adaptation is assumed. In practice, where adaptation is discrete, the closest spreading factor to the optimal value is selected.

The number of users in the cell is modeled by a $(K_{max}-1)$-state Markov process, as shown in Fig. 2.3, where $2 \leq k \leq K_{max}$. $\lambda = \lambda_k \Delta T$, $2 \leq k < K_{max}$ and $k\mu = \mu_k \Delta T$, $2 < k \leq K_{max}$, respectively, denote the probabilities of transitions occurring in a small time interval ΔT, corresponding to birth and death coefficients λ_k and μ_k, when there are k users in the cell. This design is for a multi-user system, hence, the case in which $k = 1$, is not considered. The Markov model under consideration corresponds to a M/M/m/m queuing system, which is widely employed in telephony networks [1].

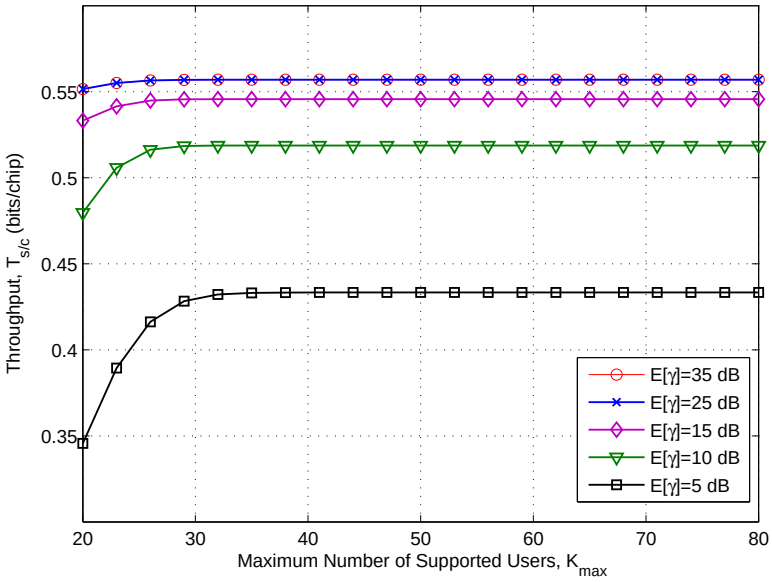

Figure 2.4: System throughput for a range of K_{max} values, $m' = 2$, $\lambda = 0.1$, $\mu = 0.005$, $\Lambda = 10^{-3}$, $\eta = 2$.

In practice, the choice of K_{max} is usually decided in such a way that it satisfies the QoS requirements of all provisioned users. In this work, for analytical convenience, K_{max} is not included in the optimization and a numerical value is assumed for it. Nevertheless, as shown in Fig. 2.4, the choice of K_{max} does not affect throughput results unless K_{max} is in the vicinity of the traffic load (channel utilization factor), λ/μ (in the figure, m' denotes the Nakagami fading parameter). For several average received SNRs, it is observed that for a traffic load of 20, the effective throughput value only changes with rising K_{max} up to approximately $K_{max} = 30$ (for the lowest $E[\gamma]$) and evens out thereafter. Looking at the results in Fig. 2.5 and Fig. 2.6 shows that the choice of K_{max} has also negligible effect on PER and η (i.e. maximum number of retransmissions which is an indicator of transmission delay) when K_{max} is well above the traffic load, λ/μ. Thus, the choice of K_{max} induces a bias (or, if so, a negligible negative bias) on our results. Numerical results indicate that for very large values of $K_{max}(> 250)$ no transmission can be performed with the typical parameters setting [147]. K_{max} values in that range are not used in this study.

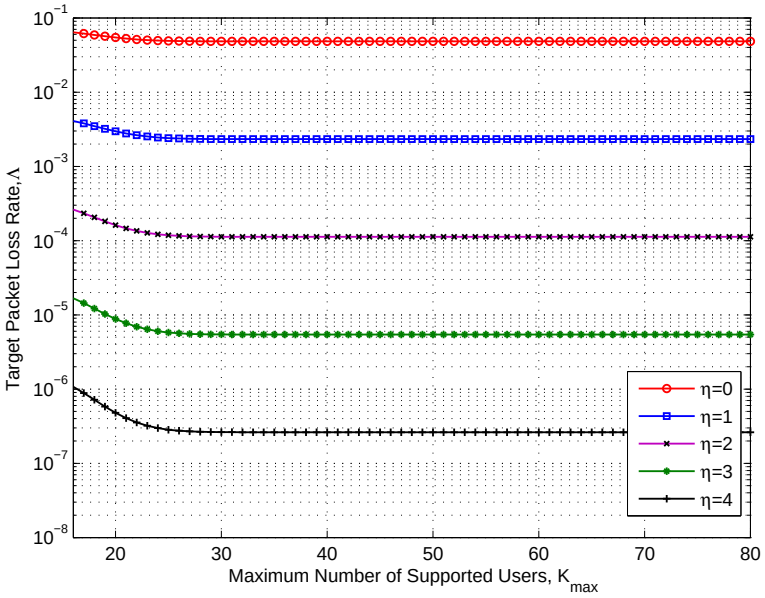

Figure 2.5: Target packet loss rate for a range of K_{max} values, $T_{s/c} = 0.53$, $E[\gamma] = 15$ dB, $m' = 2$, $\lambda = 0.1$, $\mu = 0.006$.

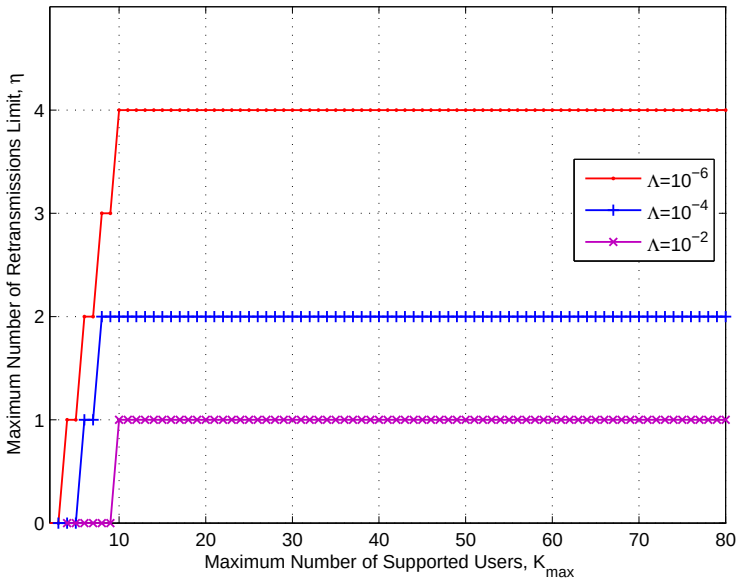

Figure 2.6: Maximum number of retransmissions delay limit for a range of K_{max} values, $T_{s/c} = 0.53$, $E[\gamma] = 15$ dB, $m' = 2$, $\lambda = 0.1$, $\mu = 0.006$.

2.3.2 Throughput Expression

For the proposed system, the effective throughput, $T_{s/c}$[1], can be calculated by

$$T_{s/c} = P_{k=2}\left[\frac{k}{N(k;PER_{target})} + \frac{P_k^{inc}(1-\epsilon)}{N(k;PER_{target})}\right]_{k=2} + \sum_{k=3}^{K_{max}-1} P_k\left[\frac{k}{N(k;PER_{target})} + \frac{P_k^{inc}(1-\epsilon)}{N(k;PER_{target})} - \frac{P_k^{dec}(1-\epsilon)}{N(k;PER_{target})}\right] + P_{k=K_{max}}\left[\frac{k}{N(k;PER_{target})} - \frac{P_k^{dec}(1-\epsilon)}{N(k;PER_{target})}\right]_{k=K_{max}} \quad \text{bits/chip} \tag{2.18}$$

where P_k is the probability that there are k active users in the cell, and P_k^{inc} and P_k^{dec} denote, respectively, the probability that the number of users increases or decreases by one. $\epsilon = \delta/T_f$, where T_f is duration of a frame, and new interfering user starts transmission δ seconds after the beginning of the frame. The probability of increase or decrease by more than one user within a frame is zero. Moreover, it is assumed that a change in the number of users can only occur at the beginning of a frame. That is, we assume that $\epsilon << 1$, and hence ϵ can be neglected in (2.18). Random arrival time for new users is considered in Chapter 3. The above throughput expression consists of three terms, respectively corresponding to events where there are 2 users, $k \in \{3, ..., K_{max} - 1\}$ users, or K_{max} users present in the system. The throughput expression in (2.18) can be simplified to

$$T_{s/c} = \sum_{k=2}^{K_{max}} P_k\left[\frac{k}{N(k;PER_{target})} + \frac{P_k^{inc}}{N(k;PER_{target})} - \frac{P_k^{dec}}{N(k;PER_{target})}\right] + \frac{P_2 P_k^{dec}}{N(k;PER_{target})_{k=2}} - \frac{P_{K_{max}} P_k^{inc}}{N(k;PER_{target})_{k=K_{max}}} \quad \text{bits/chip} \tag{2.19}$$

where $P_k^{inc} = \lambda$ and $P_k^{dec} = \mu k$. Denoting traffic load by $\rho = \lambda/\mu$, the probability of k active users in the cell is given by

$$P_k = \frac{\rho^{k-2}/k!}{\sum_{j=2}^{K_{max}}(\rho^{j-2}/j!)} \quad , \quad k = 2, 3, ..., K_{max}. \tag{2.20}$$

[1]The notation s/c stands for single-class; a multi class (m/c) scenario will be considered in a part of Chapter 4.

Hence, using (2.20) and (2.16), system effective throughput[1] can be expressed by

$$T_{s/c} = \frac{3}{\psi}\sum_{k=2}^{K_{max}} \frac{\rho^{k-2}}{k!(k-1)}[\lambda + (1-\mu)k][\frac{1}{\Psi} - \frac{1}{\sigma_{opt}(k)}] + \frac{3\mu}{\psi}[\frac{1}{\Psi} - \frac{1}{\sigma_{opt}(k)}]_{k=2} - \frac{3\lambda\rho^{K_{max}-2}}{\psi K_{max}!(K_{max}-1)}[\frac{1}{\Psi} - \frac{1}{\sigma_{opt}(k)}]_{k=K_{max}} \quad \text{bits/chip} \tag{2.21}$$

where

$$\psi = \sum_{j=2}^{K_{max}} \frac{\rho^{j-2}}{j!}. \tag{2.22}$$

2.3.3 Power Constraint

The following average power constraint is considered

$$\int_{\gamma} \sum_{k} S_i(\gamma, k) P_k p(\gamma) d\gamma \leq \rho E[S_i] \quad , \quad k = 2, 3, ..., K_{max} \tag{2.23}$$

where $p(\gamma)$ denotes the probability density function of γ. Using (2.2), the power constraint can be presented as

$$E[1/\gamma]\sigma_{opt}(k) k P_k \rho^{-1} \leq 1 \quad , \quad k = 2, 3, ..., K_{max}. \tag{2.24}$$

2.3.4 Throughput Optimization

The following optimization problem is considered by using (2.15), (2.21) and (2.24):

$$\underset{\sigma_{opt}(2),\sigma_{opt}(3),...,\sigma_{opt}(K_{max})}{\text{maximize}} \quad T_{s/c} \tag{2.25a}$$

subject to

$$C1 : E[1/\gamma]\sigma_{opt}(k) k P_k \rho^{-1} \leq 1 \quad , \quad k = 2, 3, ..., K_{max} \tag{2.25b}$$

$$C2 : PER = PER_{target}. \tag{2.25c}$$

[1]The throughput in (2.21) is derived based on continuous spreading factor and hence should be regarded as an upper-bound for practical cases with discrete spreading factors.

In order to derive the optimum SNR-target, $\sigma_{opt}(k)$, the Lagrangian optimization method is employed [148,149]. Concavity condition to use the Lagrangian method is proved in Appendix A. The Lagrangian function, $J(\sigma_{opt}(2), \sigma_{opt}(3), ..., \sigma_{opt}(K_{max}))$, is created using (2.25a)-(2.25c):

$$J(\sigma_{opt}(2), \sigma_{opt}(3), ..., \sigma_{opt}(K_{max})) = \frac{3}{\psi} \sum_{k=2}^{K_{max}} \frac{\rho^{k-2}}{k!(k-1)} [\lambda + (1-\mu)k][\frac{1}{\Psi} - \frac{1}{\sigma_{opt}(k)}] +$$
$$\frac{3\mu}{\psi}[\frac{1}{\Psi} - \frac{1}{\sigma_{opt}(k)}]_{k=2} - \frac{3\lambda\rho^{K_{max}-2}}{\psi K_{max}!(K_{max}-1)}[\frac{1}{\Psi} - \frac{1}{\sigma_{opt}(k)}]_{k=K_{max}}$$
$$+ \sum_{k=2}^{K_{max}} \phi(k) \left\{ E[1/\gamma]\sigma_{opt}(k) k P_k \rho^{-1} - 1 \right\} \tag{2.26}$$

where $\phi(k)$, $k = 2, 3, ..., K_{max}$, are the Lagrangian multipliers. Solving $\frac{\partial J}{\partial \sigma_{opt}(k)} = 0$ for $k = 2, 3, ..., K_{max}$ results in:

$$\sigma_{opt}(k) = \begin{cases} \sqrt{\frac{3\rho[\lambda+2]}{-4\phi(2)E[1/\gamma]P_2\psi}} & k = 2 \\ \sqrt{\frac{3\left\{\frac{\rho^{k-1}}{k!(k-1)}[\lambda+(1-\mu)k]\right\}}{-k\phi(k)E[1/\gamma]P_k\psi}} & k = 3, 4, ..., K_{max-1} \\ \sqrt{\frac{3\left\{\frac{\rho^{K_{max}-1}[1-\mu]}{K_{max}!(K_{max}-1)}\right\}}{-\phi(K_{max})E[1/\gamma]P_{K_{max}}\psi}} & k = K_{max}. \end{cases} \tag{2.27}$$

We use (2.20), the active constraints from (2.24), and the Kuhn-Tucker constraint qualification to solve $\frac{\partial J}{\partial \phi(k)} = 0$, for $k = 2, 3, ..., K_{max}$. Thus, $\phi(k)$, for $2 \leq k \leq K_{max}$, can be obtained as:

$$\phi(k) = \begin{cases} -3E[1/\gamma]P_2\rho^{-1}[\lambda+2]\psi^{-1} & k = 2 \\ -3E[1/\gamma]kP_k\rho^{k-3}[\lambda+(1-\mu)k]\left\{\frac{1}{\psi k!(k-1)}\right\} & k = 3, 4, ..., K_{max-1} \\ -3E[1/\gamma]K_{max}^2 P_{K_{max}}\rho^{K_{max}-3}[1-\mu]\left\{\frac{1}{\psi K_{max}!(K_{max}-1)}\right\} & k = K_{max}. \end{cases} \tag{2.28}$$

Replacing $\phi(k)$ into (3.17) yields the following optimum outer-loop SNR-target:

$$\sigma_{opt}(k) = \frac{\psi(k-1)!}{E[1/\gamma]\rho^{(k-3)}} \quad , \quad k = 2, 3, ..., K_{max}. \tag{2.29}$$

Using (2.29) in (2.21), system throughput for total channel inversion power adaptation policy can be expressed as:

$$T_{s/c} = \frac{3}{\psi}\sum_{k=2}^{K_{max}} \frac{\rho^{k-2}[\lambda+(1-\mu)k]}{k!(k-1)}\left\{\frac{1}{\Psi} - \frac{E[1/\gamma]\rho^{(k-3)}}{\psi(k-1)!}\right\} + \frac{3\mu}{\psi}\left\{\frac{1}{\Psi} - \frac{E[1/\gamma]\rho^{-1}}{\psi}\right\}$$
$$- \frac{3\lambda\rho^{K_{max}-2}}{\psi K_{max}!(K_{max}-1)}\left\{\frac{1}{\Psi} - \frac{E[1/\gamma]\rho^{(K_{max}-3)}}{\psi(K_{max}-1)!}\right\} \quad \text{bits/chip.} \tag{2.30}$$

To calculate the optimum SNR-target, $\sigma_{opt}^{tci}(k)$, when truncated channel inversion (tci) is employed, it is necessary to use $E[1/\gamma]_{\gamma_0}$ instead of $E[1/\gamma]$. The former is defined as:

$$E[1/\gamma]_{\gamma_0} = \int_{\gamma_0}^{\infty} \frac{1}{\gamma} p(\gamma) d\gamma. \tag{2.31}$$

Therefore,

$$\sigma_{opt}^{tci}(k) = \frac{\psi(k-1)!}{E[1/\gamma]_{\gamma_0}\rho^{(k-3)}}. \tag{2.32}$$

For tci, throughput can be calculated by multiplying $T_{s/c}$ by $p(\gamma > \gamma_0)$ and using $E[1/\gamma]_{\gamma_0}$ for $E[1/\gamma]$. Hence,

$$T_{s/c}^{tci} = T_{s/c} \times p(\gamma > \gamma_0) \quad \text{bits/chip.} \tag{2.33}$$

2.4 Numerical Results

This section presents theoretical and simulation results for the proposed cross-layer optimization scheme. These results are compared to those of a VSF and truncated-ARQ-assisted system where the OLPC SNR-target is not optimally exploited. Specifically, it is assumed that the OLPC in the *non-optimized* system selects the SNR-target based on the quality of the channel through the following expression [104]:

$$\sigma_{non-opt} = \frac{1}{E[1/\gamma]}. \tag{2.34}$$

Throughput improvement achieved by setting the SNR-target to its optimal value using the proposed approach is highlighted. Note that the average transmit power and the packet loss rate (or equivalently the PER-target) constraints were imposed

on the non-optimized system as well. In addition, we have compared our results to other state-of-the-art resource allocation algorithms. In particular, comparisons to the scheme in [84], where VSF and variable SNR-target are used by considering PHY-layer parameters only, and to the VSF-assisted scheme in [85], are made. In all of the above cases, continuous-rate spreading factor adaptation has been considered. Therefore, results serve as upper-bounds.

To obtain numerical results for system effective throughput, there is a need to specify $p(\gamma)$. The general Nakagami-m'[1] block fading model is considered for channel fading. Hence, γ would be Gamma-distributed:

$$p(\gamma) = \frac{1}{\Gamma(m')} \left(\frac{m'}{E[\gamma]} \right)^{m'} \gamma^{(m'-1)} e^{\frac{-m'\gamma}{E[\gamma]}} \quad , \quad \gamma \geq 0 \tag{2.35}$$

where $\Gamma(\alpha)$ is defined by $\Gamma(\alpha) \equiv \int_0^\infty t^{\alpha-1} e^{-t} dt, \alpha > 0$, and m' denotes the Nakagami fading parameter. For analytical convenience, integer m' is assumed. For $m' \geq 2$, total channel inversion policy of (2.2) is used. For $m' = 1$, i.e. Rayleigh fading, however, (2.2) is not suitable as it implies large transmit powers, and therefore the truncated channel inversion policy defined in (3.3) is employed. It can be shown that $E[1/\gamma]$ and $E[1/\gamma]_{\gamma_0}$, corresponding to total and truncated channel inversion policies, respectively, are defined by $E[1/\gamma] = \frac{m'}{(m'-1)E[\gamma]}$ and $E[1/\gamma]_{\gamma_0} = \frac{-Ei(-\gamma_0/E[\gamma])}{E[\gamma]}$, where $Ei(\alpha) \triangleq -\int_{-\alpha}^{\infty} \frac{e^{-u}}{u}\, du$. Also, the probability of non-outage, $p(\gamma > \gamma_0)$, required to calculate the throughput for truncated channel inversion policy, is computed by:

$$p(\gamma > \gamma_0) = e^{-\gamma_0/E[\gamma]}. \tag{2.36}$$

Note that all results correspond to channel inversion, unless otherwise mentioned. Moreover, it is assumed that packet length, L, is 100 bits with $r = 7$ correctable bits. In [150], it was shown that this selection of values for L and r result in the topmost performance.

Fig. 2.7 illustrates the achievable effective throughput using the optimized scheme for several values of m', a target packet loss rate of 10^{-4}, and a maxi-

[1]For notational purposes, we have denoted the Nakagami parameter with m', instead of the conventional notation, m.

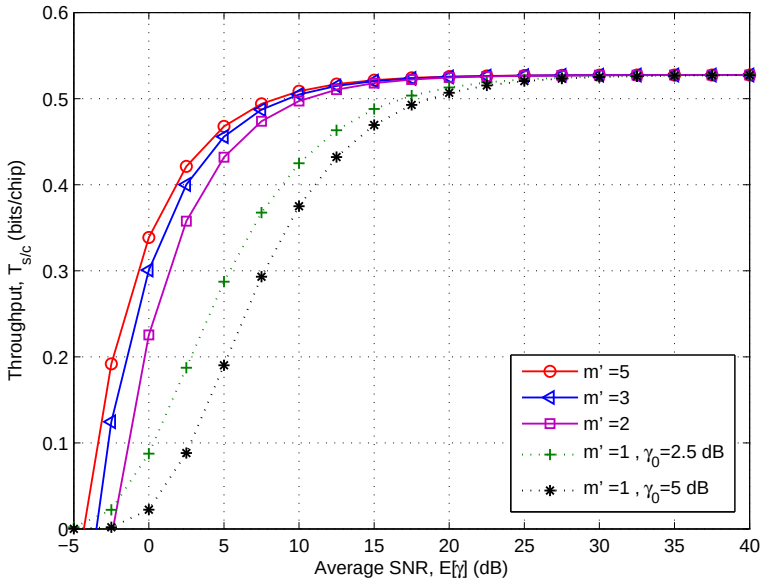

Figure 2.7: System throughput for different values of m' with different SNR threshold values, $\lambda = 0.1$, $\mu = 0.003$, $K_{max} = 50$, $\Lambda = 10^{-4}$, $\eta = 2$.

mum number of two retransmissions. It can be seen that as m' moves away from 1, higher throughput values can be realized. Also, a lower cut-off SNR, γ_0, yields better throughput. This is due to higher availability of SNRs that satisfy the non-outage condition, $\gamma > \gamma_0$. When the SNR drops below γ_0, the transmission is suspended due to outage and therefore the effective throughput is zero.

Fig. 2.8 illustrates the values selected for the spreading factor versus the number of active users in the system. Both optimal and non-optimal spreading factors are displayed for various η. Firstly, it is observed that for the same η, the optimal spreading factor is always smaller than the non-optimal one. This can be interpreted as higher transmission rate and throughput for the optimal case. Moreover, it is shown that increasing the maximum number of retransmissions causes a reduction in the value of the spreading factor, which translates to higher throughput.

The throughput rise by increasing η is depicted in Fig. 2.9. Throughput improvement, however, diminishes quickly; therefore, for $\eta = 5$ and $\eta = 6$ the throughput curves overlap.

In Fig. 2.10 optimal and non-optimal throughput values are displayed for various

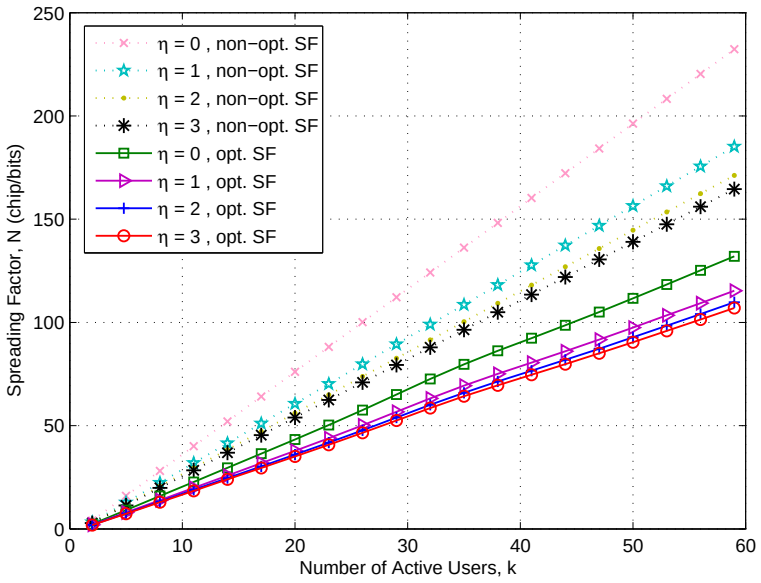

Figure 2.8: Optimal and non-optimal spreading factors as functions of the number of active users in the system for different traffics and retransmission numbers, $m' = 2$, $\lambda = 0.1$, $\mu = 0.003$, $K_{max} = 60$, $\Lambda = 10^{-3}$, $E[\gamma] = 15$ dB.

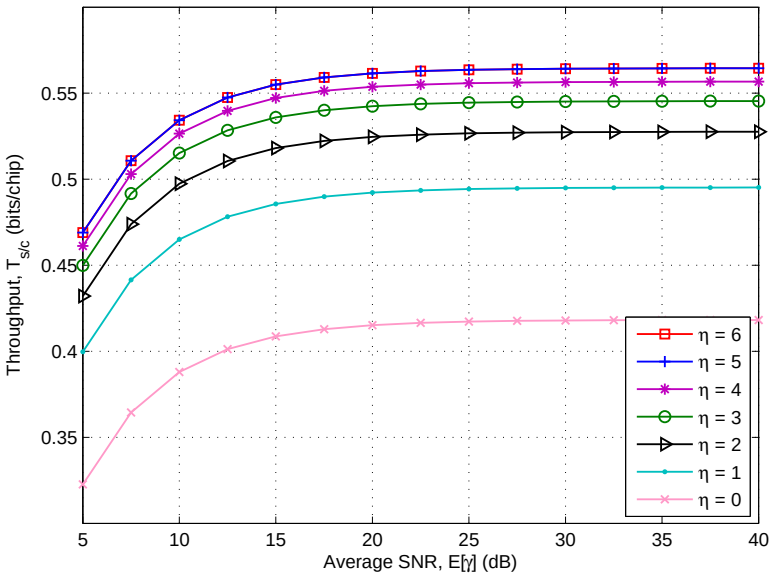

Figure 2.9: System throughput for different retransmission numbers, $m' = 2$, $\lambda = 0.1$, $\mu = 0.003$, $K_{max} = 50$, $\Lambda = 10^{-4}$.

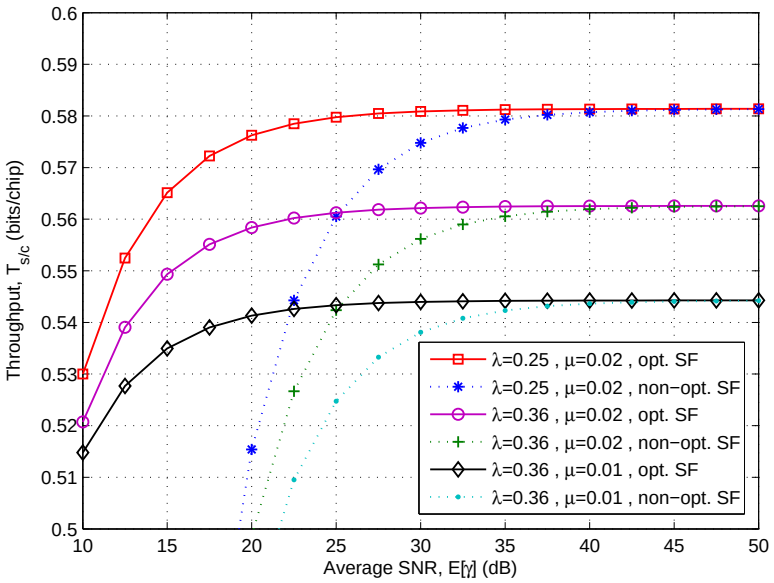

Figure 2.10: System throughput for various traffic densities, $m' = 2$, $K_{max} = 50$, $\Lambda = 10^{-3}$, $\eta = 2$.

traffic load (λ/μ) pairs. We observe that the proposed cross-layer optimization scheme always outperforms the non-optimal transmission. For instance, at 0.53 bits/chip throughput and $\lambda = 0.36$, $\mu = 0.01$ more than 13 dB gain in power is achieved. However, at higher SNRs optimal and non-optimal throughput values converge. Generally, for higher traffic loads throughput decreases. The reason is the higher MAI in the cell, which forces reduction in transmission rate in order to satisfy the PER QoS constraint.

Fig. 2.11 illustrates optimized and non-optimized throughput values for different target packet loss rates, while keeping the maximum number of retransmissions constant at two. In addition to the gains achieved by the optimized scheme over the non-optimized one, a more relaxed (higher) target packet loss rate yields higher throughput. For higher target packet loss rates, however, the throughput gain of the optimized scheme over the non-optimized one is marginally reduced. For example, at $E[\gamma] = 18$ dB and $\Lambda = 10^{-6}$, 25.1% throughput is gained; whereas the gain is reduced to 23.6% for $\Lambda = 10^{-4}$ and to 22% for $\Lambda = 10^{-2}$. Therefore, the proposed scheme produces better gains under more stringent quality requirements.

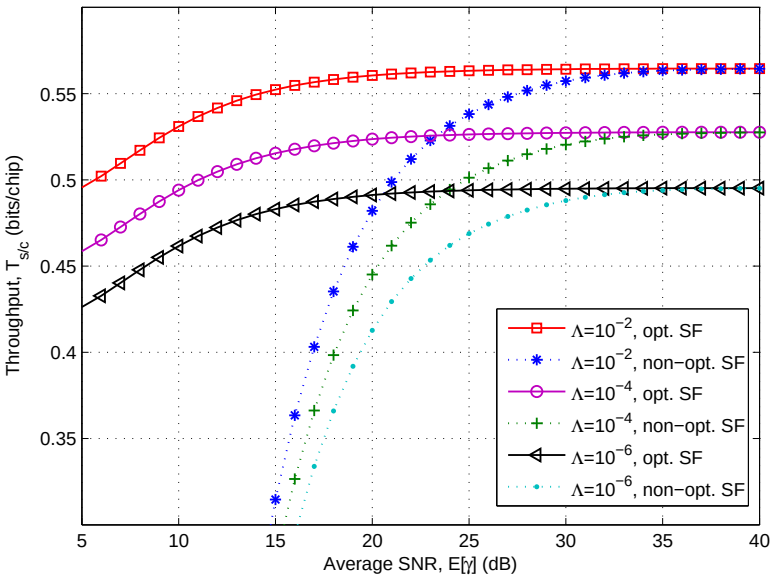

Figure 2.11: System throughput for various target packet loss rate scenarios, $m' = 2$, $\lambda = 0.1$, $\mu = 0.003$, $K_{max} = 50$, $\eta = 2$.

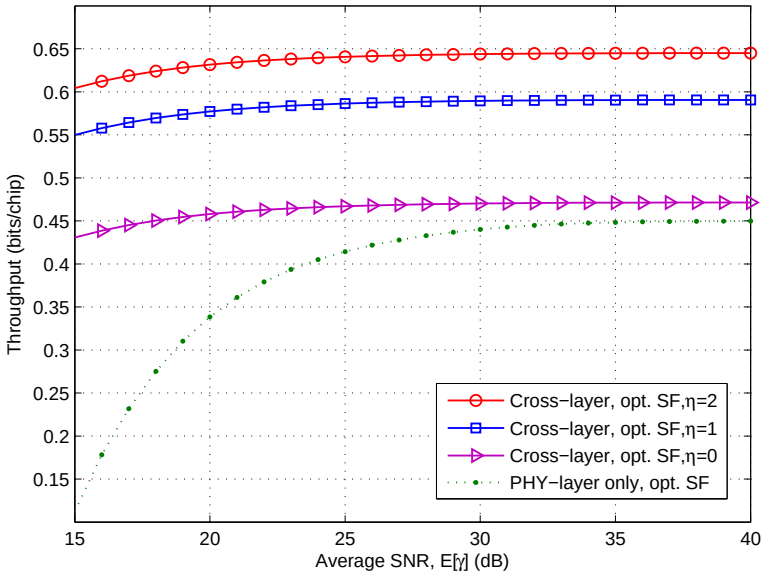

Figure 2.12: Comparison of optimized cross-layer throughput with an 'optimized PHY-layer only' scheme in [84], for different retransmission numbers, $m' = 2$, $\lambda = 0.1$, $\mu = 0.02$, $K_{max} = 50$, $\Lambda = 10^{-6}$.

In Fig. 2.12, the throughput values of our optimized cross-layer scheme, under different maximum number of retransmissions, is plotted versus the throughput performance of the scheme in [84], where a joint optimization of OLPC SNR-target and VSF in PHY-layer *only* is considered. In [84], the average throughput expression in equation (6), is provided only for one user. Therefore, in order to compare our throughput results with those in [84], we have obtained the aggregate throughput of all users at a given time based on the system model of [84]. Moreover, we made changes to the M/M/m queuing Poisson distribution model for the number of users in the PHY-layer approach, so that comparison with the cross-layer scheme would be possible. Common target packet loss rates, $\Lambda = 10^{-4}$, traffic loads, $\rho = 0.1/0.003$ and $K_{max} = 50$, under Nakagami frequency-flat fading channels with $m' = 2$, were considered for both systems. The results indicate that the cross-layer optimized system outperforms the 'optimized PHY-layer only' system even with zero number of retransmissions ($\eta = 0$). For instance, at $E[\gamma] = 25$ dB, the cross-layer scheme with $\eta = 1$ achieves 34.3% gain in throughput compared to the 'optimized PHY-layer only' scheme.

Fig. 2.13 illustrates the performance of our cross-layer scheme versus those of an 'optimized VSF scheme' proposed in [85], for different number of active users in the cell. The VSF scheme in 2.13, is derived over AWGN channels, hence, to make the comparison feasible we include the effects of fading [147], by reducing the throughput values in 2.13 (denoted with T_h) by an average of 25%. A zero average-SNR per chip, $E[\gamma_c] = 0$ dB, $\lambda = 0.35$, $\mu = 0.009$ and $\Lambda = 10^{-2}$ are assumed in both systems. It can be seen that the cross-layer scheme outperforms the VSF-assisted scheme even with zero number of retransmissions, $\eta = 0$. For higher η values, the achievable gain of our proposed cross-layer scheme over the 'optimized VSF scheme' is increased further.

Comparison of theoretical and simulation results for various settings of target packet loss rate and retransmissions number is demonstrated in Fig. 2.14. To carry out the simulation a multi-user scheme with similar conditions as in the theoretical case is considered. In particular, a practical frequency-flat *Nakagami-m shadowed* fading environment [28,151], with Log-Normal shadowing standard deviation of 4 dB

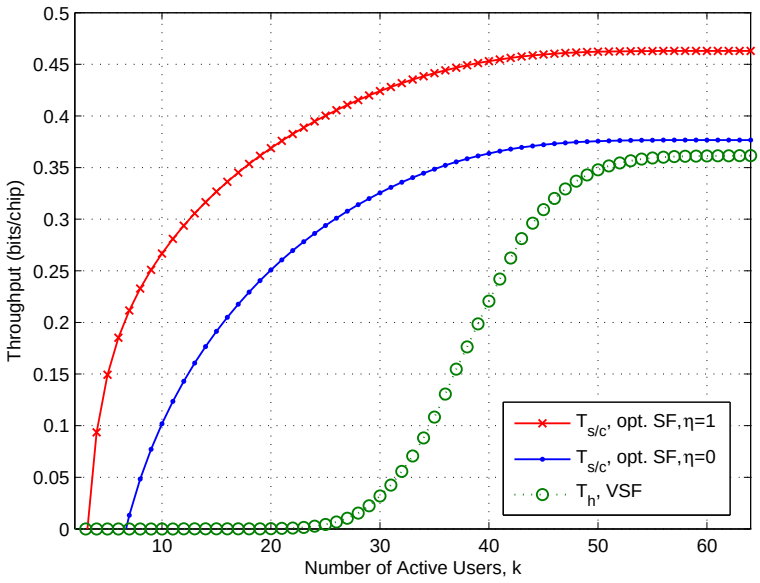

Figure 2.13: Throughput comparison of our optimized cross-layer scheme with an 'optimized VSF scheme' in [85], for different number of active users in the cell, $m' = 2$, $\lambda = 0.35$, $\mu = 0.009$, $K_{max} = 64$, $\Lambda = 10^{-2}$.

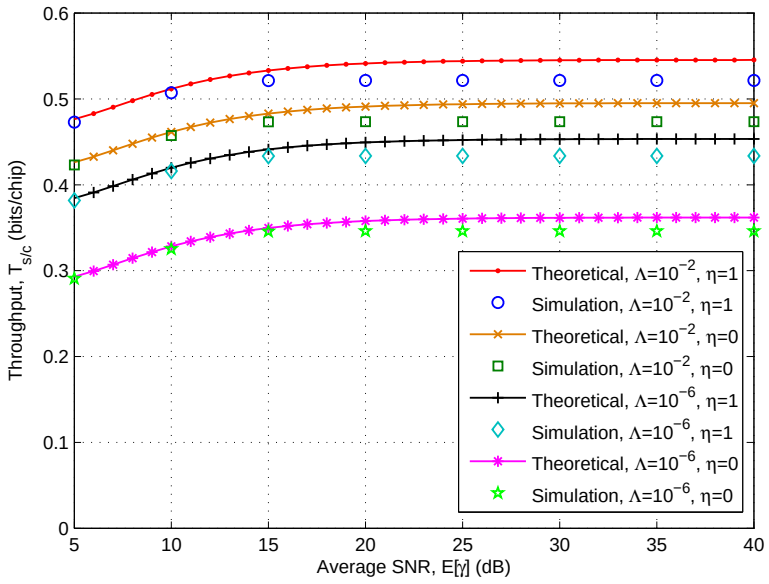

Figure 2.14: Comparison of theoretical and simulation results for various target packet loss rates and retransmission numbers, $m' = 2$, $\lambda = 0.1$, $\mu = 0.003$, $K_{max} = 50$.

and $m' = 2$, is studied. Hence, pdf of γ follows a composite Gamma/Log-Normal-distribution. It can be seen that the throughput values are degraded as a result of practical channel conditions. For higher average SNR values this degradation is increased. For instance, at $E[\gamma] = 10$ dB for $\Lambda = 10^{-6}$ with $\eta = 1$, the numerical throughput has 0.9% gain over the simulated throughput; the gain is increased to 3.5% at $E[\gamma] = 20$ dB. The reason is that the effect of shadowing on the performance is not as significant in lower SNR regions, where the channel quality is deteriorated, regardless.

2.5 Conclusions

A novel cross-layer optimization scheme was proposed to derive a closed-form expression for the optimum OLPC SNR-target and to facilitate joint optimization of outer-loop power control, variable spreading factors, and truncated-ARQ. Total and truncated channel inversion policies were implemented in the inner-loop power control. Truncated-ARQ was utilized as the error control mechanism in order to improve the throughput performance. Using this joint optimization technique, it was shown through theoretical and simulation results that, for a given target packet error rate, adapting the spreading factor to the optimum outer-loop SNR-target, a function of multiple access interference, can realize a significant gain in system effective throughput. We modeled the number of users with a one-dimensional discrete Markov chain. A considerable power gain was demonstrated by means of the proposed optimization technique. In addition, our proposed cross-layer scheme outperformed the jointly optimized outer-loop SNR-target with VSF scheme in PHY-layer [84], and the VSF scheme in [85].

Maximum achievable throughput, under continuous rate and power adaptation, and improvements achieved relative to the 'constant SNR-target' case, the 'PHY-layer based variable SNR-target' scheme in [84], and the VSF system in [85], all with continuous spreading factor adaptation, were demonstrated for various sets of system parameters. The enhanced performance was obtained without wasting power and without violating packet error rate constraints.

2.6 Contributions

Power control is the established mechanism for tackling the near-far phenomenon and minimizing the multiple access interference in UMTS standards. In practical CDMA systems, OLPC determines the target value of SNR at the receiver, mostly by using look-up tables to map bit error rates to SNR-targets. However, this does not achieve optimal throughput. In this chapter, transmission delay and target packet loss rate constraints in the data link layer were invoked in order to analytically determine the optimum outer-loop SNR-target setpoint in the PHY-layer, according to the number of active users in cell. Using the optimum SNR-target, the optimal spreading factor was determined and consequently optimal system throughput was obtained. At this point, the contributions of this chapter are summarized as follows:

- Joint optimization of outer-loop SNR-target and VSF, at the PHY-layer, with truncated-ARQ error control mechanism at the DLL was proposed.
- We show that QoS requirements at these layers, in terms of average transmit power and target packet loss rate constraints, can be simultaneously satisfied while maximizing effective throughput.
- Closed-form expression for the optimum OLPC SNR-target, and the corresponding optimal spreading factor solution, was derived for a single-service CDMA cell in the presence of Normally-distributed MAI.
- Mathematical formulations are derived for total and truncated channel inversion policies in the ILPC.
- The optimal effective throughput of a single-service CDMA cell, under continuous-rate power and rate adaptation, for the worst packet error rate case, was obtained using conventional matched-filter detection.
- System throughput performance was analysed over Nakagami-m' frequency-flat fading channels.
- The corresponding theoretical throughput, which can be regarded as upper-bound for discrete spreading factor case, is obtained numerically for various

settings of system parameters. Moreover, simulation results for practical fading channels are also provided.

- The number of active users in the cell is modeled with an M/M/m/m queuing one-dimensional discrete Markov chain.
- Our scheme is compared with 'constant SNR-target', 'PHY-layer based variable SNR-target' and 'VSF' cases -under continuous power and rate variation- to show the achievable gain through the coupling of PHY-layer and DLL parameters.
- Proof of convexity for optimization problem (2.25) is provided.

In the next chapter of this thesis, we extend our cross-layer optimization technique over frequency-selective fading channels with maximum ratio combining RAKE receiver.

2.7 Appendix A

2.7.1 Table I - Chapter Notation

Symbol	Definition
$k(t)$	Number of active users at time t
K_{max}	Maximum number of supported users
T_c	Chip duration
T_b	Bit duration
T_f	Frame duration
B	Bandwidth
$g_i(t)$	Channel gain for user-i at time t
$n(t)$	AWGN
$N_0/2$	Two sided power spectral density of AWGN
$\gamma_i(t)$	Instantaneous received SNR of i-th user
$S_i(\gamma_i(t), k(t))$	ILPC adaptive transmit signal power of user-i at time time t
$E[S_i]$	Average transmit signal power of user-i
γ_0	SNR threshold for truncated channel inversion policy
BER	Instantaneous bit error rate
L	Packet length
r	Number of bits in error correction mechanism
E_b	Bit energy
Ω	Reference user path strength
PER	Instantaneous packet error rate
PER_{target}	Target packet error rate
N	Spreading factor
$N(k; PER_{target})$	Adaptive spreading factor
η	Maximum number of retransmissions allowed per packet
Λ	Target packet loss rate
P_k	Probability that there are k active users in the cell
P_k^{inc}	Probability that the number of users increases by 1 within a frame
P_k^{dec}	Probability that the number of users decreases by 1 within a frame
δ	New user arrives δ seconds after the start of the frame
ϵ	Ratio of δ to the frame duration
ρ	Traffic load
$C1$	Average power constraint
$C2$	Target packer error rate constraint
$J(.,.,...,.)$	Lagrangian function
$\phi(k)$	Lagrangian multiplier for k users
$p(\gamma)$	Probability density function of γ
$E[\gamma]$	Average SNR
$E[\gamma_c]$	Average SNR per chip
$\sigma_{opt}(k)$	Optimum SNR-target with total channel inversion
$\sigma_{opt}^{tci}(k)$	Optimum SNR-target with truncated channel inversion
$T_{s/c}$	Throughput when total channel inversion policy is adopted
$T_{s/c}^{tci}$	Throughput when truncated channel inversion policy is adopted
$\sigma_{non-opt}$	Constant SNR-target in the non-optimized system
T_h	Throughput of the VSF scheme in [85]
m'	Nakagami fading parameter

2.7.2 Proof of convexity for optimization problem (2.25)

In this chapter, Lagrangian optimization method is used to derive $\sigma_{opt}(k)$, in order to maximize throughput, subject to average power and target packet error rate constraints. Objective function in (2.25a) and the constraint functions in (2.25b) and (2.25c) are required to be concave for this optimization method to produce an optimal value. In order to prove that objective function in optimization problem is concave in $\sigma_{opt}(k)$, where $k = 2, ..., K_{max}$, we derive the second derivative of $T_{s/c}$ with respect to $\sigma_{opt}(k)$, for $k = 2, ..., K_{max}$:

$$\frac{d^2T_{s/c}}{d\sigma^2_{opt}(k)} = \begin{cases} \frac{-6[\frac{\lambda}{2}+1]}{\psi\sigma^3_{opt}(2)} & k = 2 \\ \frac{-6\rho^{k-2}[\lambda+(1-\mu)k]}{\psi k!(k-1)\sigma^3_{opt}(k)} & k = 3, 4, ..., K_{max-1} \\ \frac{-6\rho^{K_{max}-2}[(1-\mu)K_{max}]}{\psi K_{max}!(K_{max}-1)\sigma^3_{opt}(K_{max})} & k = K_{max}. \end{cases}$$

We have $K_{max} \geq 2$ and $\rho \geq 0$, therefore according to equation (2.22), ψ takes on real positive values only. Moreover, from (2.22), $\sigma_{opt}(.)$ is always a non-negative real value. Also we note that λ and $k\mu$ in Fig. 2.3 are respectively the transition probabilities P_k^{inc} and P_k^{dec}, and therefore inequalities $k\mu \leq 1$ and $0 \leq \lambda \leq 1$ hold for $k \leq K_{max}$[1]. Hence $1-\mu > 0$ and $\lambda \geq 0$. Therefore, $\frac{d^2T_{s/c}}{d\sigma^2_{opt}(k)} < 0$ for $2 \leq k \leq K_{max}$ and the objective function in (25) is concave.

Also, the constraint functions in (2.25b) and (2.25c) are affine in $\sigma_{opt}(k)$ for $k = 2, ..., K_{max}$. Therefore the optimization problem (2.25) is a convex optimization problem and can be solved using the Lagrangian method.

[1] Although for practical reasons in this chapter we have used states $k \geq 2$ only, the theoretical values of k in general state-transition-diagram can be $'0'$ and $'1'$ as well.

Understanding is a kind of ecstasy.

Carl Sagan

Chapter 3

Cross-Layer Design and Optimization over Frequency-Selective Fading Channels

3.1 Introduction

There is still large room for improving the current 3G of wireless communication systems as CDMA-based radio access networks are expected to co-exist with the future 4G technologies for years to come. Therefore further improvements in 3G networks will be particularly valuable in the emerging heterogeneous wireless systems. One of the main objectives of this thesis is to provide motivation for further research and development into cooperative heterogeneous networks.

In the previous two chapters, we highlighted the importance of radio resource management strategies across the communication layers for achieving desirable performance. In particular, CDMA systems necessitate exigent power control algorithms to tackle MAI and near-far effect. In UMTS, the uplink power control consists of OLPC, which provides the required transmission quality by setting the SNR-target, and ILPC, which aims to attain the OLPC SNR-target [19]. In practice, predefined look-up tables select the OLPC SNR-target based on the received

bit error rate or frame error rate (FER). However, this does not result in optimal throughput.

In the previous chapter, we explicitly included the OLPC SNR-target in a cross-layer optimization problem over flat-fading Nakagami channels. In the present chapter, we extend our analysis to frequency-selective Nakagami fading channels, with coherent RAKE receiver using MRC technique. Also we relax the assumption in Chapter 2 about arrival time *for new users*. Specifically here we allow random arrival of a new user at 'any' time within a frame. Moreover, we provide simulation results for *discrete-rate* spreading factors.

For a prescribed target packet error rate (PER_{target}) and a given maximum number of ARQ retransmissions in DLL, we derive the optimum OLPC SNR-target and the corresponding adaptive spreading factor in PHY-layer, as functions of the number of active users in the cell. The main contribution of this chapter is in maximizing the sum-throughput of a frequency-selective L_p-path channel with an MRC coherent RAKE receiver. The number of users in the system is modeled with a one-dimensional discrete Markov chain. To the best knowledge of the author, this is the first time to mathematically derive the optimum OLPC SNR-target expression in a multipath multi-user scenario through coupling of PHY-layer and DLL parameters.

The reminder of this chapter is as follows. Section 3.2 presents the proposed system model and operation assumptions. Sum-throughput expression is defined and hence optimized in Sections 3.4 and 3.5, respectively. Section 3.6 presents numerical and simulation results and highlights the advantages of the proposed scheme. In Section 3.7, concluding comments on the throughput performance of the proposed system are presented, and finally Section 3.8 summarizes the chapter and its contributions. A summary of the notations used in this chapter can be found in Appendix B, Table II.

3.2 System Design

A system model similar to Chapter 2 with a frequency-selective channel and MRC coherent RAKE receiver is considered. The focus is on the uplink of a cellular single-

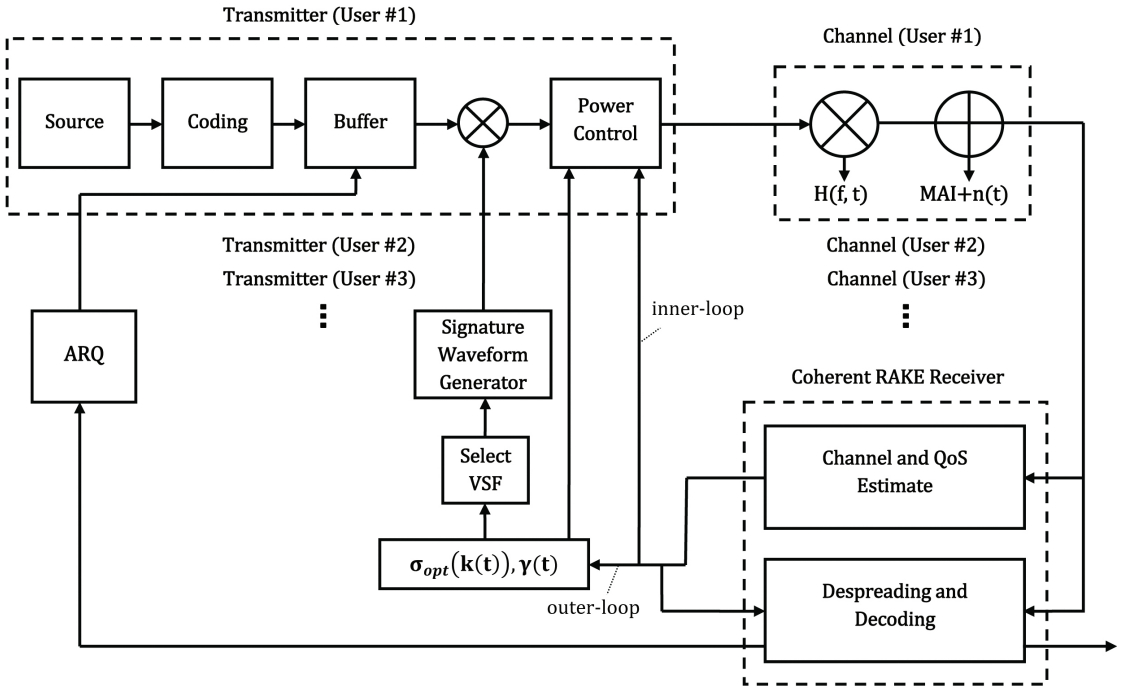

Figure 3.1: Block diagram of the proposed cross-layer optimization scheme in frequency-selective channels. $H(f,t)$ is the multiplicative variable corresponding to the frequency (f)-and-time (t)-dependent channel.

service DS-CDMA communication system, as illustrated in Fig. 3.1. Each mobile user generates a sequence of fixed-length packets of length L bits. The packets enter the buffer[1] and then are converted to DS-CDMA signals using a spreading factor $N(k(t); PER_{target})$, where $k(t)$ is the number of users at time t for a given PER_{target}. Spreading is assumed over bandwidth B with Nyquist data pulses, $B = 1/T_c$, where $T_c = T_b/N(k(t); PER_{target})$ is the fixed chip duration and T_b is the bit duration.

3.2.1 Frequency-Selective Channel

An L_p-path time-varying fading channel and stationary channel gains $H_{ij}(t)$, $j = 1, ..., L_p$ at time t for the i-th user are assumed. During transmission, zero-mean additive white Gaussian noise (i.e. AWGN), $n(t)$, with a two-sided power spectral density $N_0/2$, is added to the BPSK-modulated signal. The only interference present in the cell is assumed to be multiple access interference (i.e. MAI).

[1]For simplicity's sake, the transmission buffer is assumed to have infinite length in the analysis.

3.2.2 Maximum Ratio Combining RAKE Receiver

We denote the adaptive transmit signal power of the reference user-i at time t over the j-th path by $S_{ij}(\gamma_{ij}(t); k(t))$. $\gamma_{ij}(t)$ corresponds to the instantaneous received SNR of the i-th user over the j-th path for a constant transmit power $E[S_{ij}]$. Given that there are $k(t)$ active users present in the uplink, $\gamma_{ij}(t)$ is given by

$$\gamma_{ij}(t) = \frac{|H_{ij}(t)|^2 E[S_{ij}]}{N_0 B + \sum_{c \neq i} I_{cj}(t)} \ , \ c \in \{1, 2, ..., k\} \tag{3.1}$$

where $I_{cj}(t)$, at time t, denotes the interference imposed on the reference user over the j-th path by user-c.

Maximal ratio diversity combining is the optimal diversity scheme, and therefore provides an upper-bound in the achievable performance compared to other combining techniques. Assuming that the individual signals from each path are co-phased, the respective total SNR of user-i at the output of the MRC is given by [28]:

$$\gamma_i(t) = \sum_{j=1}^{L_p} \gamma_{ij}(t). \tag{3.2}$$

A centralized power control mechanism is assumed to maintain a uniform value for $\gamma_i(t)$ for all users. In addition, all active users are assumed to have the same SNR-target requirement. For this reason, subscript i is henceforth removed from $\gamma_i(t)$. Moreover, all further time references are omitted for stationary channel conditions.

3.2.3 System State and Transition Probabilities

The number of users is modeled with a discrete one-dimensional $(K_{max} - 1)$-state M/M/m/m queuing Markov process [1] as presented in Fig. 3.2[1]. The number of users within the cell, k, ranges between $2 \leq k \leq K_{max}$, where K_{max} is the maximum number of users allowed. The design is for a multi-user system, with at least one interfering user.

Here, the assumption is that the common *optimum* SNR-target for all users,

[1]This Markov model is presented in Chapter 2, Fig. 2.3, for the reader's convenience, we have re-illustrated the diagram here.

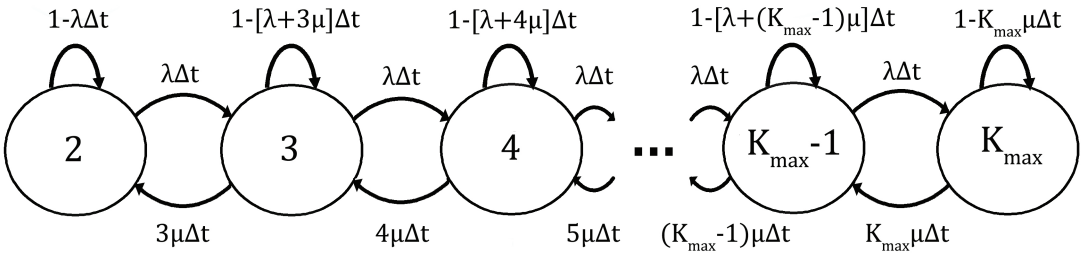

Figure 3.2: M/M/m/m queuing discrete one-dimensional Markov chain with $(K_{max} - 1)$ states modeling the number of users with probabilities of transitions occurring in a small time interval Δt.

$\sigma_{opt}(k)$, which maximizes the sum-throughput under packet error rate and transmit power constraints, is set and adjusted in the outer-loop according to the number of active users. Using $\sigma_{opt}(k)$ and PER_{target}, the corresponding spreading factor is selected at frame level, and the signature waveform is generated. Each PHY-layer frame may contain dynamic traffic from the DLL. We also assume that transmit power $S_i(\gamma, k)$ in the inner-loop is adaptive according to the total ($\gamma_0 = 0$) or truncated ($\gamma_0 > 0$) channel inversion policies

$$\frac{S_i(\gamma, k)}{E[S_i]} = \begin{cases} \frac{\sigma_{opt}(k)}{\gamma} & \gamma > \gamma_0 \\ 0 & \gamma \leq \gamma_0 \end{cases} \tag{3.3}$$

in order to attain $\sigma_{opt}(k)$, where γ_0 is a given cut-off value.

At the BS, the signal goes through a RAKE detector for despreading. For erroneous packets, the receiver may request retransmission through the truncated-ARQ scheme with maximum number of retransmissions η. Perfect channel estimation is assumed at the receiver, as is an error-free feedback path between the receiver and the transmitter.

3.3 PER Analysis

Using the approximate PER formulation for block codes with r-bit error correction capability derived in Chapter 2, we have:

$$PER = \frac{L!\left\{\frac{1}{2}\exp\left\{-\frac{1}{2}\left[SNR\right]^{-1}\right\}\right\}^{r+1}}{(r+1)!(L-r-1)!} \leq \Lambda^{\frac{1}{\eta+1}} := PER_{target} \tag{3.4}$$

where Λ is the target packet loss rate after η retransmissions and L is the fixed packet length.

For sufficiently large number of users ($K_{max} \geq 10$) in the cell, central limit theorem can be invoked to show that MAI at the receiver is asymptotically Normal with zero mean [63]. Consequently, for Normally-distributed MAI at the receiver with MRC combiner, under multipath fading, SNR at the output of the RAKE detector is given by [54]:

$$SNR = \left\{\frac{q(L_p,\delta)-1}{2N(k;PER_{target})} + \frac{(k-1)q(L_p,\delta)}{3N(k;PER_{target})} + \frac{N_0}{2E_b\Omega}\right\}^{-1} \tag{3.5}$$

where E_b is the bit energy and Ω indicates initial path strength of the reference user. $q(L_p,\delta)$ is a function of total number of paths 'L_p' received from the reference user, and the rate of exponential decay of multipath intensity profile (MIP) denoted by δ [54]:

$$q(L_p,\delta) = \sum_{i=1}^{L_p} e^{-\delta(i-1)}. \tag{3.6}$$

For the adaptive transmission scheme, $\frac{E_b\Omega}{N_0/2}$ is replaced with the OLPC optimum SNR-target, $\sigma_{opt}(k)$. As previously mentioned, this is in line with practical CDMA systems, where the OLPC updates the SNR-target value through the Load Control unit [19]. Using (3.5), the corresponding spreading factor is derived by solving (3.4) for $N(k;PER_{target})$:

$$N(k;PER_{target}) = \zeta(q(L_p,\delta),k)\left\{\frac{1}{\Psi} - \frac{1}{\sigma_{opt}(k)}\right\}^{-1} \tag{3.7}$$

where

$$\zeta(q(L_p,\delta),k)=\frac{q(L_p,\delta)-1}{2}+\frac{(k-1)q(L_p,\delta)}{3} \tag{3.8}$$

and

$$\Psi=-2\ln\left\{2\left[\frac{(r+1)!(L-r-1)!}{L!}\Lambda^{\frac{1}{\eta+1}}\right]^{\frac{1}{r+1}}\right\}. \tag{3.9}$$

3.4 Sum-Throughput Formulation with Random User Arrivals

For the proposed system, the sum-throughput, T, the rate of successfully transmitted packets by all supported users in the cell over the total channel packet rate, can be calculated by[1]

$$\begin{aligned}T=E_\epsilon[E_{k|\epsilon}(T(k)|\epsilon)]=E_\epsilon\Bigg\{&P_2\left[\frac{k}{N(k;PER_t)}+P_k^{inc}\frac{1-(\epsilon/T_f)}{N(k;PER_t)}\right]_{k=2}+\\&\sum_{k=3}^{K_{max}-1}P_k\left[\frac{k}{N(k;PER_t)}+P_k^{inc}\frac{1-(\epsilon/T_f)}{N(k;PER_t)}-P_k^{dec}\frac{1-(\epsilon/T_f)}{N(k;PER_t)}\right]+\\&P_k\left[\frac{k}{N(k;PER_t)}-P_k^{dec}\frac{1-(\epsilon/T_f)}{N(k;PER_t)}\right]_{k=K_{max}}\Bigg\}\quad\text{bits/chip}\end{aligned} \tag{3.10}$$

where E_ϵ indicate the expected value with respect to ϵ, P_k is the probability that there are k users in the cell, and $P_k^{inc}(=\lambda)$ and $P_k^{dec}(=\mu k)$ denote, respectively, the probability that the number of users increases or decreases by one. We assume that the probability of increase or decrease by more than one user within a frame is zero. T_f is the duration of a frame, and a new interfering user starts transmission ϵ seconds after the beginning of the frame. ϵ is assumed to be Uniformly-distributed over the interval $[0, N_fT_c)$, where N_f is the fixed number of chips per frame. The above sum-throughput expression consists of three terms, the first term correspond to the event where there are two users, the first and second term combined correspond to the event where there $k\in\{3,4,...,K_{max}-1\}$ users, and all three terms together correspond to the event where there are K_{max} users present in the system.

Using $\rho=\lambda/\mu$ to denote traffic load, the probability of having k active users in

[1]The system is assumed to support a single class of services.

the cell is given by [3]:

$$P_k = \frac{\rho^{k-2}/k!}{\sum_{n=2}^{K_{max}}(\rho^{n-2}/n!)}. \tag{3.11}$$

By taking the expectation (E) with respect to ϵ and from (3.7) and (3.11), sum-throughput can be written as:

$$T = \frac{1}{2\psi}\sum_{k=2}^{K_{max}}\frac{\rho^{k-2}}{k!}[\lambda+(2-\mu)k][\frac{\frac{1}{\Psi}-\frac{1}{\sigma_{opt}(k)}}{\zeta(q(L_p,\delta),k)}]+\frac{\mu}{2\psi}[\frac{\frac{1}{\Psi}-\frac{1}{\sigma_{opt}(k)}}{\zeta(q(L_p,\delta),k)}]_{k=2}-$$
$$\frac{\lambda\rho^{K_{max}-2}}{2\psi K_{max}!}[\frac{\frac{1}{\Psi}-\frac{1}{\sigma_{opt}(k)}}{\zeta(q(L_p,\delta),k)}]_{k=K_{max}} \quad \text{bits/chip} \tag{3.12}$$

where

$$\psi = \sum_{n=2}^{K_{max}}\frac{\rho^{n-2}}{n!}. \tag{3.13}$$

3.5 Optimization Problem

Consider the average power constraint from Chapter 2, Section 2.3.3:

$$C : E[1/\gamma]\sigma_{opt}(k)kP_k\rho^{-1} \leq 1\ ,\ k = 2,3,...K_{max} \tag{3.14}$$

where $p(\gamma)$ denotes the probability density function of γ. Hence, the optimization problem using (3.4), (3.12) and (3.14), can be written as:

$$\underset{\sigma_{opt}(2),\sigma_{opt}(3),...,\sigma_{opt}(K_{max})}{\text{maximize}} \quad T \tag{3.15a}$$

subject to

$$C1 : E[1/\gamma]\sigma_{opt}(k)kP_k\rho^{-1} \leq 1\ \ ,\quad k = 2,3,...,K_{max} \tag{3.15b}$$

$$C2 : PER = PER_{target}. \tag{3.15c}$$

To derive the optimum SNR-target, $\sigma_{opt}(k)$, the Lagrangian optimization method is employed. Concavity condition for applying this method is proved in Appendix B.

The Lagrangian function, $J(\sigma_{opt}(2),\sigma_{opt}(3),...,\sigma_{opt}(K_{max}))$, is constructed using

(3.15a)-(3.15c):

$$J(\sigma_{opt}(2),\sigma_{opt}(3),...,\sigma_{opt}(K_{max})) = \frac{1}{2\psi}\sum_{k=2}^{K_{max}}\frac{\rho^{k-2}}{k!}[\lambda+(2-\mu)k][\frac{\frac{1}{\Psi}-\frac{1}{\sigma_{opt}(k)}}{\zeta(q(L_p,\delta),k)}]+$$
$$\frac{\mu}{2\psi}[\frac{\frac{1}{\Psi}-\frac{1}{\sigma_{opt}(k)}}{\zeta(q(L_p,\delta),k)}]_{k=2} - \frac{\lambda\rho^{K_{max}-2}}{2\psi K_{max}!}[\frac{\frac{1}{\Psi}-\frac{1}{\sigma_{opt}(k)}}{\zeta(q(L_p,\delta),k)}]_{k=K_{max}}+$$
$$\sum_{k=2}^{K_{max}}\phi(k)\left\{E[1/\gamma]\sigma_{opt}(k)kP_k\rho^{-1}-1\right\} \tag{3.16}$$

where $\phi(k)$, $k=2,3,...,K_{max}$, are the Lagrangian multipliers. Solving $\frac{\partial J}{\partial\sigma_{opt}(k)}=0$ for $k=2,3,...,K_{max}$ results in:

$$\sigma_{opt}(k) = \begin{cases} \sqrt{\frac{\rho[\lambda+4]\{\zeta(q(L_p,\delta),2)\}^{-1}}{-8\phi(2)E[1/\gamma]P_2\psi}} & k=2 \\ \sqrt{\frac{\rho^{k-1}[\lambda+(2-\mu)k]\{\zeta(q(L_p,\delta),k)\}^{-1}}{-2k!k\phi(k)E[1/\gamma]P_k\psi}} & k=3,...,K_{max-1} \\ \sqrt{\frac{\rho^{K_{max}-1}[2-\mu]\{\zeta(q(L_p,\delta),K_{max})\}^{-1}}{-2K_{max}!\phi(K_{max})E[1/\gamma]P_{K_{max}}\psi}} & k=K_{max}. \end{cases} \tag{3.17}$$

We use (3.11), the active constraints from (3.15b) and (3.15c), and the Kuhn-Tucker constraint qualification to solve $\frac{\partial J}{\partial\phi(k)}=0$ for $k=2,3,...,K_{max}$. $\phi(k)$, for $2\leq k\leq K_{max}$ can be obtained as:

$$\phi(k) = \begin{cases} \frac{-\rho^{-1}[\lambda+4]E[1/\gamma]P_2}{2\psi\zeta(q(L_p,\delta),2)} & k=2 \\ \frac{-\rho^{k-3}[\lambda+(2-\mu)k]E[1/\gamma]kP_k}{2k!\psi\zeta(q(L_p,\delta),k)} & k=3,...,K_{max-1} \\ \frac{-\rho^{K_{max}-3}[2-\mu]E[1/\gamma]K_{max}P_{K_{max}}}{2(K_{max}-1)!\psi\zeta(q(L_p,\delta),K_{max})} & k=K_{max}. \end{cases} \tag{3.18}$$

Using (3.17) and (3.18), the following optimum outer-loop SNR-target is obtained:

$$\sigma_{opt}(k) = \frac{\psi(k-1)!}{E[1/\gamma]\rho^{k-3}}\ ,\ k=2,3,...,K_{max}. \tag{3.19}$$

It can be observed that the optimum OLPC SNR-target expression in (3.19), derived over frequency-selective fading channels, is independent of the received number of paths, L_p. Moreover, (3.19) does not depend on the Uniformly-distributed arrival time of new users.

Using (3.8) and (3.19) in (3.12), system sum-throughput for total channel inver-

sion policy can be obtained as:

$$T = \frac{1}{2\psi}\sum_{k=2}^{K_{max}}\frac{\rho^{k-2}}{k!}[\lambda+(2-\mu)k]\left\{\frac{\frac{1}{\Psi}-\frac{E[1/\gamma]\rho^{(k-3)}}{\psi(k-1)!}}{\frac{q(L_p,\delta)-1}{2}+\frac{(k-1)q(L_p,\delta)}{3}}\right\}+$$
$$\frac{\mu}{2\psi}\left\{\frac{\frac{1}{\Psi}-\frac{E[1/\gamma]\rho^{-1}}{\psi}}{\frac{q(L_p,\delta)-1}{2}+\frac{q(L_p,\delta)}{3}}\right\}-\frac{\lambda\rho^{K_{max}-2}}{2\psi K_{max}!}\left\{\frac{\frac{1}{\Psi}-\frac{E[1/\gamma]\rho^{(K_{max}-3)}}{\psi(K_{max}-1)!}}{\frac{q(L_p,\delta)-1}{2}+\frac{(K_{max}-1)q(L_p,\delta)}{3}}\right\}$$
bits/chip. (3.20)

To calculate the optimum OLPC SNR-target, $\sigma_{opt}^{tci}(k)$, when truncated channel inversion (tci) is employed, it is necessary to use $E[1/\gamma]_{\gamma_0} = \int_{\gamma_0}^{\infty}\frac{1}{\gamma}p(\gamma)d\gamma$. Therefore,

$$\sigma_{opt}^{tci}(k) = \frac{\psi(k-1)!}{E[1/\gamma]_{\gamma_0}\rho^{k-3}}\ ,\ k=2,3,...,K_{max}. \tag{3.21}$$

Hence, the respective sum-throughput, T^{tci}, can be calculated by multiplying T by the non-outage probability, $p(\gamma>\gamma_0) = e^{-\gamma_0/E[\gamma]}$:

$$T^{tci} = e^{-\gamma_0/E[\gamma]}\times\left[\frac{1}{2\psi}\sum_{k=2}^{K_{max}}\frac{\rho^{k-2}}{k!}[\lambda+(2-\mu)k]\left\{\frac{\frac{1}{\Psi}-\frac{E[1/\gamma]_{\gamma_0}\rho^{(k-3)}}{\psi(k-1)!}}{\frac{q(L_p,\delta)-1}{2}+\frac{(k-1)q(L_p,\delta)}{3}}\right\}+\right.$$
$$\left.\frac{\mu}{2\psi}\left\{\frac{\frac{1}{\Psi}-\frac{E[1/\gamma]_{\gamma_0}\rho^{-1}}{\psi}}{\frac{q(L_p,\delta)-1}{2}+\frac{q(L_p,\delta)}{3}}\right\}-\frac{\lambda\rho^{K_{max}-2}}{2\psi K_{max}!}\left\{\frac{\frac{1}{\Psi}-\frac{E[1/\gamma]_{\gamma_0}\rho^{(K_{max}-3)}}{\psi(K_{max}-1)!}}{\frac{q(L_p,\delta)-1}{2}+\frac{(K_{max}-1)q(L_p,\delta)}{3}}\right\}\right]$$
bits/chip. (3.22)

3.6 Discussion of Results

In this section theoretical and simulation results for the proposed cross-layer optimization scheme are presented under various multipath fading conditions. The optimized system results are compared to those of a non-optimized system with VSF and truncated-ARQ, where the OLPC SNR-target is kept constant through expression: $\sigma_{non-opt} = 1/E[1/\gamma]$. A frequency-selective Nakagami-m' fading channel with finite-length delay line has been considered [53, 54]. Packet length, L, is assumed to be 100 bits with $r = 7$ correctable bits.

3.6.1 Theoretical Results

Continuous-rate spreading factor adaptation, and a multipath fading channel equal to solvable paths with independent Nakagami-m-distributed path gains, are considered. Therefore, these theoretical results serve as upper-bounds for cases with discrete-rate spreading factors and practical fading channel conditions.

Optimal and non-optimal adaptive spreading factor values according to the number of active users in the cell for various values of η and L_p is presented in Fig. 3.3. For the same η, it is observed that the optimal spreading factor is always smaller than the non-optimal case, therefore the optimal scheme yields greater sum-throughput. Moreover, increasing the number of paths, for a fixed PER, requires larger spreading factors and therefore lower sum-throughput is obtained.

Fig. 3.4 illustrates the achievable sum-throughput for several values of m'. For Rayleigh fading conditions, $m' = 1$, where an SNR threshold (γ_0) is required during deep fades, sum-throughput values correspond to truncated channel inversion policy, T^{tci}, otherwise, throughput results correspond to total channel inversion policy, T. We consider a target packet loss rate of 10^{-4}, a maximum number retransmissions of one and L_p values of one and two. It is evident that as m' moves away from one, i.e. less severe fading conditions, higher sum-throughput is achieved.

In Fig. 3.5 optimal and non-optimal sum-throughput values are illustrated for various traffic loads and number of paths. It is evident that the optimal method always outperforms the non-optimal scheme. Moreover, having a lower traffic load improves the sum-throughput performance.

Fig. 3.6 illustrates optimized and non-optimized sum-throughput values for different target packet loss rates and maximum number of retransmissions. It is observed that a higher target packet loss rate, i.e. looser QoS requirement, results in greater sum-throughput. Furthermore, the gain of optimized scheme in comparison to its non-optimized counterpart is improved under more stringent quality of service constraints. For example, at $E[\gamma] = 20$ dB and $\eta = 1$, for $\Lambda = 10^{-6}$, 21.0% gain is achieved; whereas the improvement is reduced to 15.6% for $\Lambda = 10^{-1}$. However, at higher SNRs, optimized and non-optimized sum-throughputs converge.

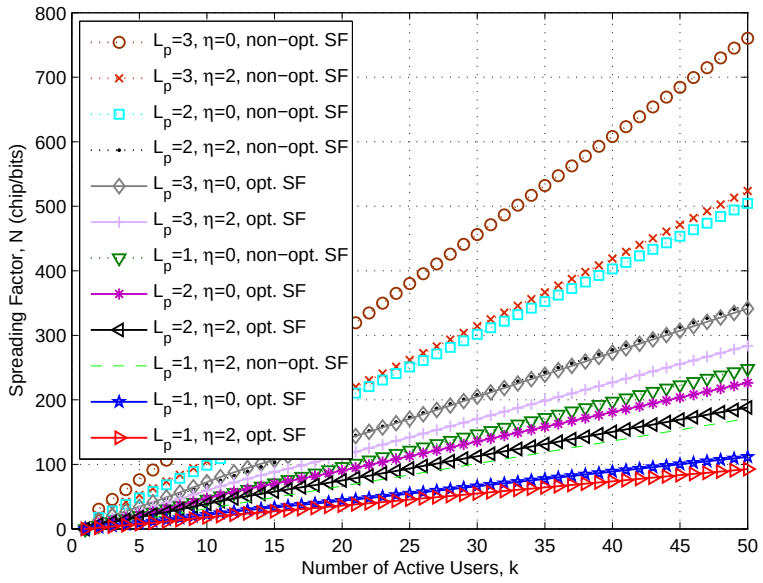

Figure 3.3: Optimal and non-optimal adaptive spreading factors as functions of the number of active users for different number of paths and number of retransmissions, $m' = 2$, $\Lambda = 10^{-4}$, $\lambda = 0.1$, $\mu = 0.005$, $K_{max} = 50$, $E[\gamma] = 20$ dB, $\delta = 0$.

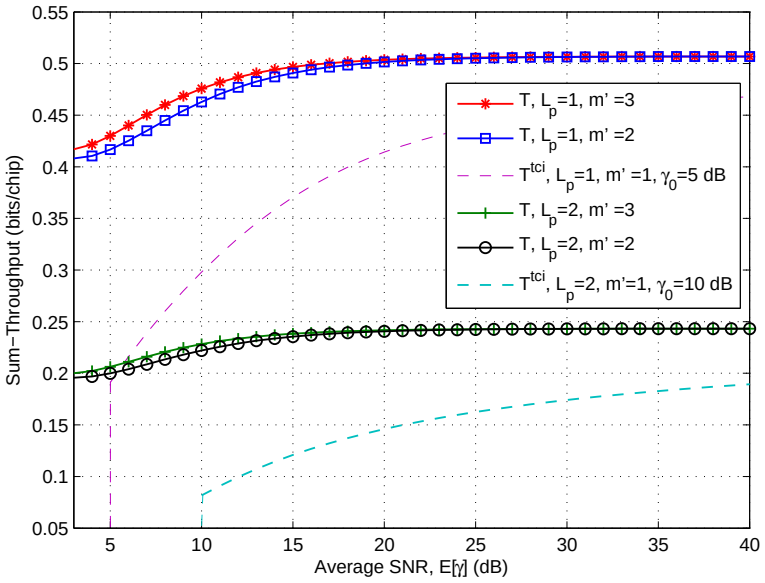

Figure 3.4: Optimized scheme sum-throughput for different values of Nakagami fading parameter, m', with different SNR threshold values, $\lambda = 0.1$, $\mu = 0.005$, $K_{max} = 50$, $\Lambda = 10^{-4}$, $\eta = 1$, $\delta = 0$.

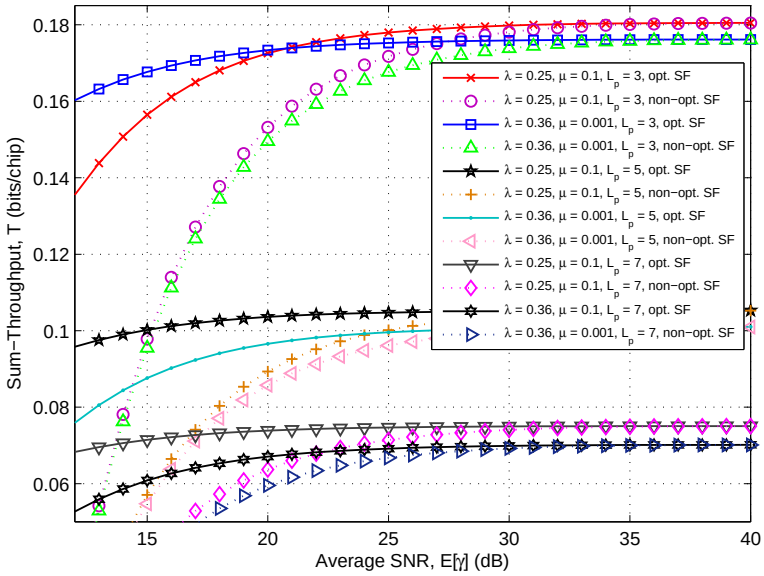

Figure 3.5: Optimized and non-optimized throughputs for various traffic loads and number of paths, $m' = 2$, $K_{max} = 50$, $\Lambda = 10^{-3}$, $\eta = 1$, $\delta = 0$.

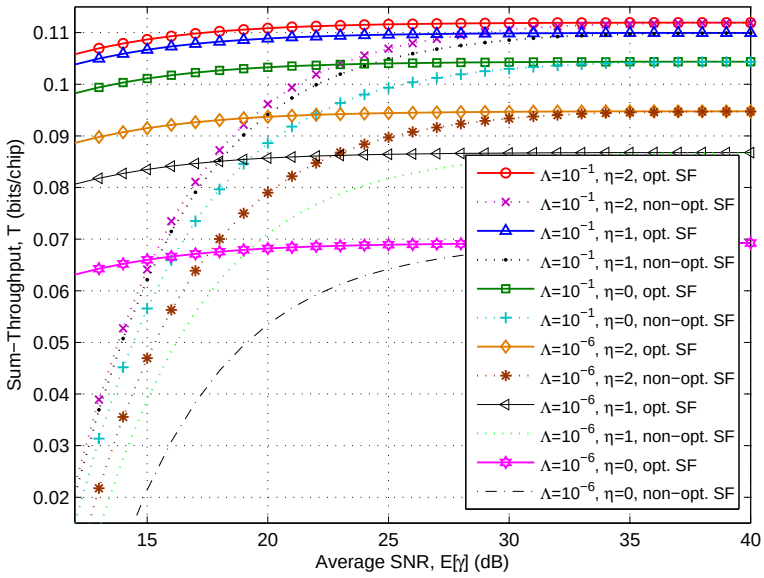

Figure 3.6: Optimized and non-optimized sum-throughputs for various target packet loss rate and retransmissions number scenarios, $L_p = 5$, $m' = 2$, $\lambda = 0.1$, $\mu = 0.006$, $K_{max} = 50$, $\delta = 0$.

3.6.2 Simulation Results with Discrete-Rate VSF

In this subsection we consider realistic cases with discrete-rate variable spreading factors and practical fading conditions.

Firstly, as demonstrated in Fig. 3.7, we analyze the performance of the optimized scheme over a practical Nakagami-m shadowed environment, with a Log-Normal shadowing standard deviation of 4 dB and $m' = 2$ [151], as was considered in Chapter 2, Fig. 2.14. To carry out the simulation a multi-user scheme with similar conditions, in particular, continuous-rate power adaptation, as in the theoretical results is considered. Comparison of theoretical and simulation results of the optimized scheme for various settings of target packet loss rate and retransmissions number is depicted in Fig. 3.7. It can be observed that the simulation carried out over the practical Nakagami-m shadowed channel has led to a slight reduction in the sum-throughput values achieved in the theoretical conditions. The slight gap in performance is more significant in better channel conditions, e.g. higher $E[\gamma]$. For instance, where $L_p = 2$, at $E[\gamma] = 10$ dB, the theoretical case achieves a throughput gain of 1% compared to the simulation scheme, whereas the gain is increased to 3.3% at $E[\gamma] = 20$ dB.

So far, we have considered continuous-rate spreading factor adaptation, hence, the sum-throughput results are optimistic and serve as upper-bounds. In practice, the choice of spreading factor is typically selected from a predefined set of discrete values. In order to adopt discrete-rate variable spreading factors in our proposed optimized scheme, we incorporate orthogonal Walsh-Hadamard spreading codes. For a frame length of 1680 chips, the set of orthogonal Walsh-Hadamard spreading factors, N_{WH}, is as follows:

$$N_{WH} \in \Big\{ 1, 2, 4, 8, 12, 16, 20, 24, 28, 40, 48, 56, 60, 80, 84, \\ 112, 120, 140, 168, 240, 280, 336, 420, 560, 840, 1680 \Big\}. \tag{3.23}$$

Comparison of optimized scheme performance, using theoretical and simulation with discrete-rate spreading codes schemes for various number of paths is demon-

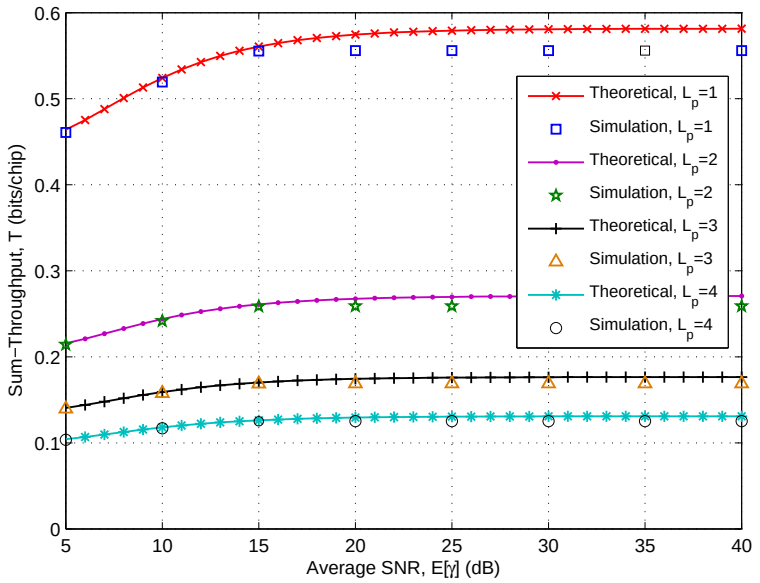

Figure 3.7: Optimized theoretical and simulation sum-throughputs for various number of paths, $m' = 2$, $\lambda = 0.25$, $\mu = 0.02$, $K_{max} = 50$, $\Lambda = 10^{-3}$, $\eta = 2$, $\delta = 0$.

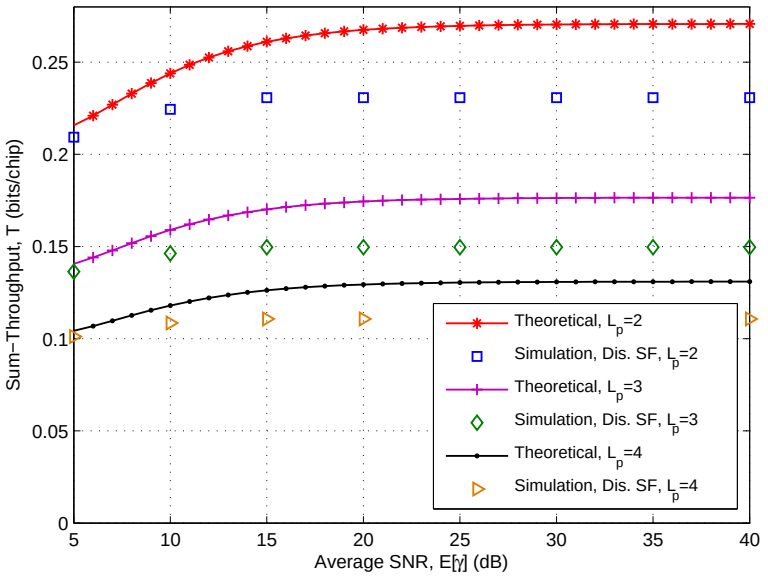

Figure 3.8: Comparison of theoretical and simulation with discrete-rate spreading factors performances for different number of paths, $m' = 2$, $\lambda = 0.25$, $\mu = 0.02$, $K_{max} = 50$, $\Lambda = 10^{-3}$, $\eta = 2$, $\delta = 0$.

strated in Fig. 3.8. The performance gap is due to the fact that in simulation results we have employed Walsh-Hadamard discrete-rate spreading codes, whereas for the theoretical results optimal continuous-rate spreading factors are used which provide an upper-bound for achievable sum-throughput. For higher average received SNRs, the gap between theoretical and simulation results increases. For example, where $L_p = 2$, at $E[\gamma] = 10$ dB, the theoretical scheme achieves a 10% gain in sum-throughput over the simulation case with discrete-rate spreading factor adaptation; whereas the gain is increased to 16% at $E[\gamma] = 20$ dB. To carry out the simulation a multi-user scheme with similar conditions as in the theoretical results is considered. In particular, orthogonal Walsh-Hadamard spreading codes for a frame length of 1680 chips and a practical multipath Nakagami-m shadowed environment with $m = 2$ is studied.

3.7 Conclusions

A throughput-optimal cross-layer scheme was analyzed for a frequency-selective channel with MRC coherent RAKE receiver. We assumed *random* arrival time for a new user within a frame, and considered *discrete* spreading factors as a practical case. It was shown that the optimal SNR-target does not vary with number of paths under MRC RAKE receiver condition. However, given a fixed packet error rate target, increasing the number of paths requires higher spreading factors and consequently reduces sum-throughput. The achievable gain through our optimization scheme, under multipath fading and random arrival time for new users, was demonstrated for various settings of the system parameters. Practical feasibility of the optimized scheme was also studied through simulation results with discrete spreading factors and practical channel conditions.

3.8 Contributions

In this chapter, the cross-layer optimization technique in Chapter 2 aws extended and analysed for frequency-selective fading channels. Given that a coherent RAKE receiver is employed with MRC, a closed-form expression for the optimum OLPC SNR-target is derived. The optimal spreading factor using the optimum OLPC SNR-target is selected at the PHY-layer, which satisfies the QoS imposed for the PER with a maximum number of allowed ARQ retransmissions at the DLL. It is shown that the optimum OLPC SNR-target expression does not depend upon the received number of paths from the reference user and is independent of the arrival time of new users within a frame. We show that an increase in L_p effectively reduces sum-throughput due to having set the PER to a fixed value. Sum-throughput performances of the optimized system and the non optimized case, over various multipath fading conditions, are studied. A considerable gain in sum-throughput is achieved through joint optimization of PHY-layer and DLL variables, under frequency-selective channel condition. At this point, the contributions of this chapter are summarized as follows:

- Cross-layer optimization technique in Chapter 2 is extended and analysed for frequency-selective channels with MRC coherent RAKE receiver.
- We assume random arrival time for a new user within a frame and consider discrete-rate Walsh-Hadamard spreading codes as a practical case.
- We show that the optimum outer-loop SNR-target does not depend on the received number of paths (L_p), and neither is dependent on the Uniformly-distributed arrival time of new users.
- Sum-throughput performances of the optimized system and a non optimized case, where the SNR-target is assumed to be constant, under various settings of the system parameters is studied.
- A considerable gain in sum-throughput is achieved through joint optimization of PHY-layer and DLL variables, under frequency-selective fading conditions.

- Practical feasibility of the optimized scheme was studied by comparing theoretical and simulation results. A performance gap was observed between theoretical and simulation results, as a result of discrete spreading factors and composite fading/shadowing channel conditions.

- Proof of convexity for optimization problem (3.5) is provided.

In the next chapter of this thesis, firstly, a cross-layer optimization scheme, in the sense of maximizing network sum-throughput, is proposed for a multi-service CDMA cell of heterogeneous data traffic. Secondly, the performance of the cross-layer algorithm is investigated and extended in the context of shared-spectrum heterogeneous OFDM/CDMA networks.

3.9 Appendix B

3.9.1 Table II - Chapter Notation

Symbol	Definition
$k(t)$	Number of active users at time t
K_{max}	Maximum number of supported users
T_c	Chip duration
T_b	Bit duration
T_f	Frame duration
B	Bandwidth
$H_{ij}(t)$	Channel gain for user-i over j-th path at time t
$n(t)$	AWGN
$N_0/2$	Two sided power spectral density of AWGN
$\gamma_{ij}(t)$	Received SNR of i-th user over j-th path at time t
$\gamma_i(t)$	Received SNR of i-th user at the output of MRC combiner at time t
$S_{ij}(\gamma_i(t), k(t))$	ILPC adaptive transmit signal power of user-i over j-th path at time time t
$E[S_{ij}]$	Average transmit signal power of user-i over j-th path
γ_0	SNR threshold for truncated channel inversion policy
BER	Instantaneous bit error rate
L	Packet length
r	Number of bits in error correction mechanism
L_p	Number of paths
E_b	Bit energy
Ω	Reference user initial path strength
PER	Instantaneous packet error rate
PER_{target}	Target packet error rate
N_f	Fixed number of chips per frame
N	Spreading factor
$N(k; PER_{target})$	Adaptive spreading factor
N_{WH}	Walsh-Hadamard discrete spreading codes
η	Maximum number of retransmissions allowed per packet
Λ	Target packet loss rate
P_k	Probability that there are k active users in the cell
P_k^{inc}	Probability that the number of users increases by 1 within a frame
P_k^{dec}	Probability that the number of users decreases by 1 within a frame
δ	New interfering user starts transmission δ seconds after the beginning of the frame
ϵ	Ratio of δ to the frame duration
ρ	Traffic load
$C1$	Average power constraint
$C2$	Target packer error rate constraint
$J(.,.,...,.)$	Lagrangian function
$\phi(k)$	Lagrangian multiplier for k users
$p(\gamma)$	Probability density function of γ
$E[\gamma]$	Average SNR
$\sigma_{opt}(k)$	OLPC optimum SNR-target for k users with total channel inversion ILPC
$\sigma_{opt}^{tci}(k)$	OLPC optimum SNR-target for k users with truncated channel inversion ILPC

Continued on next page

Symbol	Definition
T	Sum-throughput when total channel inversion policy is adopted
T^{tci}	Sum-throughput when truncated channel inversion policy is adopted
$\sigma_{non-opt}$	Constant SNR-target in the non-optimized case
m'	Nakagami fading parameter

3.9.2 Proof of convexity for optimization problem (3.15)

In order to prove that the use of Lagrangian optimization method is justified, we prove that the optimization problem (3.15a)-(3.15c) is convex. Taking the second derivative of T with respect to $\sigma_{opt}(k)$ for $k = 2, 3, ...K_{max}$ results in:

$$\frac{d^2T}{d\sigma^2_{opt}(k)} = \begin{cases} \frac{\lambda+4}{-2\psi\zeta(q(L_p,\delta),2)\sigma^3_{opt}(2)} & k = 2 \\ \frac{\rho^{k-2}[\lambda+(2-\mu)k]}{-k!\psi\zeta(q(L_p,\delta),k)\sigma^3_{opt}(k)} & k = 3, 4, ..., K_{max-1} \\ \frac{-2\rho^{K_{max}-2}[(2-\mu)K_{max}]}{K_{max}!\psi\zeta(q(L_p,\delta),K_{max})\sigma^3_{opt}(K_{max})} & k = K_{max}. \end{cases}$$

We have $K_{max} \geq 2$ and $\rho \geq 0$, therefore according to equation (3.13), $\psi > 0$. Also from (4.49), $q(L_p, \delta) > 0$. Specifically since $L_p \geq 1$, we have $q(L_p, \delta) \geq 1$, therefore based on (3.8), $\zeta(q(L_p, \delta), k) > 0$. Moreover, from (3.19), $\sigma_{opt}(.)$ is always a non-negative real value. Also we note that λ and $k\mu$ are respectively the transition probabilities P^{inc}_k and P^{dec}_k, and therefore inequalities $k\mu \leq 1$ and $0 \leq \lambda \leq 1$ hold for $k \leq K_{max}$[1]. Hence, $2 - \mu > 0$ and $\lambda \geq 0$. Therefore, $\frac{d^2T}{d\sigma^2_{opt}(k)} < 0$ for $2 \leq k \leq K_{max}$ and the objective function in (3.15a) is concave.

Also, the constraint functions in (3.15b) and (3.15c) are affine in $\sigma_{opt}(k)$ for $k = 2, ..., K_{max}$. Therefore the optimization problem (3.15) is convex.

[1]For practical reasons in this paper we have used states $k \geq 2$ only, however, the theoretical values of k in general state-transition-diagram can be $'0'$ and $'1'$ as well.

The greatest challenge to any thinker is stating the problem in a way that will allow a solution.

Bertrand Russell

Chapter 4

Throughput-Optimal Dynamic Cross-Layer Resource Allocation in Heterogeneous Networks

4.1 Introduction

There is still large room for enriching the existing 3G services as UMTS standards are expected to co-exist with the emerging 4G-LTE technologies for years to come. It is understood that upgrading the current 3G networks to 4G cannot be done all at once, and the transition would take several years. During this changeover, it is predicted that service providers accommodate both 3G and 4G technologies at the same time. Co-operation among the cells that incorporate different radio access technologies can be considered as an effective tool to utilize the shared resources more efficiently, and to support high network capacity. Hence, further enhancements in current 3G networks, the main motivation behind this research, would be particularly valuable in future cooperative heterogeneous wireless networks.

As extensively discussed throughout previous chapters, radio resource management algorithms, in particular dynamic power control, are essential for achieving desirable performance in mobile communication networks under limited radio resources. The significance of RRM to support high data rates is heightened by the wireless environment limitations, such as noise, interference, shadowing and fading.

In the previous two chapters, we proposed a cross-layer scheme, facilitating joint optimization of PHY-layer and DLL parameters, in the context of a single-service CDMA mobile communication network. As a consequence of the single-service assumption, a common variable spreading factor was selected for all users in the cell. However, practical CDMA systems accommodate users of different services in the network simultaneously. Hence, in the first part of this chapter, we extend our analysis to a multi-service network of heterogeneous non-real-time data traffic [152–154], in order to improve the practical feasibility of our proposed cross-layer design approach.

Here, OLPC SINR-targets of heterogeneous data classes are distinctly included in a joint PHY-layer and DLL optimization problem. Considering different ARQ delay limits and prescribed maximum packet loss rates for each class in DLL, we derive the unique optimum outer-loop SINR-target setpoint of each class and the corresponding adaptive spreading factors in PHY-layer, as functions of users' activity in the system. Optimality in this case, means maximizing sum-throughput of the *multi-service* mobile communication network. The number of users in the network is modeled with a two-dimensional discrete Markov chain. To the best of my knowledge, this is the first time to derive closed-form expressions of the optimum SINR-targets in a multi-service network by coupling PHY-layer and DLL parameters.

Further, to overcome bandwidth scarcity, cognitive radio techniques are widely used to enhance the utilization of spectrum [82, 155–158]. In cognitive radio networks, the secondary service may access the frequency band that is licensed to the primary service, subject to pre-determined constraints. The main objective of cognitive radio algorithms is to maximize the throughput of the secondary users whilst minimizing the imposed interference on the primary receiver. In a shared-spectrum implementation, the secondary service detects the unused and under-used parts of the primary spectrum, and together with estimating the current interference temperature levels, it adapts power and bandwidth accordingly. Opportunistic spectrum sharing schemes incorporate this idea by imposing *interference tolerance* and *sensing* limits. In AL-OSA, the secondary service exploits the parts of the primary spectrum that are unused by the primary users. Utilizing the primary spectrum

subject to interference temperature constraints, corresponds to interference-limited opportunistic spectrum access.

Cognitive radio networks have been extensively studied in the literature. In [158] the capacity of the secondary service is maximized by using an OSA scheme based on the primary users' activity. The performance of the secondary service subject to average and peak received power constraints at the primary receiver was studied in [157]. In [159], the achievable gain by employing adaptive transmit power and variable spreading factors is studied for cognitive radio CDMA networks. [82] studies the trade-off between maximizing the performance of secondary network and minimizing the imposed interference on the primary users. By far, most of the resource allocation algorithms in the literature do not employ spectrum sharing strategies. However, without dynamic sharing of bandwidth, optimal performance is not achievable. Furthermore, the cognitive radio research in the literature, mostly focus on spectrum sharing strategies among networks that adopt the same radio access technology. However, with the rapid emergence of new technologies, co-operation among cells that incorporate different radio access technologies can be very effective towards increasing connectivity and supporting high performance [160].

In the second part of this chapter, the proposed cross-layer design strategy is extended and analysed in the context of shared-spectrum CDMA/OFDM heterogeneous networks. Our goal is to maximize the secondary network sum-throughput by exploiting the idle parts of the primary spectrum, using an AL-OSA scheme with a zero tolerable interference limit on the primary receiver. Primary service uses OFDM, hence the practical requisite flexibility is provided for the secondary CDMA service to access the idle parts of the primary spectrum. This is particularly beneficial in terms of minimizing the imposed MAI levels at the secondary receiver by reducing the number of active users in the secondary spectrum. We model the number of primary and secondary users with one-dimensional discrete Markov chains, and examine the performance of our proposed cross-layer shared-spectrum scheme over frequency-selective Nakagami fading channels with MRC RAKE receiver. To the best of author's knowledge, this is the first time to devise a dynamic spectrum sharing algorithm, jointly considering parameters from PHY-layer and DLL, in the

context of a primary OFDM cell and a secondary CDMA cell heterogeneous network.

The organization of the reminder of this chapter is outlined here. Following this introduction, analysis on a multi-service network of heterogeneous data traffic is presented in Section 4.2. Subsection 4.2.1, presents the proposed multi-service architecture and system assumptions. In Subsection 4.2.2, the dual-class data traffic cross-layer analysis for sum-throughput optimization is provided. Subsection 4.2.3 presents numerical and simulation results and highlights the advantages of the proposed cross-layer scheme. In Section 4.3, a shared-spectrum heterogeneous OFDM/CDMA network is considered. Subsection 4.3.1 presents the shared-spectrum heterogeneous network model under consideration and elaborates on the operation assumptions. In Subsection 4.3.2, the methodology for secondary sum-throughput optimization is provided. Subsection 4.3.3 provides numerical results and highlights the advantages of the proposed cross-layer shared-spectrum scheme. In Section 4.4, concluding comments on the sum-throughput performance of the proposed networks under consideration are presented. In Section 4.5, novel contributions are drawn and the most important results are summarized. Lists of the notations used in Sections 4.2 and 4.3 can be found in Appendix C, Table III and Table IV, respectively.

4.2 Multi-Service Network of Heterogeneous Data Traffic

4.2.1 System Architecture Model

This section outlines the system architecture model and describes the approach to maximizing network sum-throughput whilst obeying QoS constraints. Sum-throughput is defined as the total number of successfully transmitted packets by all supported users in the network, over total number of transmitted packets. The focus is on the uplink of a single-cell multi-user multi-service conventional cellular DS-CDMA communication mobile network. It is assumed that a single BS, situated in the centre of the cell, receives communication signals from Uniformly-distributed

mobile users. A multi-service packet-based network, with a dual-class non-real-time data/voice traffic, is considered. Moreover, asynchronous operation is assumed.

The block diagram in Fig. 4.1 illustrates the selection of parameters used for the proposed network. Mobile users (sources) of the two classes generate sequences of fixed-length packets of length L bits. These packets enter the buffer after coding. The data-class buffer contents and the voice-class buffer contents are then converted to DS-CDMA signals, using spreading factors $N_d(k_d(t), k_v(t); PER_{target-d}$,-$PER_{target-v})$ and $N_v(k_d(t), k_v(t); PER_{target-d}, PER_{target-v})$, respectively, where $k_d(t)$, $k_v(t)$, $PER_{target-d}$, and $PER_{target-v}$, in the order given, denote the number of data users at time t, the number of voice users at time t, the packer error rate (PER)-target for data users, and the PER-target for voice users. This methodology will be elucidated as analysis proceeds.

The channel is frequency-flat and time-varying with stationary channel gains $g_{di}(t)$ for the i-th data user, and $g_{vj}(t)$ for the j-th voice user. Data packets are spread over channel bandwidth B with Nyquist pulses, $B = 1/T_{chip-d}$, where $T_{chip-d} = T_{bit-d}/N_d(k_d(t), k_v(t); PER_{target-d}, PER_{target-v})$ is the data chip duration, and T_{bit-d} is the data bit duration. Similarly, spreading of voice packets is done over B with Nyquist pulses, $B = 1/T_{chip-v}$, where $T_{chip-v} = T_{bit-v}/N_v(k_d(t), k_v(t); PER_{target-d}$,-$PER_{target-v})$ is the voice chip duration, and T_{bit-v} is the voice bit duration. To avoid bandwidth expansion, a common chip rate is assumed for the two service, i.e. $T_{chip-d} = T_{chip-v}$. During transmission, zero-mean AWGN, $n(t)$, with a two-sided power spectral density, $N_0/2$, is added to the BPSK-modulated data/voice signal. The only interference present in the cell is assumed to be MAI, generated by other active users within the cell. Let $S_{di}(\gamma_{di}(t), k_d(t), k_v(t))$ and $S_{vj}(\gamma_{vj}(t), k_d(t), k_v(t))$ denote the adaptive transmit signal powers of the i-th data user and j-th voice user at time t, respectively. $\gamma_{di}(t)$ and $\gamma_{vj}(t)$ correspond to instantaneous received SINRs of data user-i and voice user-j with constant transmit powers $E[S_{di}]$ and $E[S_{vj}]$, respectively. Given there are $k_d(t) + k_v(t) = h(t)$ active users in the uplink,

$$\gamma_{di}(t) = \frac{|g_{di}(t)|^2 E[S_{di}]}{N_0 B + \sum_{c \neq i} I_c(t)} \ , \ c \in \{1, 2, ..., h\} \tag{4.1}$$

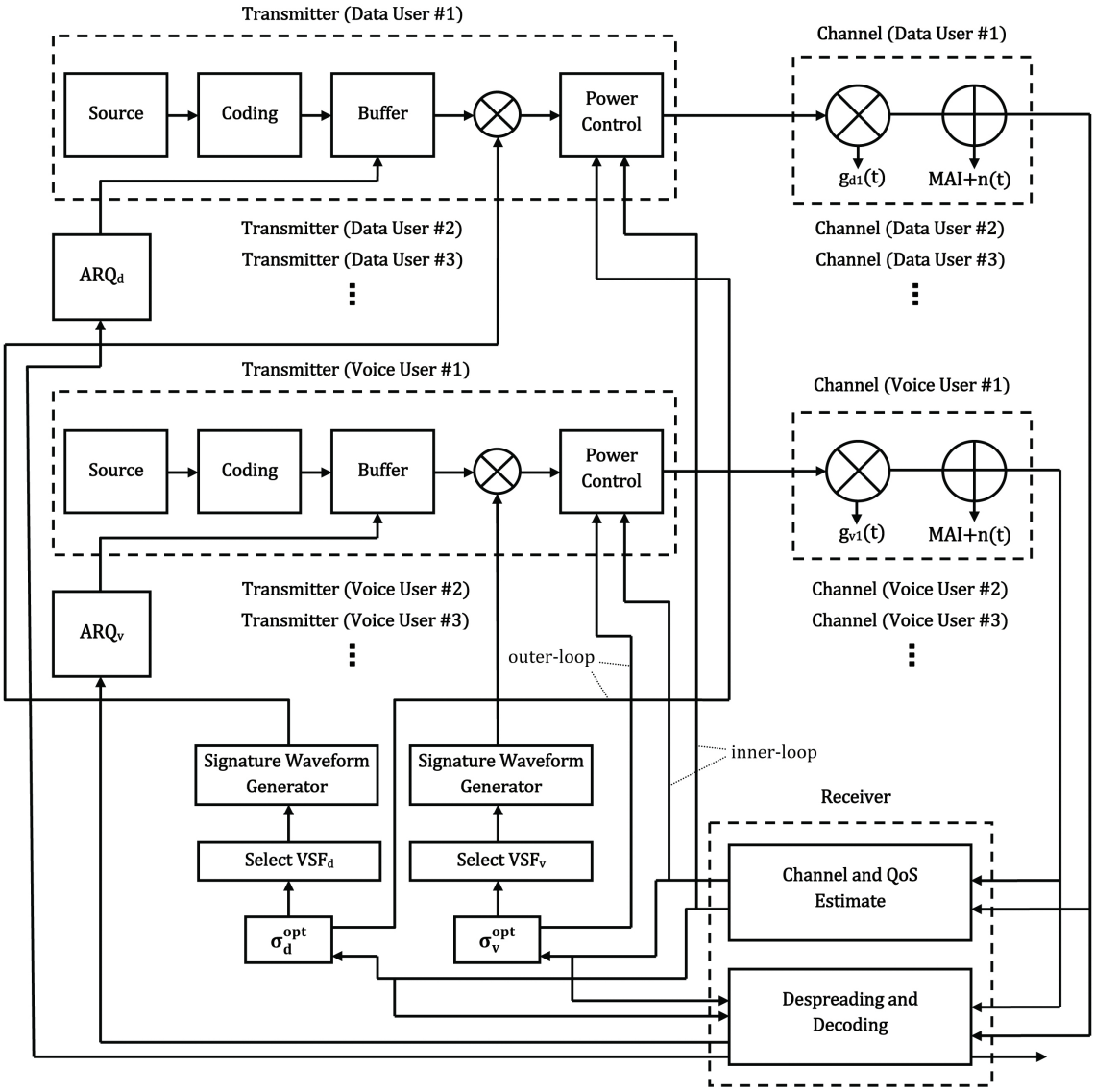

Figure 4.1: Block diagram of the proposed multi-user multi-service system. The diagram depicts the inner- and outer- loop power control schemes of the non-real-time data/voice packet-based network, that adapt, uniquely for each service class, transmit power and optimum SINR-target, and the corresponding variable spreading factor, to physical link variations, number of users, and the requisite PER-target.

and

$$\gamma_{vj}(t) = \frac{|g_{vj}(t)|^2 E[S_{vj}]}{N_0 B + \sum_{c \neq j} I_c(t)} \ , \ c \in \{1, 2, ..., h\} \tag{4.2}$$

are the respective $\gamma_{di}(t)$ and $\gamma_{vj}(t)$, where $I_c(t)$, at time t, denotes the interference imposed on the reference user by the interfering user-c. Similar to our framework in Chapter 3, with some adjustments, the analysis in this chapter can be extended for

frequency-selective channels with MRC coherent RAKE receiver.

As a remedy to near-far effect in CDMA networks, it is vital for the power control mechanism to maintain equal received SINRs for all users at the BS. Moreover, the proposed multi-service network is assumed to support a dual-class of data and voice users, therefore all active users in each class are assumed to have the same SINR-target requirement, which is obtained based on the unique service specification of each class. Therefore, here we assume that the centralized power control mechanism retains uniform values of γ_{di}, for all data users, and γ_{vj}, for all voice users. As a result of this and for brevity, subscripts i and j are hereafter eliminated from γ_{di} and γ_{vj}, respectively. In addition, all time references are discarded for stationary channel conditions.

In this work, the assumption is that the optimum SINR-target of data users $\sigma_d^{opt}(k_d, k_v)$, and the optimum SINR-target of voice users $\sigma_v^{opt}(k_d, k_v)$, which maximize the sum-throughput under PER and transmit power constraints of the two classes, are set and adjusted in the outer-loop according to the number of active users of each class in the cell. According to $\sigma_d^{opt}(k_d, k_v)$, $\sigma_v^{opt}(k_d, k_v)$, $PER_{target-d}$ and $PER_{target-v}$, the relevant spreading factors are selected at frame level, and the signature waveform is generated. We also assume that transmit powers $S_{di}(\gamma_d, k_d, k_v)$ and $S_{vj}(\gamma_v, k_d, k_v)$ for all data and voice users in the inner-loop are adapted to received data-class and voice-class SINRs and the number of data and voice users, through the channel inversion power adaptation policy in order to attain $\sigma_d^{opt}(k_d, k_v)$ and $\sigma_v^{opt}(k_d, k_v)$, respectively. The total ($\gamma_{d0} = 0, \gamma_{v0} = 0$) and truncated ($\gamma_{d0} > 0, \gamma_{v0} > 0$) channel inversion policies for the two classes of traffic are expressed as follows:

$$\frac{S_{di}(\gamma_d, k_d, k_v)}{E[S_{di}]} = \begin{cases} \frac{\sigma_d^{opt}(k_d,k_v)}{\gamma_d} & \gamma_d > \gamma_{d0} \\ 0 & \gamma_d \leq \gamma_{d0} \end{cases} \tag{4.3}$$

$$\frac{S_{vj}(\gamma_v, k_d, k_v)}{E[S_{vj}]} = \begin{cases} \frac{\sigma_v^{opt}(k_d,k_v)}{\gamma_v} & \gamma_v > \gamma_{v0} \\ 0 & \gamma_v \leq \gamma_{v0} \end{cases} \tag{4.4}$$

where γ_{d0} and γ_{v0} are the SINR cut-off values for data and voice classes respectively.

Two classes of data and voice, in the network, are assumed to have different user

arrival rates ($\lambda_{d/v}$) and average service rates ($\mu_{d/v}$). Furthermore, users of the two services are supposed to be constrained by different delay limits, and therefore by different maximum number of ARQ retransmissions, $\eta_{d/v}$. For example, $\eta_d = 2$ can be imposed for data users, whereas, due to the undesired delay, $\eta_v = 0$ or 1 is set for the voice users. Correspondingly, different packet loss rate constraints are imposed on each of the services, since in practice, users of data-class tolerate less stringent packet error rate constraints in comparison to the users of voice-class.

4.2.2 Analysis

This section develops a cross-layer sum-throughput optimization scheme for a multi-service CDMA cell.

Dual-Class Traffic

It is assumed that non-real-time heterogeneous data traffic, consisting of k_d data users and k_v voice users, are active in the cell[1], where

$$2 \leq k_d; \quad 2 \leq k_v; \quad 4 \leq k_d + k_v \leq K_{max}. \tag{4.5}$$

In practice, the selected value of K_{max} must satisfy the QoS constraints of all provisioned users. For analytical convenience, here, we do not include K_{max} in the optimization problem, however, in Chapter 2, we have shown that the choice of K_{max} does not affect the throughput performance unless it is in the vicinity of the traffic load. A multi-dimensional discrete Markov process with two independent truncated M/M/m/m queues, shown in Fig. 4.2, is used to model the number of users in the proposed dual-class network. $\lambda_d = \lambda_{dk}\Delta t$ and $k_d\mu_d = \mu_{dk}\Delta t$, for $2 \leq k_d < K_{max}$, respectively, denote the probabilities of transitions occurring in a small time interval Δt, corresponding to birth and death coefficients λ_{dk} and μ_{dk} when there are k_d data users in the cell [1]. Similar notation applies to the voice-class with respective birth and death coefficients λ_{vk} and μ_{vk} with k_v voice users in the network.

[1]The design is for a multi-user network, with at least one interfering user in each service class. Hence, in this work we have used states $k_d \geq 2$ and $k_v \geq 2$, however, the theoretical values of k_d and k_v in general state-transition-diagram can be '0' and '1' as well.

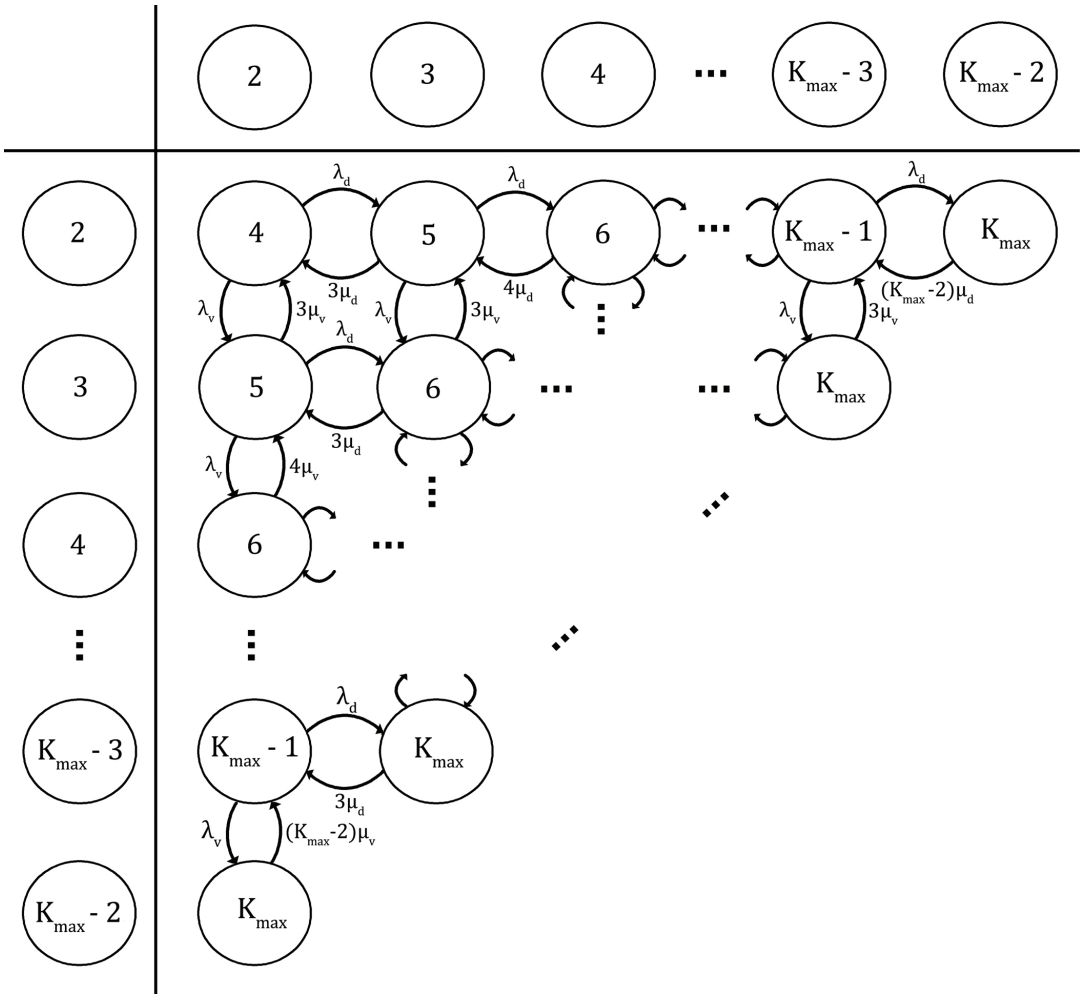

Figure 4.2: Two-dimensional Markov chain for the dual-class network under consideration. Number of data and voice users increases horizontally and vertically, respectively. For simplification, self-transitions are not shown.

Unique Data/Voice PER and VSF Formulation

As discussed in previous chapters, for sufficiently large number of users ($K_{max} \geq 10$) in the cell, central limit theorem can be invoked to show that MAI at the receiver is asymptotically Normal with zero mean. Consequently, for Normally-distributed MAI at the receiver, under flat fading, SINR at the output of the matched-filter detector for data users can be expressed as [16]:

$$SINR_d = \left\{ \frac{k_d - 1}{3N_d} + \frac{k_v}{3N_v} + \frac{N_0}{2E_b\Omega} \right\}^{-1} \tag{4.6}$$

where E_b denotes bit energy, Ω indicates reference user path strength, and for notational brevity, N_d and N_v are hereafter used to denote $N_d(k_d, k_v; PER_{target-d}, PER_{target-v})$ and $N_v(k_d, k_v; PER_{target-d}, PER_{target-v})$, respectively. In a similar approach to the single-service scenario in Chapter 2, $BER_d = Q(\sqrt{SINR_d})$ can be used with the upper bound PER formulation (i.e. worst case of PER) of block codes with r-bits error correction capability, to derive an approximate PER expression for data users (PER_d):

$$PER_d = \frac{L! \left\{ \frac{1}{2} e^{-\frac{1}{2}\left[\frac{k_d-1}{3N_d} + \frac{k_v}{3N_v} + \frac{1}{\sigma_d^{opt}(k_d,k_v)}\right]^{-1}} \right\}^{r+1}}{(r+1)!(L-r-1)!}. \tag{4.7}$$

As previously mentioned, the maximum number of ARQ retransmissions allowed per data and voice packets, in the order given, are denoted with η_d and η_v. The maximum packet loss probability after η_d and η_v retransmissions will be denoted by Λ_d and Λ_v, respectively. Therefore, to satisfy the packet loss constraint for data users, we have:

$$PER_d{}^{\eta+1} \leq \Lambda_d. \tag{4.8}$$

Subsequently, in order to maintain $PER_d \leq PER_{target-d}$, the following equation holds:

$$PER_d \leq \Lambda_d^{\frac{1}{\eta_d+1}} := PER_{target-d}. \tag{4.9}$$

Hence from (4.7) and (4.9), we obtain:

$$\begin{aligned} PER_d &= \frac{L! \left\{ \frac{1}{2} e^{-\frac{1}{2}\left[\frac{k_d-1}{3N_d} + \frac{k_v}{3N_v} + \frac{1}{\sigma_d^{opt}(k_d,k_v)}\right]^{-1}} \right\}^{r+1}}{(r+1)!(L-r-1)!} \\ &= PER_{target-d} := \Lambda_d^{\frac{1}{\eta_d+1}}. \end{aligned} \tag{4.10}$$

Now, N_d, the optimal spreading factor for the data-class, can be determined by

$$N_d = \frac{k_d - 1}{3} \left[\frac{1}{\Psi_d} - \frac{k_v}{3N_v} - \frac{1}{\sigma_d^{opt}(k_d, k_v)} \right]^{-1} \tag{4.11}$$

where

$$\Psi_d = -2\ln\left\{2\left[\frac{(r+1)!(L-r-1)!\Lambda_d^{\frac{1}{\eta_d+1}}}{L!}\right]^{\frac{1}{r+1}}\right\}. \tag{4.12}$$

Therefore, N_d is derived according to the optimum SINR-target for data users, $\sigma_d^{opt}(k_d, k_v)$. Similar to (4.6), the SINR expression of voice users at the output of the matched filter detector is given by:

$$SINR_v = \left\{\frac{k_d}{3N_d} + \frac{k_v - 1}{3N_v} + \frac{N_0}{2E_b\Omega}\right\}^{-1}. \tag{4.13}$$

Applying the analysis (4.6)-(4.10) used for the data-class, we obtain the optimal spreading factor expression for voice users:

$$N_v = \frac{k_v - 1}{3}\left[\frac{1}{\Psi_v} - \frac{k_d}{3N_d} - \frac{1}{\sigma_v^{opt}(k_d, k_v)}\right]^{-1} \tag{4.14}$$

where

$$\Psi_v = -2\ln\left\{2\left[\frac{(r+1)!(L-r-1)!\Lambda_v^{\frac{1}{\eta_v+1}}}{L!}\right]^{\frac{1}{r+1}}\right\}. \tag{4.15}$$

It is observed that N_d and N_v are represented in terms of each other. Equations (4.11) and (4.14) can therefore be used to derive explicit expressions:

$$N_d = \frac{k_d k_v - (k_d - 1)(k_v - 1)}{3k_v(\frac{1}{\Psi_v} - \frac{1}{\sigma_v^{opt}}) - 3(k_v - 1)(\frac{1}{\Psi_d} - \frac{1}{\sigma_d^{opt}})} \tag{4.16}$$

$$N_v = \frac{k_d k_v - (k_d - 1)(k_v - 1)}{3k_d(\frac{1}{\Psi_d} - \frac{1}{\sigma_d^{opt}}) - 3(k_d - 1)(\frac{1}{\Psi_v} - \frac{1}{\sigma_v^{opt}})} \tag{4.17}$$

where for notational convenience, σ_d^{opt} and σ_v^{opt}, in the order given, are used to express $\sigma_d^{opt}(k_d, k_v)$ and $\sigma_v^{opt}(k_d, k_v)$.

Multi-Service Network Sum-Throughput

In order to calculate the sum-throughput for the dual-class network, $T_{d/c}$, the following equation is constructed

$$T_{d/c} = \sum_{h=4}^{K_{max}} \sum_{k_d=2}^{h-2} p(k_d, h-k_d)\Big(k_d\frac{1}{N_d} + \lambda_d\frac{1-\epsilon}{N_d} + k_v\frac{1}{N_v} + \lambda_v\frac{1-\epsilon}{N_v} - k_d\mu_d\frac{1-\epsilon}{N_d} - k_v\mu_v\frac{1-\epsilon}{N_v}\Big) - \sum_{k_d=2}^{K_{max}-2} p(k_d, K_{max}-k_d)\Big(\lambda_d\frac{1-\epsilon}{N_d} + \lambda_v\frac{1-\epsilon}{N_v}\Big) + 2\sum_{k_d=2}^{K_{max}-2} p(k_d, 2)\Big(\mu_v\frac{1-\epsilon}{N_v}\Big) + 2\sum_{k_v=2}^{K_{max}-2} p(2, k_v)\Big(\mu_d\frac{1-\epsilon}{N_d}\Big) \quad \text{bits/chip} \tag{4.18}$$

where $p(x, y)$ denotes the joint equilibrium probability that the network is in state (x, y); where there are x active data users ($k_d = x$) and y active voice users ($k_v = y$) in the network. $\epsilon = \delta/T_f$, where T_f is the duration of a frame, and new interfering user starts transmission δ seconds after the beginning of the frame. In our model, the probability of increase or decrease by more than one user within a frame is zero. Moreover, it is assumed that a change in the number of users can only occur at the beginning of a frame. That is, we assume that $\epsilon << 1$, and hence ϵ can be neglected in (4.18). Random arrival time for new users in a frame is considered in Chapter 3.

The global balance equation for the two-dimensional Markov process under consideration, with compensation of impossible states enforced in (4.5), is given by

$$\sum_{h=4}^{K_{max}} \sum_{k_d=2}^{h-2} p(k_d, k_v)\Big(\lambda_d + \lambda_v + k_d\mu_d + k_v\mu_v\Big) = \sum_{h=4}^{K_{max}} \sum_{k_d=2}^{h-2} p(k_d-1, k_v)\lambda_d + \sum_{h=4}^{K_{max}} \sum_{k_d=2}^{h-2} p(k_d, k_v-1)\lambda_v + \sum_{h=4}^{K_{max}} \sum_{k_d=2}^{h-2} p(k_d+1, k_v)(k_d+1)\mu_d + \sum_{h=4}^{K_{max}} \sum_{k_d=2}^{h-2} p(k_d, k_v+1)(k_v+1)\mu_v - \sum_{k_v=2}^{K_{max}-2} p(1, k_v)\lambda_d - \sum_{k_d=2}^{K_{max}-2} p(k_d, 1)\lambda_v - \sum_{k_d=2}^{K_{max}-2} p(k_d+1, K_{max}-k_d)(k_d+1)\mu_d - \sum_{k_v=2}^{K_{max}-2} p(K_{max}-k_v, k_v+1)(k_v+1)\mu_v \tag{4.19}$$

where

$$h = k_d + k_v. \tag{4.20}$$

Employing LU decomposition [149], equation (4.19) can be solved for steady-state probabilities using the detailed balance equation together with the normalization condition (condition for total probability of all states):

$$\sum_{h=4}^{K_{max}} \sum_{k_d=2}^{h-2} p(k_d, k_v = h - k_d) = 1. \tag{4.21}$$

Denoting the traffic loads of data and voice services by $\rho_d = \lambda_d/\mu_d$ and $\rho_v = \lambda_v/\mu_v$, respectively, the joint probability of k_d active data and k_v active voice users in the cell is given by

$$p(k_d, k_v) = \frac{1}{G}\Big\{\frac{\rho_d^{k_d-2}/k_d!}{\sum_{i=2}^{K_{max}-2}(\rho_d^{i-2}/i!)} \frac{\rho_v^{k_v-2}/k_v!}{\sum_{j=2}^{K_{max}-2}(\rho_v^{j-2}/j!)}\Big\} \tag{4.22}$$

where G is a normalization constant obtained from the set of states in the truncated Markov chain:

$$G = \sum_{h=4}^{K_{max}} \sum_{k_d=2}^{h-2} \frac{\rho_d^{k_d-2}/k_d!}{\sum_{i=2}^{K_{max}-2}(\rho_d^{i-2}/i!)} \frac{\rho_v^{h-k_d-2}/(h-k_d)!}{\sum_{j=2}^{K_{max}-2}(\rho_v^{j-2}/j!)}. \tag{4.23}$$

Using (4.11) and (4.14) sum-throughput in (4.18) is simplified to:

$$\begin{aligned}
T_{d/c} = {} & 3 \sum_{h=4}^{K_{max}} \sum_{k_d=2}^{h-2} \frac{p(k_d, k_v = h - k_d)}{k_d k_v - (k_d - 1)(k_v - 1)} \Bigg\{ [\lambda_d + (1 - \mu_d)k_d] \Big[k_v (\frac{1}{\Psi_v} - \frac{1}{\sigma_v^{opt}}) - \\
& (k_v - 1)(\frac{1}{\Psi_d} - \frac{1}{\sigma_d^{opt}}) \Big] + [\lambda_v + (1 - \mu_v)k_v] \Big[k_d (\frac{1}{\Psi_d} - \frac{1}{\sigma_d^{opt}}) - (k_d - 1)(\frac{1}{\Psi_v} - \frac{1}{\sigma_v^{opt}}) \Big] \Bigg\} \\
& - 3 \sum_{k_d=2}^{K_{max}-2} \frac{p(k_d, k_v = K_{max} - k_d)}{k_d k_v - (k_d - 1)(k_v - 1)} \Bigg\{ \lambda_d \Big[k_v (\frac{1}{\Psi_v} - \frac{1}{\sigma_v^{opt}}) - (k_v - 1)(\frac{1}{\Psi_d} - \frac{1}{\sigma_d^{opt}}) \Big] + \\
& \lambda_v \Big[k_d (\frac{1}{\Psi_d} - \frac{1}{\sigma_d^{opt}}) - (k_d - 1)(\frac{1}{\Psi_v} - \frac{1}{\sigma_v^{opt}}) \Big] \Bigg\} + 6 \sum_{k_d=2}^{K_{max}-2} \frac{p(k_d, k_v = 2)}{k_d k_v - (k_d - 1)(k_v - 1)} \times \\
& \Bigg\{ \mu_v \Big[k_d (\frac{1}{\Psi_d} - \frac{1}{\sigma_d^{opt}}) - (k_d - 1)(\frac{1}{\Psi_v} - \frac{1}{\sigma_v^{opt}}) \Big] \Bigg\} + 6 \sum_{k_v=2}^{K_{max}-2} \frac{p(k_d = 2, k_v)}{k_d k_v - (k_d - 1)(k_v - 1)} \times \\
& \Bigg\{ \mu_d \Big[k_v (\frac{1}{\Psi_v} - \frac{1}{\sigma_v^{opt}}) - (k_v - 1)(\frac{1}{\Psi_d} - \frac{1}{\sigma_d^{opt}}) \Big] \Bigg\} \quad \text{bits/chip.}
\end{aligned} \tag{4.24}$$

The average power constraints of the dual-class network, for $\forall(k_d, k_v),\ 2 \leq k_d;\ 2 \leq k_v;\ 4 \leq k_d+k_v \leq K_{max}$, are defined as:

$$C_d : \int_{\gamma_d} \sum_{k_d} S_{di}(\gamma_d, k_d, k_v) k_d p(k_d, k_v) p(\gamma_d) d\gamma_d \leq \left(\frac{\lambda_d}{\mu_d}\right) E[S_{di}] \tag{4.25}$$

$$C_v : \int_{\gamma_v} \sum_{k_v} S_{vj}(\gamma_v, k_d, k_v) k_v p(k_d, k_v) p(\gamma_v) d\gamma_v \leq \left(\frac{\lambda_v}{\mu_v}\right) E[S_{vj}]. \tag{4.26}$$

Using (4.3) and (4.4), the power constraints for $\forall(k_d, k_v),\ 2 \leq k_d;\ 2 \leq k_v;\ 4 \leq k_d+k_v \leq K_{max}$, can be simplified to

$$C_d : E[\frac{1}{\gamma_d}]\sigma_d^{opt} k_d p(k_d, k_v)\left(\frac{\lambda_d}{\mu_d}\right)^{-1} \leq 1 \tag{4.27}$$

$$C_v : E[\frac{1}{\gamma_v}]\sigma_v^{opt} k_v p(k_d, k_v)\left(\frac{\lambda_v}{\mu_v}\right)^{-1} \leq 1. \tag{4.28}$$

Optimization Problem

The following optimization problem is considered by using (4.5), (4.10), (4.24), (4.27) and (4.28):

$$\underset{\sigma_d^{opt}, \sigma_v^{opt}}{\text{maximize}} \quad T_{d/c} \tag{4.29a}$$

subject to

$$\frac{E[\frac{1}{\gamma_d}]\sigma_d^{opt} k_d p(k_d, k_v)}{\frac{\lambda_d}{\mu_d}} \leq 1; \quad \frac{E[\frac{1}{\gamma_v}]\sigma_v^{opt} k_v p(k_d, k_v)}{\frac{\lambda_v}{\mu_v}} \leq 1; \tag{4.29b}$$

$$PER_d = PER_{target-d}; \quad PER_v = PER_{target-v}; \tag{4.29c}$$

$$\forall(k_d, k_v)\ ,\ 2 \leq k_d;\ 2 \leq k_v;\ 4 \leq k_d + k_v \leq K_{max}. \tag{4.29d}$$

To obtain the optimum SINR-targets, σ_d^{opt} and σ_v^{opt}, the Lagrangian optimization technique is employed. Similar to our proofs in Chapter 2 and 3, it can easily be shown that the concavity condition for applying this method is satisfied for practical network settings. The Lagrangian function, $J(\sigma_d^{opt}, \sigma_v^{opt})$, is constructed

using (4.29a)-(4.29c), for $\forall(k_d, k_v)$, $2 \leq k_d$; $2 \leq k_v$; $4 \leq k_d{+}k_v \leq K_{max}$:

$$J(\sigma_d^{opt}, \sigma_v^{opt}) = T_{d/c} + \sum_{h=4}^{K_{max}} \sum_{k_d=2}^{h-2} \Bigg\{ \phi_d \Big[E[\frac{1}{\gamma_d}] \sigma_d^{opt} k_d p(k_d, k_v = h - k_d) \left(\frac{\lambda_d}{\mu_d} \right)^{-1} - 1 \Big] + \phi_v \Big[E[\frac{1}{\gamma_v}] \sigma_v^{opt} k_v p(k_d, k_v = h - k_d) \left(\frac{\lambda_v}{\mu_v} \right)^{-1} - 1 \Big] \Bigg\} \tag{4.30}$$

where $\phi_d(k_d, k_v)$ and $\phi_v(k_d, k_v)$ are the Lagrangian multipliers, which for brevity, are denoted with ϕ_d and ϕ_v, respectively.

Solving $\frac{\partial J}{\partial \sigma_d^{opt}} = 0$ and $\frac{\partial J}{\partial \sigma_v^{opt}} = 0$, for $\forall(k_d, k_v)$, $2 \leq k_d$; $2 \leq k_v$; $4 \leq k_d{+}k_v \leq K_{max}$, results in:

$$\sigma_d^{opt} = \sqrt{\frac{\omega_d(k_d, k_v) \left(\frac{\lambda_d}{\mu_d} \right)}{-\phi_d E[\frac{1}{\gamma_d}] k_d p(k_d, k_v)[k_d k_v - (k_d - 1)(k_v - 1)]}} \tag{4.31}$$

$$\sigma_v^{opt} = \sqrt{\frac{\omega_v(k_d, k_v) \left(\frac{\lambda_v}{\mu_v} \right)}{-\phi_v E[\frac{1}{\gamma_v}] k_v p(k_d, k_v)[k_d k_v - (k_d - 1)(k_v - 1)]}} \tag{4.32}$$

where

$$\omega_d(k_d, k_v) = 3p(k_d, k_v = h - k_d) \Big\{ k_d[\lambda_v + (1 - \mu_v)k_v] - (k_v - 1)[\lambda_d + (1 - \mu_d)k_d] \Big\} - 3p(k_d, k_v = K_{max} - k_d) \Big\{ k_d \lambda_v - (k_v - 1)\lambda_d \Big\} + 6p(k_d, k_v = 2) \Big\{ k_d \mu_v \Big\} + 6p(k_d = 2, k_v) \Big\{ (k_v - 1)\mu_d \Big\} \tag{4.33}$$

$$\omega_v(k_d, k_v) = 3p(k_d, k_v = h - k_d) \Big\{ k_v[\lambda_d + (1 - \mu_d)k_d] - (k_d - 1)[\lambda_v + (1 - \mu_v)k_v] \Big\} - 3p(k_d, k_v = K_{max} - k_d) \Big\{ k_v \lambda_d - (k_d - 1)\lambda_v \Big\} + 6p(k_d, k_v = 2) \Big\{ - (k_d - 1)\mu_v \Big\} + 6p(k_d = 2, k_v) \Big\{ k_v \mu_d \Big\}. \tag{4.34}$$

For simplicity, the arguments 'k_d, k_v' in $\omega_d(k_d, k_v)$ and $\omega_v(k_d, k_v)$ are omitted hereafter. The active constraints from (4.27) and (4.28), and the Kuhn-Tucker constraint qualification are then invoked to solve $\frac{\partial J}{\partial \phi_d} = 0$ and $\frac{\partial J}{\partial \phi_v} = 0$, for $\forall(k_d, k_v)$,

$2 \leq k_d;\ 2 \leq k_v;\ 4 \leq k_d+k_v \leq K_{max}$. Thus, ϕ_d and ϕ_v are obtained:

$$\phi_d(k_d,k_v) = -\omega_d E[\frac{1}{\gamma_d}]k_d p(k_d,k_v)\Big(\frac{\lambda_d}{\mu_d}\Big)^{-1} \tag{4.35}$$

$$\phi_v(k_d,k_v) = -\omega_v E[\frac{1}{\gamma_v}]k_v p(k_d,k_v)\Big(\frac{\lambda_v}{\mu_v}\Big)^{-1}. \tag{4.36}$$

Hence, the following optimum OLPC SINR-targets for the data-class and the voice-class are obtained, for $\forall(k_d,k_v),\ 2 \leq k_d;\ 2 \leq k_v;\ 4 \leq k_d+k_v \leq K_{max}$:

$$\sigma_d^{opt}(k_d,k_v) = \frac{\frac{\lambda_d}{\mu_d}}{E[\frac{1}{\gamma_d}]k_d p(k_d,k_v)} \tag{4.37}$$

$$\sigma_v^{opt}(k_d,k_v) = \frac{\frac{\lambda_v}{\mu_v}}{E[\frac{1}{\gamma_v}]k_v p(k_d,k_v)}. \tag{4.38}$$

Replacing σ_d^{opt} and σ_v^{opt} into (4.24), the network optimal sum-throughput with total channel inversion can be determined by:

$$T_{d/c} = 3\sum_{h=4}^{K_{max}}\sum_{k_d=2}^{h-2}\frac{p(k_d,k_v=h-k_d)}{k_dk_v-(k_d-1)(k_v-1)}\Bigg\{[\lambda_d+(1-\mu_d)k_d]\Bigg[k_v(\frac{1}{\Psi_v}-\frac{E[\frac{1}{\gamma_v}]k_vp(k_d,k_v)}{\frac{\lambda_v}{\mu_v}})$$
$$-(k_v-1)(\frac{1}{\Psi_d}-\frac{E[\frac{1}{\gamma_d}]k_dp(k_d,k_v)}{\frac{\lambda_d}{\mu_d}})\Bigg]+[\lambda_v+(1-\mu_v)k_v]\Bigg[k_d(\frac{1}{\Psi_d}-\frac{E[\frac{1}{\gamma_d}]k_dp(k_d,k_v)}{\frac{\lambda_d}{\mu_d}})-$$
$$(k_d-1)(\frac{1}{\Psi_v}-\frac{E[\frac{1}{\gamma_v}]k_vp(k_d,k_v)}{\frac{\lambda_v}{\mu_v}})\Bigg]\Bigg\}-3\sum_{k_d=2}^{K_{max}-2}\frac{p(k_d,k_v=K_{max}-k_d)}{k_dk_v-(k_d-1)(k_v-1)}\Bigg\{\lambda_d\Bigg[k_v(\frac{1}{\Psi_v}-$$
$$\frac{E[\frac{1}{\gamma_v}]k_vp(k_d,k_v)}{\frac{\lambda_v}{\mu_v}})-(k_v-1)(\frac{1}{\Psi_d}-\frac{E[\frac{1}{\gamma_d}]k_dp(k_d,k_v)}{\frac{\lambda_d}{\mu_d}})\Bigg]+\lambda_v\Bigg[k_d(\frac{1}{\Psi_d}-\frac{E[\frac{1}{\gamma_d}]k_dp(k_d,k_v)}{\frac{\lambda_d}{\mu_d}})$$
$$-(k_d-1)(\frac{1}{\Psi_v}-\frac{E[\frac{1}{\gamma_v}]k_vp(k_d,k_v)}{\frac{\lambda_v}{\mu_v}})\Bigg]\Bigg\}+6\sum_{k_d=2}^{K_{max}-2}\frac{p(k_d,k_v=2)}{k_dk_v-(k_d-1)(k_v-1)}\Bigg\{\mu_v\Bigg[k_d(\frac{1}{\Psi_d}$$
$$-\frac{E[\frac{1}{\gamma_d}]k_dp(k_d,k_v)}{\frac{\lambda_d}{\mu_d}})-(k_d-1)(\frac{1}{\Psi_v}-\frac{E[\frac{1}{\gamma_v}]k_vp(k_d,k_v)}{\frac{\lambda_v}{\mu_v}})\Bigg]\Bigg\}+$$
$$6\sum_{k_v=2}^{K_{max}-2}\frac{p(k_d=2,k_v)}{k_dk_v-(k_d-1)(k_v-1)}\Bigg\{\mu_d\Bigg[k_v(\frac{1}{\Psi_v}-\frac{E[\frac{1}{\gamma_v}]k_vp(k_d,k_v)}{\frac{\lambda_v}{\mu_v}})-(k_v-1)\times$$
$$(\frac{1}{\Psi_d}-\frac{E[\frac{1}{\gamma_d}]k_dp(k_d,k_v)}{\frac{\lambda_d}{\mu_d}})\Bigg]\Bigg\}\quad\text{bits/chip.} \tag{4.39}$$

In order to calculate the sum-throughput, $T_{d/c}^{tci}$, with truncated channel inversion implementation, $E[\frac{1}{\gamma_d}]_{\gamma_{d0}} = \int_{\gamma_{d0}}^{\infty} \frac{1}{\gamma_d} p(\gamma_d) d\gamma_d$ and $E[\frac{1}{\gamma_v}]_{\gamma_{v0}} = \int_{\gamma_{v0}}^{\infty} \frac{1}{\gamma_v} p(\gamma_v) d\gamma_v$, should respectively replace $E[\frac{1}{\gamma_d}]$ and $E[\frac{1}{\gamma_v}]$ in the preceding equation. Also, the result should be multiplied by the non-outage probability:

$$p(\gamma_d > \gamma_{d0}, \gamma_v > \gamma_{v0}) = e^{-\gamma_{d0}/E[\gamma_d]} \times e^{-\gamma_{v0}/E[\gamma_v]}. \tag{4.40}$$

Hence, the network sum-throughput for truncated channel inversion policy can be expressed as:

$$T_{d/c}^{tci} = e^{-\gamma_{d0}/E[\gamma_d]} \times e^{-\gamma_{v0}/E[\gamma_v]} \times \Bigg[3 \sum_{h=4}^{K_{max}} \sum_{k_d=2}^{h-2} \frac{p(k_d, k_v = h - k_d)}{k_d k_v - (k_d - 1)(k_v - 1)} \Bigg\{ [\lambda_d + (1-\mu_d) k_d] \times$$
$$\Bigg[k_v \Big(\frac{1}{\Psi_v} - \frac{E[\frac{1}{\gamma_v}]_{\gamma_{v0}} k_v p(k_d, k_v)}{\frac{\lambda_v}{\mu_v}} \Big) - (k_v - 1) \Big(\frac{1}{\Psi_d} - \frac{E[\frac{1}{\gamma_d}]_{\gamma_{d0}} k_d p(k_d, k_v)}{\frac{\lambda_d}{\mu_d}} \Big) \Bigg] + [\lambda_v + (1-\mu_v) k_v] \times$$
$$\Bigg[k_d \Big(\frac{1}{\Psi_d} - \frac{E[\frac{1}{\gamma_d}]_{\gamma_{d0}} k_d p(k_d, k_v)}{\frac{\lambda_d}{\mu_d}} \Big) - (k_d - 1) \Big(\frac{1}{\Psi_v} - \frac{E[\frac{1}{\gamma_v}]_{\gamma_{v0}} k_v p(k_d, k_v)}{\frac{\lambda_v}{\mu_v}} \Big) \Bigg] \Bigg\} - 3 \times$$
$$\sum_{k_d=2}^{K_{max}-2} \frac{p(k_d, k_v = K_{max} - k_d)}{k_d k_v - (k_d - 1)(k_v - 1)} \Bigg\{ \lambda_d \Bigg[k_v \Big(\frac{1}{\Psi_v} - \frac{E[\frac{1}{\gamma_v}]_{\gamma_{v0}} k_v p(k_d, k_v)}{\frac{\lambda_v}{\mu_v}} \Big) - (k_v - 1) \times$$
$$\Big(\frac{1}{\Psi_d} - \frac{E[\frac{1}{\gamma_d}]_{\gamma_{d0}} k_d p(k_d, k_v)}{\frac{\lambda_d}{\mu_d}} \Big) \Bigg] + \lambda_v \Bigg[k_d \Big(\frac{1}{\Psi_d} - \frac{E[\frac{1}{\gamma_d}]_{\gamma_{d0}} k_d p(k_d, k_v)}{\frac{\lambda_d}{\mu_d}} \Big) - (k_d - 1) \times$$
$$\Big(\frac{1}{\Psi_v} - \frac{E[\frac{1}{\gamma_v}]_{\gamma_{v0}} k_v p(k_d, k_v)}{\frac{\lambda_v}{\mu_v}} \Big) \Bigg] \Bigg\} + 6 \sum_{k_d=2}^{K_{max}-2} \frac{p(k_d, k_v = 2)}{k_d k_v - (k_d - 1)(k_v - 1)} \Bigg\{ \mu_v \Bigg[k_d \Big(\frac{1}{\Psi_d}$$
$$- \frac{E[\frac{1}{\gamma_d}]_{\gamma_{d0}} k_d p(k_d, k_v)}{\frac{\lambda_d}{\mu_d}} \Big) - (k_d - 1) \Big(\frac{1}{\Psi_v} - \frac{E[\frac{1}{\gamma_v}]_{\gamma_{v0}} k_v p(k_d, k_v)}{\frac{\lambda_v}{\mu_v}} \Big) \Bigg] \Bigg\} + 6 \times$$
$$\sum_{k_v=2}^{K_{max}-2} \frac{p(k_d = 2, k_v)}{k_d k_v - (k_d - 1)(k_v - 1)} \Bigg\{ \mu_d \Bigg[k_v \Big(\frac{1}{\Psi_v} - \frac{E[\frac{1}{\gamma_v}]_{\gamma_{v0}} k_v p(k_d, k_v)}{\frac{\lambda_v}{\mu_v}} \Big) - (k_v - 1) \times$$
$$\Big(\frac{1}{\Psi_d} - \frac{E[\frac{1}{\gamma_d}]_{\gamma_{d0}} k_d p(k_d, k_v)}{\frac{\lambda_d}{\mu_d}} \Big) \Bigg] \Bigg\} \Bigg] \quad \text{bits/chip.} \tag{4.41}$$

4.2.3 Theoretical and Simulation Results

This section presents theoretical and simulation results for the proposed cross-layer optimization scheme. These results are compared to a VSF- and truncated-ARQ- assisted network where the outer-loop SINR-targets are not optimally selected. Specifically, it is assumed in the non-optimized case that the SINR-targets are kept constant: $\sigma_d = 1/E[1/\gamma_d]$, $\sigma_v = 1/E[1/\gamma_v]$. Sum-throughput improvement achieved by setting the SINR-targets to their optimal values using the proposed approach is highlighted. Note that the average transmit power and the packet loss rates constraints were imposed on the non-optimized case as well. In all of above, continuous-rate spreading factor adaptation has been considered, therefore, results serve as upper-bounds. The general Nakagami-m' block fading model is considered for channel fading. Hence, γ_d and γ_v are Gamma-distributed. For numerical results, without loss of generality, $E[\gamma]$ is taken as the average received SINR of all users within the cell. Note that all results correspond to total channel inversion in the inner-loop, unless otherwise mentioned. Moreover, it is assumed that packet length is $L = 100$ bits with $r = 5$ correctable bits.

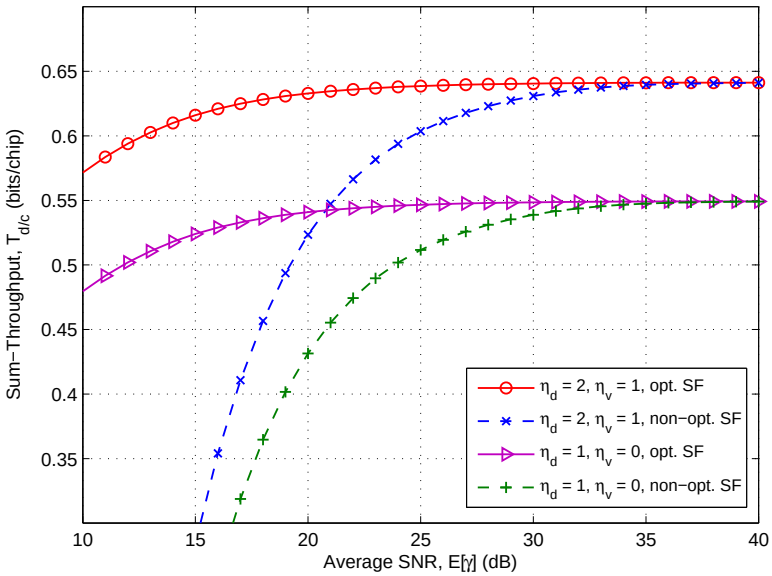

Figure 4.3: Network sum-throughput of the optimized and non-optimized dual-class schemes for different η_d, η_v pairs, $m' = 2$, $\lambda_d = 0.2$, $\lambda_v = 0.3$, $\mu_d = 0.04$, $\mu_v = 0.01$, $K_{max} = 10$, $\Lambda_d = 10^{-3}$, $\Lambda_v = 10^{-4}$.

Fig. 4.3 shows the dual-class network sum-throughput of the optimized and non-optimized schemes. Performance was examined for different ARQ truncation levels. For the data-class, η_d was switched between 2 and 1, and for the voice-class, η_v was set to 1 and 0; as a result of the delay-sensitivity of voice communication a lower ARQ is assumed for this class in comparison to the data-class. Target packet loss rates of data-class and voice-class were set to, $\Lambda_d = 10^{-3}$ and $\Lambda_v = 10^{-4}$, respectively, since typically in practice voice-transmission requires higher quality of service in comparison to data communication. A higher power gain is possible via the optimized scheme. For instance, with $\eta_d = 1$ and $\eta_v = 0$, at sum-throughput of 0.5 bits/chip, a power gain of more than 10 dB is achieved by the optimized scheme over the non-optimized system. In general, voice users have higher terminal priority in comparison to data users, therefore we have assigned a higher traffic load for voice service in our results.

Fig. 4.4 illustrates sum-throughputs of the optimized and non-optimized networks for various target packet loss rates, whilst maximum ARQ levels are kept at $\eta_d = 1$ and $\eta_d = 0$. It can be observed that the optimized network outperforms the non-optimal scheme. For example, for $\Lambda_d = 10^{-3}$, $\Lambda_v = 10^{-5}$, at $E[\gamma] = 20$ dB, a 28% gain in sum-throughput is achieved. Moreover, the optimized scheme yields better gains over the non-optimized scheme under more rigorous QoS requirements.

Simulation results of the optimized and non-optimized systems, for truncated channel inversion policy with a cut-off SINR value of 5 dB for both classes, with various traffic load pairs is demonstrated in Fig. 4.5. To carry out the simulation a practical *Rayleigh shadowed* channel ($m' = 1$) with Log-Normal shadowing standard deviation of 4 dB is considered. Hence, probability density functions of γ_d and γ_v follow composite Exponential/Log-Normal distributions. Moreover, similar conditions, in particular continuous-rate power and rate adaptation, as in the theoretical results are considered. It can be observed that for higher traffic loads sum-throughput decreases and that the optimized scheme sum-throughput performance is superior over the non-optimized scheme.

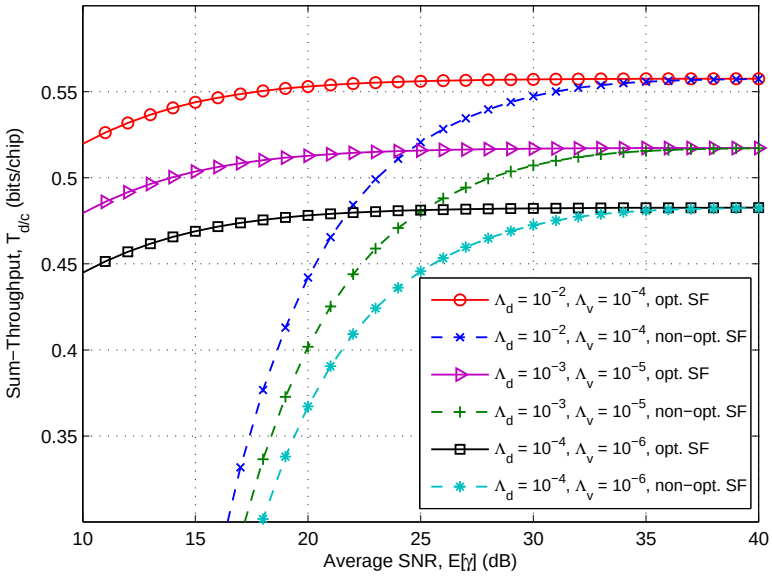

Figure 4.4: Optimized and non-optimized dual-class schemes sum-throughput performances for various Λ_d and Λ_v values, $m' = 2$, $\lambda_d = 0.2$, $\lambda_v = 0.3$, $\mu_d = 0.02$, $\mu_v = 0.01$, $K_{max} = 10$, $\eta_d = 1$, $\eta_v = 0$.

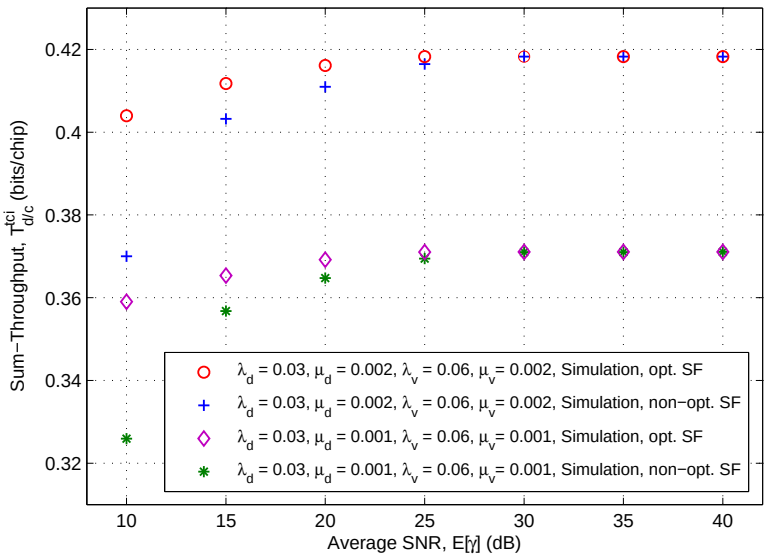

Figure 4.5: Sum-throughput simulation of the optimized and non-optimized dual-class networks with truncated channel inversion policy with several traffic load values, $m' = 1$, $\gamma_{d0} = 5$ dB, $\gamma_{v0} = 5$ dB, $K_{max} = 10$, $\eta_d = 1$, $\eta_v = 0$, $\Lambda_d = 10^{-3}$, $\Lambda_v = 10^{-4}$.

4.3 Shared-Spectrum Heterogeneous OFDM/CDMA Network

4.3.1 Primary/Secondary Network Model

This section outlines the proposed shared-spectrum heterogeneous network model and elucidates the methodology for exploiting spectrum of the primary service in order to maximize the sum-throughput of the secondary service. As it is illustrated in Fig. 4.6, the heterogeneous network consists of two adjacent (uplink) cellular cells: the primary OFDM cell and the secondary CDMA cell. The secondary service does not have the license to access the primary service spectrum, however, it may acquire access through the OSA schemes. Specifically here, the secondary users can access the idle primary spectrum through an AL-OSA scheme. In the AL-OSA scheme, the primary spectrum is divided into a number of sub-channels and the secondary service may exploit one or more of these sub-channels on the condition that the sub-channels are detected to be idle to commence cognitive transmission.

The design is for multi-user cellular mobile systems, with at least one active user in each OFDM/CDMA cell. Fig. 4.7(a) and Fig. 4.7(b) illustrate the number of primary, $k_p(t)$, and secondary, $k_s(t)$, users at time t, which are modeled with discrete one-dimensional K_{pmax}-state and K_{smax}-state M/M/m/m queuing Markov processes, respectively. Hence, the following holds:

$$1 \leq k_p(t) \leq K_{pmax}; \quad 1 \leq k_s(t) \leq K_{smax}. \tag{4.42}$$

User arrival rate and average service time, for primary and secondary services, are denoted with λ_p, $1/\mu_p$, λ_s and $1/\mu_s$, respectively.

The primary network is assumed to spectrum, B_p, is equally divided between $k_p(t)$ active OFDM users. Consequently, each primary radio is allocated an equal channel resource, with an extent of $\frac{1}{k_p(t)}$ over the total spectrum, for transmission of data [82]. Sub-channels that are licensed to primary radios, are partitioned into time slots that are idle on average, with a probability of $(1 - p_B)$, where p_B

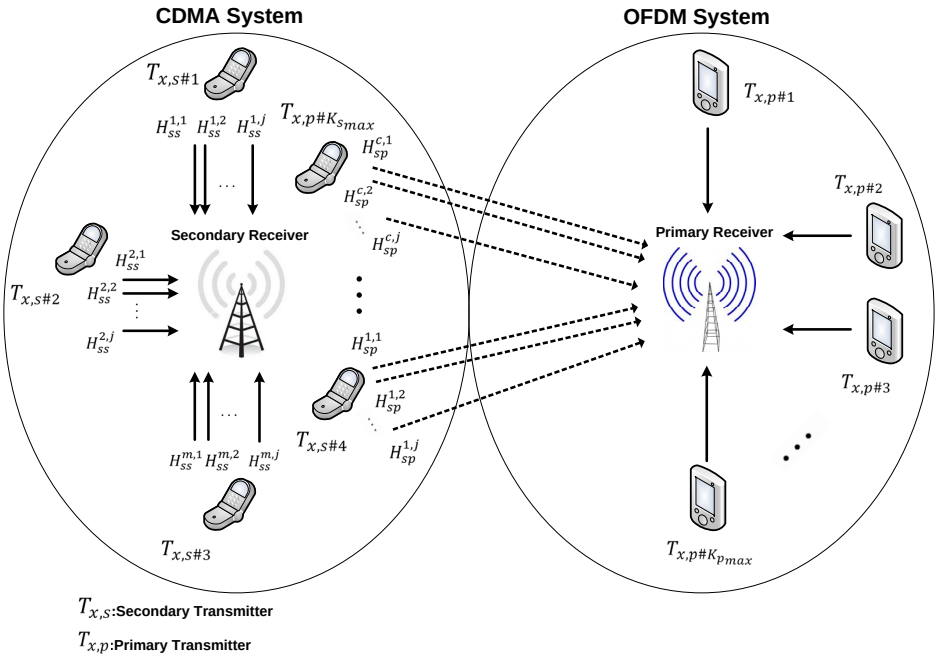

Figure 4.6: Shared-spectrum heterogeneous network with adjacent primary OFDM- and secondary CDMA- cells. The diagram depicts primary and secondary users in operation over L_p-path frequency-selective channels.

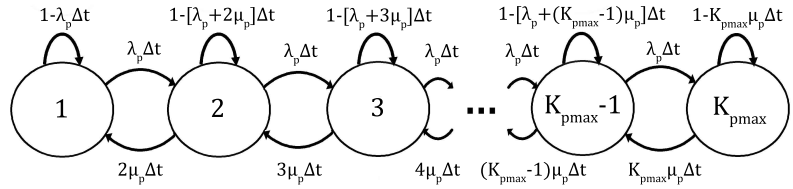

(a)

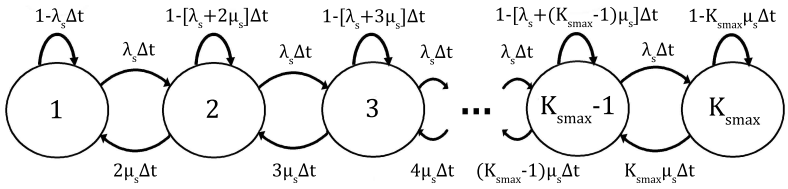

(b)

Figure 4.7: M/M/m/m queuing discrete one-dimensional Markov chains modeling the number of primary users with K_{pmax}-states (Fig. 4.7(a)) and secondary users with K_{smax}-states (Fig. 4.7(b)), in a small time interval Δt, respectively.

denotes the primary users' activity factor, i.e. the probability of inactivity of each primary user. To achieve higher deliverable throughputs, AL-OSA is employed in the heterogeneous network. In AL-OSA, idle parts of the primary spectrum are opportunistically exploited by the secondary users without imposing any interference on the primary receiver. Perfect primary service detection is considered, meaning the secondary users can precisely sense as to whether a given sub-channel is active or idle. Moreover, a zero interference tolerance on both primary and secondary receivers is imposed, and the perfect sensing assumption precludes the probability of any collisions between primary and secondary users. In practice, accurate detection of idle parts of the primary spectrum is challenging and necessitates intelligent and reliable spectrum sensing mechanisms [82, 83].

The secondary service accommodates $k_s(t)$ active secondary CDMA mobile users at time t, with $k_{ss}(t)$ of these users employing the spectrum allocated to the secondary service, whereas $k_{sp}(t)$ users communicate through primary sub-channels. Therefore $k_{ss}(t)$ secondary users operate in a *CDMA-CDMA layout*, whilst $k_s(t) - k_{ss}(t) = k_{sp}(t)$ secondary (*cognitive*) users engage in a *CDMA-OFDM layout*. In this work, the radios in the CDMA-CDMA layout, $k_{ss}(t)$, are referred to as secondary-secondary (SS) users, and the radios in the CDMA-OFDM layout, $k_{sp}(t)$, are labeled as secondary-primary (SP) or cognitive users.

Secondary users generate fixed-length packets of L bits which are added to a buffer after coding. The buffer contents are then converted to DS-CDMA signals using spreading factors $N_{ss}(k_{ss}(t), PER_{ss}^{target})$ and $N_{sp}(PER_{sp}^{target})$, for $k_{ss}(t)$ and $k_{sp}(t)$ users, with target packet error rates, PER_{ss}^{target} and PER_{sp}^{target}, respectively. This methodology will be elaborated as analysis proceeds.

Spreading factor adaptation for secondary-secondary users, $k_{ss}(t)$, is assumed over the secondary bandwidth, B_s. An L_p-path frequency-selective time-varying fading channel and stationary channel gains $H_{ss}^{mj}(t)$, $j = 1, ..., L_p$ at time t for m-th (mobile) user is considered in the CDMA-CDMA layout. The spreading factor adaptation for each of the $k_{sp}(t)$ cognitive users is assumed over a primary sub-channel bandwidth, $B_{sp}(t) = \frac{B_p}{k_p(t)}$. An L_p-path time-varying frequency-selective sub-channel with stationary channel gains $H_{sp}^{cj}(t)$, $j = 1, ..., L_p$ at time t for the c-th *cogni-*

tive (mobile) user in the CDMA-OFDM layout is assumed. We denote the adaptive transmit signal powers of the m-th secondary-secondary user and c-th cognitive user, at time t, over their j-th path, with $S_{ss}^{mj}(\gamma_{ss}^{mj}(t), k_{ss}(t))$ and $S_{sp}^{cj}(\gamma_{sp}^{cj}(t))$, respectively. $E[S_{ss}^{mj}]$ and $E[S_{sp}^{cj}]$ are the corresponding average transmit signal powers, and

$$\gamma_{ss}^{mj}(t) = \frac{|H_{ss}^{mj}(t)|^2 E[S_{ss}^{mj}]}{N_0 B} \tag{4.43}$$

and

$$\gamma_{sp}^{cj}(t) = \frac{|H_{sp}^{cj}(t)|^2 E[S_{sp}^{cj}]}{N_0 B} \tag{4.44}$$

respectively correspond to the instantaneous received SNRs of the m-th secondary-secondary user and c-th secondary-primary user for constant transmit powers of $E[S_{ss}^{mj}]$ and $E[S_{sp}^{cj}]$. The respective total SNR of the m-th secondary-secondary user and the c-th secondary-primary user at time t at the output of the MRC combiner are respectively given by [54]:

$$\gamma_{ss}^{m}(t) = \sum_{j=1}^{L_p} \gamma_{ss}^{mj}(t) \tag{4.45}$$

and

$$\gamma_{sp}^{c}(t) = \sum_{j=1}^{L_p} \gamma_{sp}^{cj}(t). \tag{4.46}$$

Here we assume that a centralized power control mechanism maintains a uniform value, $\gamma_{ss}^{m}(t)$, for all SS users in the CDMA-CDMA layout, and a uniform value, $\gamma_{sp}^{c}(t)$, for all SP users in the CDMA-OFDM layout. In addition, the focus is on single-service cellular cells, therefore all active users in each layout are assumed to have the same SNR-target requirements. For this reason, subscripts m and c are henceforth eliminated from $\gamma_{ss}^{m}(t)$ and $\gamma_{sp}^{c}(t)$, respectively. Moreover, all further time references are omitted for stationary channel conditions.

At the secondary BS, the signal, either transmitted via the secondary or primary bandwidth, goes through a RAKE detector for despreading. After despreading and decoding the received packet, the receiver may, due to erroneous bits, request a retransmission through the truncated-ARQ scheme with maximum number of

retransmissions, η_{ss} and η_{sp}, for SS and SP users, respectively. Perfect channel estimation is assumed at the receiver, as is an error-free feedback path between the receiver and the transmitter.

4.3.2 Dynamic Spectrum Sharing Analysis

In this section, the analysis for integrating the cross-layer design approach with a spectrum sharing strategy is provided. The objective is to devise an algorithm for dynamic allocation of idle primary sub-channels to secondary users, based on random variations in the number of primary and secondary users. To incorporate this idea, firstly, the unique PER and adaptive spreading factor expressions for each CDMA-CDMA and CDMA-OFDM layouts are derived. Next, the secondary sum-throughput expression, T_s, based on random variations in the primary users' activity, is defined. Thirdly, for a given number of idle primary sub-channels, k_{pi}, the secondary sum-throughput expression, $T_s(k_{pi})$, according to random variations in the number of secondary users, is formulated. Finally the optimization problem is constructed, and the unique OLPC optimum SNR-target expression for each layout is obtained. Through employing dynamic AL-OSA, the proposed algorithm exploits the idle primary sub-channels, thus effectively reduces the MAI levels in the CDMA cell, and ultimately maximizes the total deliverable secondary throughput.

CDMA-CDMA Layout

In the CDMA-CDMA layout, the assumption is that the common *optimum* SNR-target for all secondary users in the secondary channel, $\sigma_{ss}^{opt}(k_{ss})$, which maximizes the layout sum-throughput under PER and transmit power constraints, is set and adjusted in the outer-loop according to the number of active SS users, k_{ss}. Using $\sigma_{ss}^{opt}(k_{ss})$ and PER_{ss}^{target}, the corresponding spreading factor $N_{ss}(k_{ss}, PER_{ss}^{target})$ is selected at the frame level, and the signature waveform is generated. Each PHY-layer frame may contain dynamic traffic from the DLL. We also assume that the SS transmit power $S_{ss}^{m}(\gamma_{ss}, k_{ss})$ in the inner-loop is adapted to γ_{ss} and k_{ss} through the

total ($\gamma_{ss}^{trunc} = 0$) or truncated ($\gamma_{ss}^{trunc} > 0$) channel inversion policies

$$\frac{S_{ss}^{m}(\gamma_{ss}, k_{ss})}{E[S_{ss}^{m}]} = \begin{cases} \frac{\sigma_{ss}^{opt}(k_{ss})}{\gamma_{ss}} & \gamma_{ss} > \gamma_{ss}^{trunc} \\ 0 & \gamma_{ss} \leq \gamma_{ss}^{trunc} \end{cases} \tag{4.47}$$

in order to attain $\sigma_{ss}^{opt}(k_{ss})$, where γ_{ss}^{trunc} is a given SS cut-off SNR threshold.

For Normally-distributed MAI at the secondary MRC RAKE receiver, under frequency-selective fading, received SNR of the SS user at the output of the RAKE detector is given by [54]:

$$\gamma_{ss} = \left\{ \frac{q(L_p, \delta) - 1}{2N_{ss}(k_{ss}, PER_{ss}^{target})} + \frac{(k_{ss} - 1)q(L_p, \delta)}{3N_{ss}(k_{ss}, PER_{ss}^{target})} + \frac{N_0}{2E_b\Omega} \right\}^{-1} \tag{4.48}$$

where E_b is the bit energy and Ω indicates the initial path strength of the reference SS user. $q(L_p, \delta)$[1] is a function of total number of paths (L_p) received from the reference user, and the rate of exponential decay of MIP denoted with δ:

$$q(L_p, \delta) = \sum_{m=1}^{L_p} e^{-\delta(m-1)}. \tag{4.49}$$

For the adaptive transmission scheme, $\frac{E_b\Omega}{N_0/2}$ is replaced with the SS users' OLPC optimum SNR-target, $\sigma_{ss}^{opt}(k_{ss})$, which in this work is set and adjusted based on the number of active SS users.

Using the approximate PER formulation of block codes with r-bits error correction capability in Chapter 2, the target packet error rate for SS users, PER_{ss}, is obtained:

$$PER_{ss} = \frac{L! \left\{ \frac{1}{2} \exp\left\{ -\frac{1}{2} \left[\gamma_{ss}\right]^{-1} \right\} \right\}^{r+1}}{(r+1)!(L-r-1)!} \leq \Lambda_{ss}^{\frac{1}{\eta_{ss}+1}} := PER_{ss}^{target} \tag{4.50}$$

where Λ_{ss} is the target packet loss rate after η_{ss} retransmissions. Using (2.6), the corresponding SS spreading factor is derived by solving (4.50) for $N_{ss}(k_{ss}, PER_{ss}^{target})$:

$$N_{ss}(k_{ss}, PER_{ss}^{target}) = \zeta_{ss}(q(L_p, \delta), k_{ss}) \left\{ \frac{1}{\Psi_{ss}} - \frac{1}{\sigma_{ss}^{opt}(k_{ss})} \right\}^{-1} \tag{4.51}$$

[1]Without loss of generality, the notation $q(L_p, \delta)$, is also used for SP users.

where

$$\zeta_{ss}(q(L_p,\delta),k_{ss}) = \frac{q(L_p,\delta)-1}{2} + \frac{(k_{ss}-1)q(L_p,\delta)}{3} \tag{4.52}$$

and

$$\Psi_{ss} = -2\ln\left\{2\left[\frac{(r+1)!(L-r-1)!}{L!}\Lambda_{ss}^{\frac{1}{\eta_{ss}+1}}\right]^{\frac{1}{r+1}}\right\}. \tag{4.53}$$

CDMA-OFDM Layout

In the CDMA-OFDM layout, k_{sp} secondary users exploit the idle primary spectrum, with the aim of minimizing the MAI levels in the CDMA cell. As previously mentioned, each SP user selects one free primary sub-channel at random for secondary communication. The assumption is that the idle primary sub-channels are wide enough to provide suitable bandwidth for transmission of spread-spectrum CDMA data. Perfect sensing is assumed, therefore the probability of a collision among SP users is zero. Further, primary sub-channels are partitioned among independent users in non-overlapping sets of orthogonal sub-channels, therefore there is no MAI experienced by secondary users in the idle sub-channels.

The SP transmit power $S_{sp}^{c}(\gamma_{sp})$ in the inner-loop is adapted to γ_{sp} and k_p through the total ($\gamma_{sp}^{trunc}=0$) or truncated ($\gamma_{sp}^{trunc}>0$) channel inversion policies

$$\frac{S_{sp}^{c}(\gamma_{sp})}{E[S_{sp}^{c}]} = \begin{cases} \frac{\sigma_{sp}^{opt}}{\gamma_{sp}} & \gamma_{sp} > \gamma_{sp}^{trunc} \\ 0 & \gamma_{sp} \leq \gamma_{sp}^{trunc} \end{cases} \tag{4.54}$$

in order to attain σ_{sp}^{opt}, where γ_{sp}^{trunc} is a given SP cut-off SNR threshold. Consequently, with zero MAI, the SNR expression for cognitive users at the output of the MRC RAKE detector is given by:

$$\gamma_{sp} = \left\{\frac{q(L_p,\delta)-1}{2N_{sp}(PER_{sp}^{target})} + \frac{N_0}{2E_b\Omega}\right\}^{-1} \tag{4.55}$$

where E_b is the bit energy and Ω indicates the initial path strength of the reference SP user. For secondary-primary users, $\frac{E_b\Omega}{N_0/2}$ is replaced with the SP users' optimum OLPC SNR-target expression, σ_{sp}^{opt}. The cognitive users operate in individual OFDM sub-channels, therefore they experience no interference from other users. As

a result of this, σ_{sp}^{opt} is obtained based on the quality of the primary channel. This methodology will be elaborated further as analysis proceeds.

Using the approximate PER formulation of block codes with r-bit error correction capability in Chapter 2, the target packet error rate for SP users, PER_{sp}^{target}, is derived:

$$PER_{sp} = \frac{L!\left\{\frac{1}{2}\exp\left\{-\frac{1}{2}\left[\gamma_{sp}\right]^{-1}\right\}\right\}^{r+1}}{(r+1)!(L-r-1)!} \leq \Lambda_{sp}^{\frac{1}{\eta_{sp}+1}} := PER_{sp}^{target} \tag{4.56}$$

where Λ_{sp} is the target packet loss rate after η_{sp} retransmissions. Using (4.55), the corresponding SP spreading factor is derived by solving (4.56) for $N_{sp}(PER_{sp}^{target})$:

$$N_{sp}(PER_{sp}^{target}) = \zeta_{sp}(q(L_p,\delta))\left\{ \frac{1}{\Psi_{sp}} - \frac{1}{\sigma_{sp}^{opt}} \right\}^{-1} \tag{4.57}$$

where

$$\zeta_{sp}(q(L_p,\delta)) = \frac{q(L_p,\delta)-1}{2} \tag{4.58}$$

and

$$\Psi_{sp} = -2\ln\left\{ 2\left[\frac{(r+1)!(L-r-1)!}{L!}\Lambda_{sp}^{\frac{1}{\eta_{sp}+1}} \right]^{\frac{1}{r+1}} \right\}. \tag{4.59}$$

Secondary Sum-Throughput

For the proposed AL-OSA shared-spectrum heterogeneous network, the secondary sum-throughput, T_s, with randomly varying k_p primary users with activity of p_B, can be computed by

$$\begin{aligned} T_s = {} & P_{k_p=1}\left[\sum_{k_{pi}=0}^{k_p} \binom{k_p}{k_{pi}} (1-p_B)^{k_{pi}} {p_B}^{k_p-k_{pi}} T_s(k_{pi}) + P_{k_p}^{inc}(1-\epsilon_p)(1-p_B)T_s(k_{pi}^{++}) \right]_{k_p=1} \\ & + \sum_{k_p=2}^{K_{pmax}-1} P_{k_p}\left[\sum_{k_{pi}=0}^{k_p} \binom{k_p}{k_{pi}} (1-p_B)^{k_{pi}} p_B^{k_p-k_{pi}} T_s(k_{pi}) + P_{k_p}^{inc}(1-\epsilon_p)(1-p_B)T_s(k_{pi}^{++}) - \right. \\ & \left. P_{k_p}^{dec}(1-\epsilon_p)(1-p_B)T_s(k_{pi}^{++}) \right] + P_{k_p=K_{pmax}}\left[\sum_{k_{pi}=0}^{k_p} \binom{k_p}{k_{pi}} (1-p_B)^{k_{pi}} p_B^{k_p-k_{pi}} T_s(k_{pi}) - \right. \\ & \left. P_{k_p}^{dec}(1-\epsilon_p)(1-p_B)T_s(k_{pi}^{++}) \right]_{k_p=K_{pmax}} \quad \text{bits/chip} \end{aligned} \tag{4.60}$$

where $T_s(k_{pi})$ is the secondary sum-throughput given k_{pi} primary sub-channels, out of a total of k_p, are not active. P_{k_p} is the probability that there are k_p active primary users in the OFDM cell, and $P_{k_p}^{inc}(=\lambda_p)$ and $P_{k_p}^{dec}(=\mu_p k_p)$ denote, respectively, the probability that the number of primary users increases or decreases by one. Moreover, $T_s(k_{pi}^{++})$ denotes the additional secondary sum-throughput, given a new primary sub-channel becomes free, with a probability of $(1-p_B)P_{k_p}^{inc}$, in a given frame. In the event that the number of idle primary sub-channels is reduced by one, with a probability of $(1-p_B)P_{k_p}^{dec}$, $T_s(k_{pi}^{++})$ is deducted from the achievable sum-throughput in the respective frame. $\epsilon_p = \frac{\delta_p}{T_{pf}}$, where T_{pf} denotes primary users' frame duration and new interfering primary user starts transmission δ_p seconds after the start of a new frame.

The secondary sum-throughput expression in (4.60) consists of three terms, corresponding to the achievable throughputs for events where the number of active primary users is $k_p = 1$, $k_p \in \{3, ..., K_{pmax} - 1\}$ and $k_p = K_{pmax}$, respectively. Using $\rho_p = \lambda_p/\mu_p$ to denote the primary service traffic load, the probability of k_p active users in the primary cell is expressed as:

$$P_{k_p} = \frac{\rho_p^{k_p - 1}}{k_p! \psi_p} \tag{4.61}$$

where

$$\psi_p = \sum_{n=1}^{K_{pmax}} \frac{\rho_p^{n-1}}{n!}. \tag{4.62}$$

The secondary sum-throughput, given there are k_s active secondary users and k_{pi} idle primary sub-channels, $T_s(k_{pi})$, is defined as the aggregate throughputs of the SS users in the CDMA channel and the SP users exploiting the idle OFDM sub-channels. The protocol for dynamic allocation of secondary users into CDMA-CDMA and CDMA-OFDM layouts, is formulated through the following two cases.

Case 1. $k_s > k_{pi}$

This case corresponds to the event where the number of free primary sub-channels is less than the number of active secondary users. Here, each idle sub-channel is allocated to one secondary user for transmission of data. The other secondary

users would have to operate in the secondary spectrum. Hence, in this case, $k_{ss} \in \{1, 2, ..., K_{smax} - k_{sp}\}$ and $k_{sp} = k_{pi}$. If a new secondary user becomes active, it will be placed in the CDMA-CDMA layout, since all the free primary sub-channels are occupied by the k_{sp} SP users.

Case 2. $k_s \leq k_{pi}$

In this scenario, the number of idle primary sub-channels is more than the number of active secondary users. Therefore we allocate each free primary sub-channel to one CDMA user with the goal of minimizing MAI in the secondary channel. The design is so that at least one secondary user is present in the secondary spectrum at all times. Therefore, in this case, $k_{ss} = 1$ and $k_{sp} \in \{1, 2, ..., K_{smax} - 1\}$. Upon arrival of a new secondary user within a frame, it is allocated to the OFDM-CDMA layout and thus exploits one idle primary sub-channel.

Consequently, denoting the occurrence of events *Case 1* and *Case 2* with '$1_{k_s>k_{pi}}$' ($\equiv 1$ if $k_s > k_{pi}$, else 0) and '$1_{k_s \leq k_{pi}}$' ($\equiv 1$ if $k_s \leq k_{pi}$, else 0), respectively, the secondary sum-throughput, given k_{pi} primary sub-channels are idle, is derived:

$$T_s(k_{pi}) = P_{k_s=1}\Bigg\{1_{k_s>k_{pi}} \times \Bigg[\Big[\frac{k_{ss}}{N_{ss}(k_{ss}, PER_{ss}^{target})}\Big]_{k_{ss}=1} + \frac{P_{k_s}^{inc}(1-\epsilon_s)}{N_{ss}(k_{ss}, PER_{ss}^{target})}\Bigg]_{k_s=1} +$$
$$1_{k_s \leq k_{pi}} \times \Bigg[\Big[\frac{k_{ss}}{N_{ss}(k_{ss}, PER_{ss}^{target})}\Big]_{k_{ss}=1} + \frac{P_{k_s}^{inc}(1-\epsilon_s)}{N_{sp}(PER_{sp}^{target})}\Bigg]_{k_s=1}\Bigg\} + \sum_{k_s=2}^{K_{smax}-1} P_{k_s}\Bigg\{1_{k_s>k_{pi}} \times$$
$$\Bigg[\Big[\frac{k_{ss}}{N_{ss}(k_{ss}, PER_{ss}^{target})}\Big]_{k_{ss}=k_s-k_{pi}} + \Big[\frac{k_{sp}}{N_{sp}(PER_{sp}^{target})}\Big]_{k_{sp}=k_{pi}} + \frac{P_{k_s}^{inc}(1-\epsilon_s)}{N_{ss}(k_{ss}, PER_{ss}^{target})} -$$
$$\frac{P_{k_s}^{dec}(1-\epsilon_s)}{N_{ss}(k_{ss}, PER_{ss}^{target})}\Bigg] + 1_{k_s \leq k_{pi}} \times \Bigg[\Big[\frac{k_{ss}}{N_{ss}(k_{ss}, PER_{ss}^{target})}\Big]_{k_{ss}=1} + \Big[\frac{k_{sp}}{N_{sp}(PER_{sp}^{target})}\Big]_{k_{sp}=k_s-1}$$
$$+ \frac{P_{k_s}^{inc}(1-\epsilon_s)}{N_{sp}(PER_{sp}^{target})} - \frac{P_{k_s}^{dec}(1-\epsilon_s)}{N_{sp}(PER_{sp}^{target})}\Bigg]\Bigg\} + P_{k_s=k_{smax}}\Bigg\{1_{k_s>k_{pi}} \times$$
$$\Bigg[\Big[\frac{k_{ss}}{N_{ss}(k_{ss}, PER_{ss}^{target})}\Big]_{k_{ss}=k_s-k_{pi}} + \Big[\frac{k_{sp}}{N_{sp}(PER_{sp}^{target})}\Big]_{k_{sp}=k_{pi}} - \frac{P_{k_s}^{dec}(1-\epsilon_s)}{N_{ss}(k_{ss}, PER_{ss}^{target})}\Bigg]_{k_s=k_{smax}}$$
$$+ 1_{k_s \leq k_{pi}} \times \Bigg[\Big[\frac{k_{ss}}{N_{ss}(k_{ss}, PER_{ss}^{target})}\Big]_{k_{ss}=1} + \Big[\frac{k_{sp}}{N_{sp}(PER_{sp}^{target})}\Big]_{k_{sp}=k_s-1} -$$
$$\frac{P_{k_s}^{dec}(1-\epsilon_s)}{N_{sp}(PER_{sp}^{target})}\Bigg]_{k_s=k_{smax}}\Bigg\} \quad \text{bits/chip} \tag{4.63}$$

where $P_{k_s}^{inc}(=\lambda_s)$ and $P_{k_s}^{dec}(=\mu_s k_s)$ denote, respectively, the probability that the number of secondary users increases or decreases by one. $\epsilon_s = \frac{\delta_s}{T_{sf}}$, where T_{sf} is the duration of a secondary user frame and new interfering secondary user starts transmission δ_s seconds after the start of a new frame. The probability of increase or decrease by more than one user within a frame is assumed to be zero, in both primary and secondary queueing processes. For analytical convenience, we assume that a change in the number of primary/secondary users can only occur at the beginning of a frame, i.e. $\epsilon_p \ll 1$ and $\epsilon_s \ll 1$. Hence, ϵ_p and ϵ_s can be neglected in (4.60) and (4.63), respectively. Denoting the secondary service traffic load by $\rho_s = \lambda_s/\mu_s$, the probability of k_s active users in the secondary cell is given by:

$$P_{k_s} = \frac{\rho_s^{k_s-1}}{k_s!\psi_s} \tag{4.64}$$

where

$$\psi_s = \sum_{n=1}^{K_{smax}} \frac{\rho_s^{n-1}}{n!}. \tag{4.65}$$

Optimization Problem

The following optimization problem is considered:

$$\underset{\sigma_{ss}^{opt}(k_{ss});\sigma_{sp}^{opt}}{\text{maximize}} \quad T_s(k_{pi}) \tag{4.66a}$$

subject to:

$$C_{ss} \tag{4.66b}$$

$$C_{sp} \tag{4.66c}$$

$$PER_{ss} = PER_{ss}^{target}; \quad PER_{sp} = PER_{sp}^{target}; \tag{4.66d}$$

$$\forall(k_s, k_p)\ ,\ 1 \le k_s \le k_{smax};\ 1 \le k_p \le k_{pmax} \tag{4.66e}$$

where C_{ss} and C_{sp} are used to denote the average power constraints on secondary-secondary and secondary-primary users, respectively. To maximize the objective function, the SS optimum SNR-target, $\sigma_{ss}^{opt}(k_{ss})$, has to be derived. SP optimum SNR-target, σ_{sp}^{opt}, serves as a non-adaptive parameter in the optimization problem. Similar to previous chapters, the Lagrangian algorithm can be employed to solve

this optimization problem. The maximum total deliverable secondary throughput for total channel inversion policy, according to random variations in the number of secondary users, can therefore be expressed as:

$$T_s(k_{pi}) = P_{k_s=1}\Bigg\{1_{k_s>k_{pi}}\times\Bigg[\Bigg[(k_{ss}+\lambda_s)\zeta_{ss}^{-1}(q(L_p,\delta))\{\frac{1}{\Psi_{ss}}-\frac{E[1/\gamma_{ss}]P_{k_{ss}}}{\rho_s-(1-p_B)}\}\Bigg]_{k_{ss}=1}\Bigg]_{k_s=1}$$
$$+1_{k_s\leq k_{pi}}\times\Bigg[\Bigg[\zeta_{ss}^{-1}(q(L_p,\delta))\{\frac{1}{\Psi_{ss}}-E[1/\gamma_{ss}]P_{k_{ss}}\}\Bigg]_{k_{ss}=1}+\lambda_s\zeta_{sp}^{-1}(q(L_p,\delta))\times$$
$$\{\frac{1}{\Psi_{sp}}-E[1/\gamma_{sp}]\}\Bigg]_{k_s=1}\Bigg\}+\sum_{k_s=2}^{K_{smax}-1}P_{k_s}\Bigg\{1_{k_s>k_{pi}}\times\Bigg[\Bigg[(k_{ss}+\lambda_s-\mu_s k_s)\zeta_{ss}^{-1}(q(L_p,\delta))\times$$
$$\{\frac{1}{\Psi_{ss}}-\frac{E[1/\gamma_{ss}]P_{k_{ss}}k_{ss}}{\rho_s-(1-p_B)}\}\Bigg]_{k_{ss}=k_s-k_{pi}}+\Bigg[k_{sp}\zeta_{sp}^{-1}(q(L_p,\delta))\{\frac{1}{\Psi_{sp}}-E[1/\gamma_{sp}]\}\Bigg]_{k_{sp}=k_{pi}}\Bigg]+$$
$$1_{k_s\leq k_{pi}}\times\Bigg[\Bigg[k_{ss}\zeta_{ss}^{-1}(q(L_p,\delta))\{\frac{1}{\Psi_{ss}}-E[1/\gamma_{ss}]P_{k_{ss}}\}\Bigg]_{k_{ss}=1}+\Bigg[(k_{sp}+\lambda_s-\mu_s k_s)\times$$
$$\zeta_{sp}^{-1}(q(L_p,\delta))\{\frac{1}{\Psi_{sp}}-E[1/\gamma_{sp}]\}\Bigg]_{k_{sp}=k_s-1}\Bigg]\Bigg\}+P_{k_s=k_{smax}}\Bigg\{1_{k_s>k_{pi}}\times\Bigg[\Bigg[(k_{ss}-\mu_s k_s)\times$$
$$\zeta_{ss}^{-1}(q(L_p,\delta))\{\frac{1}{\Psi_{ss}}-\frac{E[1/\gamma_{ss}]P_{k_{ss}}k_{ss}}{\rho_s-(1-p_B)}\}\Bigg]_{k_{ss}=k_s-k_{pi}}+\Bigg[k_{sp}\zeta_{sp}^{-1}(q(L_p,\delta))\{\frac{1}{\Psi_{sp}}-$$
$$E[1/\gamma_{sp}]\}\Bigg]_{k_{sp}=k_{pi}}\Bigg]_{k_s=k_{smax}}+1_{k_s\leq k_{pi}}\times\Bigg[\Bigg[k_{ss}\zeta_{ss}^{-1}(q(L_p,\delta))\{\frac{1}{\Psi_{ss}}-E[1/\gamma_{ss}]P_{k_{ss}}\}\Bigg]_{k_{ss}=1}+$$
$$\Bigg[(k_{sp}-\mu_s k_{smax})\zeta_{sp}^{-1}(q(L_p,\delta))\times\{\frac{1}{\Psi_{sp}}-E[1/\gamma_{sp}]\}\Bigg]_{k_{sp}=k_s-1}\Bigg]_{k_s=k_{smax}}\Bigg\}\quad\text{bits/chip.}\tag{4.67}$$

In order to employ the truncated channel inversion (tci) policy, $E[1/\gamma_{ss}]_{\gamma_{ss}^{trunc}} = \int_{\gamma_{ss}^{trunc}}^{\infty}\frac{1}{\gamma_{ss}}p(\gamma_{ss})d\gamma_{ss}$ and $E[1/\gamma_{sp}]_{\gamma_{sp}^{trunc}} = \int_{\gamma_{sp}^{trunc}}^{\infty}\frac{1}{\gamma_{sp}}p(\gamma_{sp})d\gamma_{sp}$, should respectively replace $E[1/\gamma_{ss}]$ and $E[1/\gamma_{sp}]$. The optimal total deliverable secondary sum-throughput for truncated channel inversion policy, given there are k_{pi} idle primary sub-channels, can therefore be obtained by inserting $E[1/\gamma_{ss}]_{\gamma_{ss}^{trunc}}$ and $E[1/\gamma_{sp}]_{\gamma_{sp}^{trunc}}$ in the preceding sum-throughput expression in (4.67) and multiplying it by the non-outage transmission probability, $p(\gamma_{ss}>\gamma_{ss}^{trunc},\gamma_{sp}>\gamma_{sp}^{trunc}) = e^{-\gamma_{ss}^{trunc}/E[\gamma_{ss}]}\times e^{-\gamma_{sp}^{trunc}/E[\gamma_{sp}]}$.

4.3.3 Performance Evaluation

In this section we evaluate the performance of the shared-spectrum heterogeneous network using our proposed dynamic cross-layer resource allocation algorithm. The performance of the cross-layer shared-spectrum system is compared to a *non-shared-spectrum* cross-layer scheme. It is assumed that all secondary users in the non-shared-spectrum case operate in the CDMA channels. Improvements in total deliverable secondary throughput achieved by employing dynamic AL-OSA to the primary spectrum and setting the OLPC SNR-targets of SS and SP users to their optimal values, is highlighted. The achievable gain in secondary sum-throughput is studied for various settings of the parameters in the secondary and primary systems. In particular the impact of adopting different primary users' activity factors is investigated. Continuous-rate power and rate adaptation is incorporated in the results. Furthermore, perfect sensing and perfect CSI availability is assumed. Hence, the results presented in this section should be regarded as upper-bounds for practical cases with discrete-rate adaptation, imperfect sensing and non/partial CSI. The secondary channels and primary sub-channels are modeled by frequency-selective Nakagami-m fading. Hence, γ_{ss} and γ_{sp} are Gamma-distributed. Note that all results correspond to total channel inversion in the inner-loop, unless otherwise mentioned. Moreover, it is assumed that packet length is $L = 100$ bits with $r = 7$ correctable bits.

Fig. 4.8 illustrates the achievable secondary sum-throughput in optimized AL-OSA system for different number of idle primary sub-channels. In the case of $k_{pi} = 0$, results correspond to the non-shared-spectrum system, where all users operate in the secondary spectrum. It can be observed that, as the number of available sub-channels moves away from 0, significant gains in total deliverable secondary throughput are achieved. This is due to two main reasons: 1) Cognitive users in the primary sub-channels experience no MAI from other CDMA users, therefore they can operate at significantly higher data rates (lower spreading factors) with more transmit power, 2) consequently, the MAI in the secondary spectrum is minimized as SP users exploit the inactive parts of the primary spectrum, thus the throughout performance of SS users in the CDMA cell is enhanced. The performance with

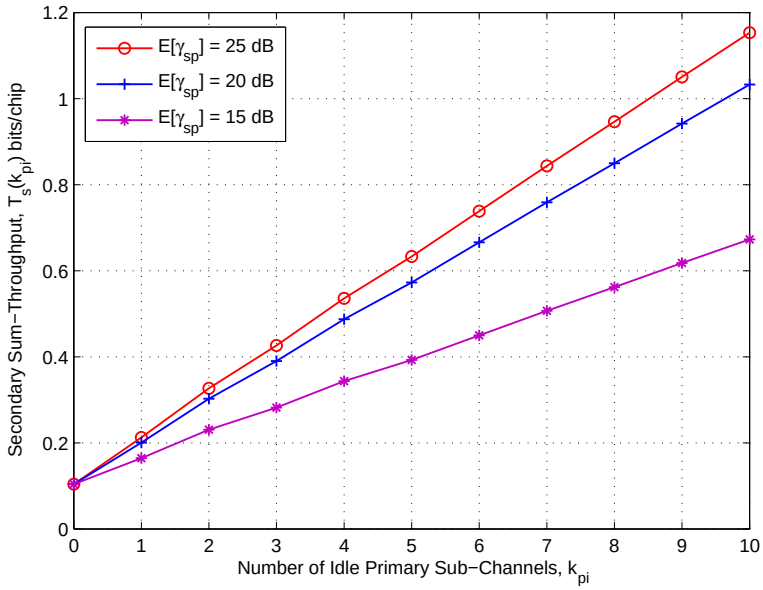

Figure 4.8: Optimized AL-OSA system secondary sum-throughput based on the number of idle primary sub-channels, with different average received SP SNR values, $m = 2$, $L_p = 4$, $\delta = 0$, $E[\gamma_{ss}] = 10$ dB, $K_{smax} = 30$, $K_{pmax} = 20$, $\Lambda_{ss} = 10^{-4}$, $\Lambda_{sp} = 10^{-3}$, $\eta_{ss} = 1$, $\eta_{sp} = 1$, $\lambda_s = 0.4$, $\lambda_p = 0.3$, $\mu_s = 0.02$, $\mu_p = 0.06$.

various average SP SNR values ($E[\gamma_{sp}]$), whilst the average SS SNR is set to a constant lower number, $E[\gamma_{ss}] = 10$ dB, is also depicted in Fig. 4.8. A higher average SP SNR results in better throughputs; however, it can be seen that the gain is reduced for higher $E[\gamma_{sp}]$ values.

Fig. 4.9 presents the achievable improvements in total deliverable secondary throughput by exploiting the idle primary sub-channels and effectively reducing the interference levels. To better observe the impact of AL-OSA scheme in minimizing MAI, without loss of generality, average SNR of SS and SP users are taken to be the same. In addition to the gains achieved by exploiting more primary sub-channels, for higher average SNRs, the sum-throughput gain of the 'AL-OSA scheme with higher idle primary sub-channels', over the 'AL-OSA scheme with lower primary spectrum availability' and the 'non-shared-spectrum case', is considerably increased. The reason behind this is the fact that under better channel conditions and without any MAI, cognitive users can utilize the primary spectrum much more effectively.

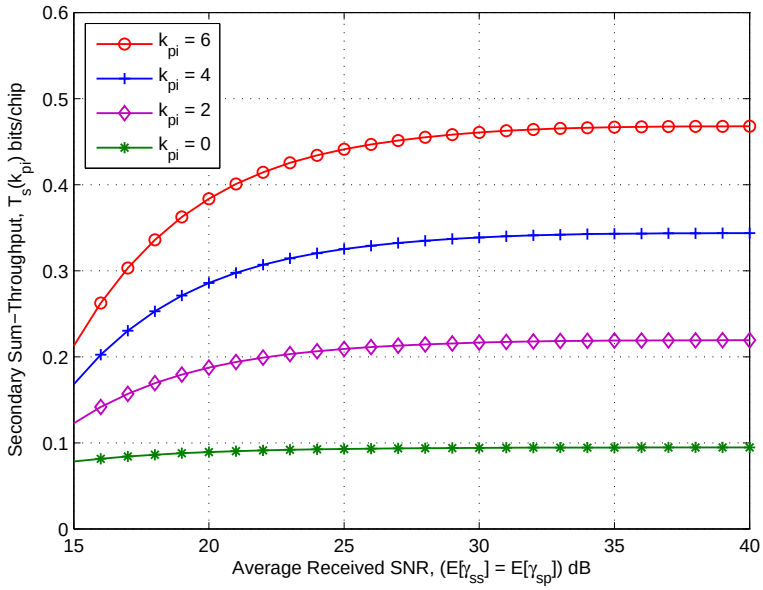

Figure 4.9: Total deliverable secondary throughput using the optimized shared-spectrum scheme with different SNR and k_{pi} values, $m = 2$, $L_p = 5$, $\delta = 0$, $K_{smax} = 20$, $K_{pmax} = 10$, $\Lambda_{ss} = 10^{-3}$, $\Lambda_{sp} = 10^{-5}$, $\eta_{ss} = 1$, $\eta_{sp} = 0$, $\lambda_s = 0.4$, $\lambda_p = 0.3$, $\mu_s = 0.01$, $\mu_p = 0.03$.

Total deliverable secondary throughput for various values of L_p, η_{ss}, η_{sp}, Λ_{ss} and Λ_{sp} is presented in Fig. 4.10. Increasing η_{ss} and η_{sp}, improves sum-throughput, however, in practice high number of ARQ retransmissions is not desirable due to the induced delay. Specifically, here, lower maximum number of retransmissions is assigned to SP users over SS users, to take into account the probability of primary users returning or new ones arriving. However, we assign less stringent packet loss rate constraints to SP users in comparison to SS users (i.e. $\Lambda_{sp} > \Lambda_{ss}$), considering the cognitive users in primary sub-channels experience no MAI. Increasing the number of paths for fixed PER_{ss} and PER_{sp}, requires larger spreading factors and thus lower secondary sum-throughput is obtained.

Fig. 4.11, illustrates the achievable secondary sum-throughput in optimized AL-OSA system based on number of primary users with different activity factors. The case where $p_B = 1$, corresponds to the non-shared-spectrum system. Evidently, higher number of primary users with low activity (i.e. small p_B) increases the

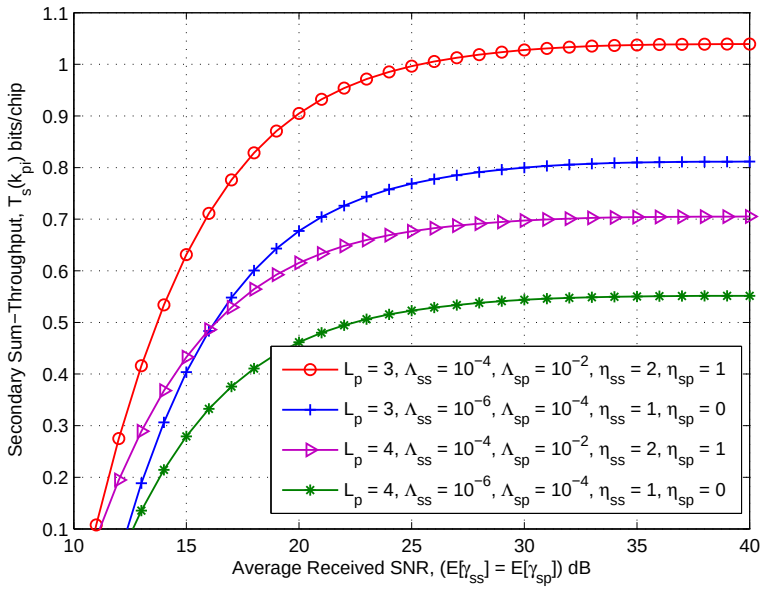

Figure 4.10: Optimized AL-OSA system secondary performance with various number of paths, target packet error rates, and ARQ retransmissions, $k_{pi} = 5$, $m = 2$, $\delta = 0$, $K_{smax} = 30$, $K_{pmax} = 10$, $\lambda_s = 0.2$, $\lambda_p = 0.3$, $\mu_s = 0.01$, $\mu_p = 0.01$.

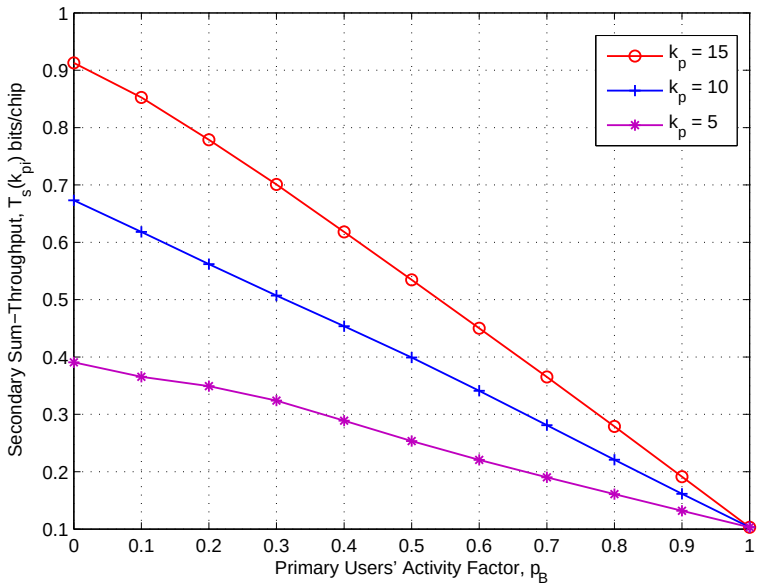

Figure 4.11: Maximum achievable secondary sum-throughput in optimized AL-OSA system based on number of active primary users with different activity factors, $m = 2$, $L_p = 4$, $\delta = 0$, $K_{smax} = 30$, $K_{pmax} = 20$, $\Lambda_{ss} = 10^{-4}$, $\Lambda_{sp} = 10^{-3}$, $\eta_{ss} = 1$, $\eta_{sp} = 1$, $\lambda_s = 0.4$, $\lambda_p = 0.3$, $\mu_s = 0.02$, $\mu_p = 0.06$.

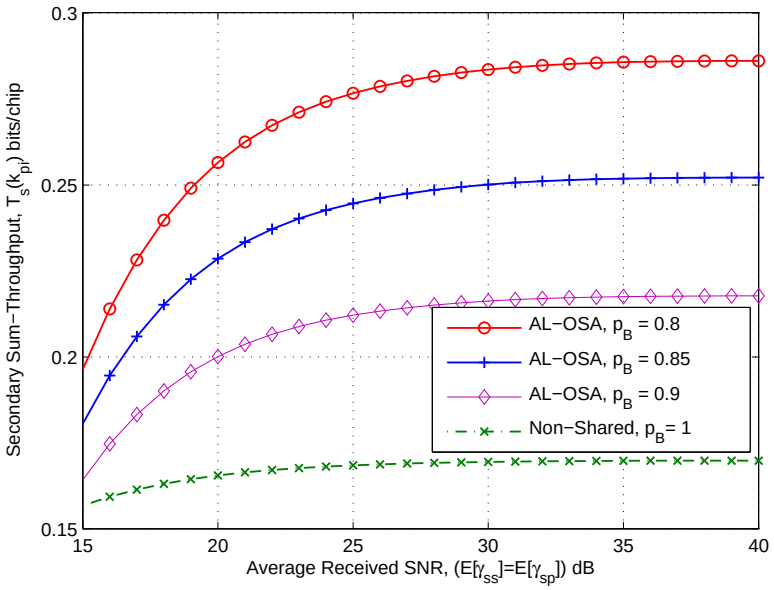

Figure 4.12: Maximum achievable secondary sum-throughput of AL-OSA and non-shared-spectrum schemes, $k_p = 5$, $m = 2$, $L_p = 3$, $\delta = 0$, $K_{smax} = 20$, $K_{pmax} = 20$, $\Lambda_{ss} = 10^{-3}$, $\Lambda_{sp} = 10^{-2}$, $\eta_{ss} = 2$, $\eta_{sp} = 0$, $\lambda_s = 0.4$, $\lambda_p = 0.2$, $\mu_s = 0.1$, $\mu_p = 0.2$.

availability of idle primary sub-channels and therefore enhances the total deliverable secondary throughput. It can be observed that the reduction in achievable sum-throughput is almost linear with increase in primary users' activity factor. In addition, for the same p_B, the achievable gain by the increase in number of primary users, k_p, is greater for lower primary users' activity factors. For example, for $p_B = 0.8$, with $k_p = 15$, a 26% gain in sum-throughput is achieved compared to $k_p = 10$; whereas this relative improvement is increased to 30% for $p_B = 0.7$.

Fig. 4.12 takes a closer look at the performance of the optimized AL-OSA system versus the optimized non-shared-spectrum case using realistic (high) primary network activity factors. It can be observed that employing opportunistic spectrum access significantly enhances throughput performance even with small availability of idle primary sub-channels. In the AL-OSA system the cognitive users can achieve near-optimum capacity performance, whereas in the non-shared-spectrum scheme, CDMA users experience high MAI, in particular due to multipath fading conditions, hence, their throughput performance is severely degraded.

4.4 Conclusions

During the past decade, there has been huge improvement and development in all layers of communication networks, except the PHY-layer. This is mostly because physical layer techniques focused on maximizing capacity under limited radio resources, have already been innovated and implemented. The best (relatively) recent innovation in PHY-layer design, is perhaps the development of MIMO technology. Cognitive radio is a prominent candidate to be the next step towards improving capacity by intelligent and effective utilization of unused and under-used parts of the available radio spectrum. Further, without cross-layer design in context of cognitive radio, e.g. just focusing on PHY-layer performance without considering parameters from higher layers, QoS satisfaction acoss all layers cannot be guaranteed. On the other hand, spectrum sharing among 3G and 4G networks may have great potential, particularly because the transition of upgrading the current 3G UMTS to 4G-LTE is expected to take many years. Dynamic opportunistic spectrum access techniques in heterogeneous networks could improve connectivity and provide more effective utilization of shared-spectrum resources.

In this chapter, firstly, a novel throughput-optimal cross-layer scheme was proposed for a multi-service system of heterogeneous data traffic. The proposed dynamic resource allocation algorithm, implements inner- and outer- loop power control mechanisms, that adapt, uniquely for each service class, transmit power and optimum SINR-target, and hence the corresponding variable spreading factor, to channel variations, number of users, and the requisite PER-target. The number of users was modeled with a two-dimensional discrete Markov chain. The achievable gain in network sum-throughput through our optimized scheme, was demonstrated with theoretical and simulation results for various sets of system parameters.

Next, a novel dynamic spectrum sharing algorithm with cross-layer design for heterogeneous OFDM/CDMA networks was proposed. AL-OSA was employed to exploit the idle parts of the primary spectrum, without imposing any disruption to primary OFDM service. Based on randomly-varying number of users in the cells, each secondary user was dynamically assigned to either an idle primary sub-

channel (CDMA-OFDM layout) or the secondary spectrum (CDMA-CDMA layout), for transmission of data. Using this dynamic spectrum sharing strategy, the cognitive SP users experienced no MAI, and therefore can transmit at higher rate and power. Consequently, exploiting the idle primary sub-channels minimized the MAI in the CDMA channels, hence, SS users achieved higher throughputs. Total deliverable secondary throughput in the optimized AL-OSA system, and improvements achieved relative to the non-shared-spectrum case, were illustrated for various settings of the systems parameters. It was observed that due to the absent of MAI, SP users can achieve near-optimal capacity performance, whilst minimizing the MAI imposed on the SS users. On the other hand, specially due to multipath fading conditions, the CDMA users in the non-shared-spectrum system experienced high levels of MAI, and therefore their sum-throughput performance was severely lowered. Hence, using the optimized cross-layer AL-OSA scheme realized significant improvements in secondary sum-throughput performance, even with high primary users' activity factor and low number of idle primary sub-channels.

4.5 Contributions

In part of this chapter, the cross-layer design technique in Chapter 2 is extended and analysed for a multi-service network of heterogeneous data traffic. According to the service specifications of the classes, we derived unique optimum OLPC SINR-targets and hence optimal spreading factor expressions, as functions of the number of active users in the two classes. We modeled the number of users in the network with a multi-dimensional discrete Markov chain corresponding to two truncated M/M/m/m queuing processes. Different user arrival rates and average service times were considered for the classes. To incorporate the higher terminal priority of voice users, in our results, higher traffic loads were assigned for the voice-class in comparison to the data-class. Due to the delay sensitivity of voice-transmission, a lower maximum number of retransmissions was imposed on the voice users compared to the users of data service. Moreover, different DLL packet loss rate constraints were imposed on the services, since in practice, data users tolerate less stringent

QoS constraints. Sum-throughput performance of the optimized system and the improvements achieved, relative to the non-optimized case, were demonstrated with theoretical and simulation results for various traffic loads, packet loss rates, and ARQ retransmissions. At this point, the contributions of this part of the chapter are summarized:

- Cross-layer optimization technique in Chapter 2 was extended and analysed for a multi-service network of non-real-time data/voice classes.
- Unique expressions for optimum OLPC SINR-targets and hence optimal spreading factors were derived for the heterogeneous data classes.
- Lower target packet loss rates were imposed on the voice-transmission, since in practice data users tolerate less stringent QoS constraints.
- As a result of delay sensitivity of voice service, lower maximum number of retransmissions was assigned to the voice users.
- Higher traffic loads were adopted for the non-real-time voice service, in order to incorporate the higher terminal priority of voice-transmission.
- Sum-throughput performances of the optimized system, and the non-optimized case, where the services SINR-targets were kept constant, under various settings of the network parameters, were studied.
- A considerable gain in the multi-service network sum-throughput is achieved through coupling of PHY-layer and DLL parameters.
- Practical feasibility of the optimized and non-optimized schemes were studied by conducting simulations over a Rayleigh shadowed environment.

Next, a dynamic spectrum sharing algorithm with cross-layer design, was proposed in the context of heterogeneous OFDM/CDMA networks. AL-OSA was employed to utilize the idle parts of the primary spectrum, effectively minimizing the interference levels. Together with dynamic AL-OSA, cross-layer optimization of the PHY-layer and DLL parameters was incorporated to maximize the total deliverable

secondary throughput. To the best of my knowledge, dynamic resource allocation, considering the PHY-layer and DLL parameters, has not yet been addressed in the context of OFDM/CDMA cognitive radio networks. At this point, the contributions of this part of the chapter are summarized below:

- A novel dynamic spectrum sharing algorithm with cross-layer design for heterogeneous OFDM/CDMA networks was proposed.
- Using AL-OSA, idle primary SC-FDMA sub-channels were dynamically allocated to secondary WCDMA users, based on random variations in the number of primary and secondary users.
- Secondary users only exploited the idle primary sub-channels, hence, they imposed no interference on the primary OFDM service.
- Allocating SP users to the primary spectrum, effectively minimized the MAI levels in the CDMA channel. Hence, SS users' throughput performance was significantly improved.
- Cognitive users in the idle primary sub-channels experienced no MAI, therefore they achieved near-optimum capacity performance.
- Total deliverable secondary throughput in the optimized AL-OSA system, and improvements achieved relative to the non-shared-spectrum case, were illustrated for various settings of the systems parameters.
- Without dynamic spectrum sharing, optimized system experienced high MAI, particularly due to multipath fading conditions. Hence, the proposed dynamic AL-OSA algorithm realized high gains in secondary sum-throughput over the non-shared-spectrum case, even with high primary users' activity factor and low number of idle primary sub-channels.

4.6 Appendix C

4.6.1 Table III - Section 4.2 Notation

Symbol	Definition
$k_d(t)$	Number of active data users in the cell at time t
$k_v(t)$	Number of active voice users in the cell at time t
K_{max}	Maximum number of active users supported by the cell
PER_d	Instantaneous packet error rate of data users
PER_v	Instantaneous packet error rate of voice users
$PER_{target-d}$	Packet error rate target for data users
$PER_{target-v}$	Packet error rate target for voice users
B	Channel bandwidth
T_{chip-d}	Data chip duration
T_{chip-v}	Voice chip duration
T_{bit-d}	Data bit duration
T_{bit-v}	Voice bit duration
$g_{di}(t)$	Channel gain for data user-i at time t
$g_{vj}(t)$	Channel gain for voice user-j at time t
$n(t)$	AWGN
$N_0/2$	Two sided power spectral density of AWGN
$I_c(t)$	Interference imposed on reference user by interfering user-c at time t
$\gamma_{di}(t)$	Instantaneous received SINR of data user-i
$\gamma_{vj}(t)$	Instantaneous received SINR of voice user-j
γ_d	Equal received SINR for data-class
γ_v	Equal received SINR for voice-class
$S_{di}(\gamma_d, k_d, k_v)$	ILPC adaptive transmit signal power of data user-i
$S_{vj}(\gamma_v, k_d, k_v)$	ILPC adaptive transmit signal power of voice user-j
$E[S_{di}]$	Average transmit signal power of data user-i
$E[S_{vj}]$	Average transmit signal power of voice user-j
γ_{d0}	Data service SINR threshold for truncated channel inversion policy
γ_{v0}	Voice service SINR threshold for truncated channel inversion policy
BER_d	Instantaneous bit error rate of data users
BER_v	Instantaneous bit error rate of voice users
L	Packet length
δ	New interfering user starts transmission δ seconds after the beginning of the frame
T_f	Frame duration
ϵ	Ratio of δ over frame duration
r	Number of error correction capability bits
E_b	Bit energy
Ω	Reference user path strength
N_d	Adaptive spreading factor for data users
N_v	Adaptive spreading factor for voice users
η_d	Maximum number of retransmissions allowed per data packet
η_v	Maximum number of retransmissions allowed per voice packet
Λ_d	Target packet loss rate for data-class
Λ_v	Target packet loss rate for voice-class
$p(k_d, k_v)$	Joint equilibrium probability of k_d data and k_v voice active users in the network
G	Normalization constant obtained from the set of states in truncated Markov chain

Continued on next page

Symbol	Definition
h	Dummy variable indicating the total number of active users in the network
λ_d	Data-class user arrival rate
λ_v	Voice-class user arrival rate
μ_d	Data-class average service rate
μ_v	Voice-class average service rate
ρ_d	Data-class traffic load
ρ_v	Voice-class traffic load
Δt	Small time interval
C_d	Average power constraint for data service
C_v	Average power constraint for voice service
$\sigma_d^{opt}(k_d, k_v)$	OLPC optimum SINR-target for data service
$\sigma_v^{opt}(k_d, k_v)$	OLPC optimum SINR-target for voice service
$J(\sigma_d^{opt}, \sigma_v^{opt})$	Lagrangian function
$\phi_d(k_d, k_v)$	Lagrangian multiplier for data service
$\phi_v(k_d, k_v)$	Lagrangian multiplier for voice service
$E[\gamma_d]$	Average received SINR of data users with total channel inversion
$E[\gamma_v]$	Average received SINR of voice users with total channel inversion
$E[\frac{1}{\gamma_d}]$	Average inverted received SINR of data users with total channel inversion
$E[\frac{1}{\gamma_v}]$	Average inverted received SINR of voice users with total channel inversion
$E[\gamma_d]_{\gamma_{d0}}$	Average received SINR of data users with truncated channel inversion
$E[\gamma_v]_{\gamma_{v0}}$	Average received SINR of voice users with truncated channel inversion
$E[\frac{1}{\gamma_d}]_{\gamma_{d0}}$	Average inverted received SINR of data users with truncated channel inversion
$E[\frac{1}{\gamma_v}]_{\gamma_{v0}}$	Average inverted received SINR of voice users with truncated channel inversion
$T_{d/c}$	Dual-class network sum-throughput
σ_d	SINR-target for data service in the non-optimized case
σ_v	SINR-target for voice service in the non-optimized case
m'	Nakagami fading parameter

4.6.2 Table IV - Section 4.3 Notation

Symbol	Definition
$k_p(t)$	Number of primary OFDM users at time t
$k_s(t)$	Number of secondary CDMA users at time t
K_{smax}	Maximum number of secondary users supported by the CDMA cell
K_{pmax}	Maximum number of primary users supported by the OFDM cell
$k_{pi}(t)$	Number of idle primary sub-channels at time t
$k_{sp}(t)$	Number of SP users in the CDMA-OFDM layout at time t
$k_{ss}(t)$	Number of SS users in the CDMA-CDMA layout at time t
B_p	Primary service bandwidth
B_s	Secondary service bandwidth
B_{sp}	Primary sub-channel bandwidth
p_B	Primary users' activity factor
PER_{sp}	Instantaneous packet error rate of SP users
PER_{ss}	Instantaneous packet error rate of SS users
PER_{sp}^{target}	Target packet error rate for SP users
PER_{ss}^{target}	Target packet error rate for SS users
$H_{sp}^{cj}(t)$	Channel gain for SP user-c over j-th path at time t
$H_{ss}^{mj}(t)$	Channel gain for SS user-m over j-th path at time t
$n(t)$	AWGN
$N_0/2$	Two sided power spectral density of AWGN
$\gamma_{sp}^{cj}(t)$	Instantaneous SNR of SP user-c over j-th path at time t, with constant transmit power
$\gamma_{ss}^{mj}(t)$	Instantaneous SNR of SS user-m over j-th path at time t, with constant transmit power
$S_{sp}^{cj}(\gamma_{sp}^{cj}(t))$	ILPC adaptive transmit signal power of SP user-c over j-th path at time time t
$S_{ss}^{mj}(\gamma_{ss}^{mj}(t), k_{ss}(t))$	ILPC adaptive transmit signal power of SS user-m over j-th path at time time t
$\gamma_{sp}^{c}(t)$	Received SNR of SP user-c at the output of MRC at time t, with variable transmit power
$\gamma_{ss}^{m}(t)$	Received SNR of SS user-m at the output of MRC at time t, with variable transmit power
$E[S_{sp}^{cj}]$	Average transmit signal power of SP user-c over j-th path
$E[S_{ss}^{mj}]$	Average transmit signal power of SS user-m over j-th path
γ_{sp}^{trunc}	SP users' cut-off SNR threshold for truncated channel inversion policy
γ_{ss}^{trunc}	SS users' cut-off SNR threshold for truncated channel inversion policy
L_p	Number of paths
L	Packet length
r	Number of error correction capability bits
δ	rate of exponential MIP decay
E_b	Bit energy
Ω	Reference user path strength
η_{sp}	Maximum number of retransmissions for SP users
η_{ss}	Maximum number of retransmissions for SS users
T_{pf}	Primary users' frame duration
T_{sf}	Secondary users' frame duration

Continued on next page

Symbol	Definition
ϵ_p	Ratio of δ over T_{pf}
ϵ_s	Ratio of δ over T_{sf}
Δt	Small time interval
N_{sp}	Adaptive spreading factor for SP users
N_{ss}	Adaptive spreading factor for SS users
Λ_{sp}	Target packet loss rate for SP users
Λ_{ss}	Target packet loss rate for SS users
T_s	Total deliverable secondary sum-throughput with random variations in number of primary and secondary users
$T_s(k_{pi}^{++})$	Additional secondary sum-throughput, given a new primary subchannel becomes idle
λ_p	Primary service user arrival rate
λ_s	Secondary service user arrival rate
μ_p	Primary users' average service rate
μ_s	Secondary users' average service rate
ρ_p	Primary service traffic load
ρ_s	Secondary service traffic load
P_{k_p}	Probability that there are k_p active users in the primary cell
P_{k_s}	Probability that there are k_s active users in the secondary cell
$P_{k_{ss}}$	Probability that there are k_{ss} SS users in operation
$P_{k_p}^{inc}$	Probability that the number of primary users increases by one within a frame
$P_{k_p}^{dec}$	Probability that the number of primary users decreases by one within a frame
$P_{k_s}^{inc}$	Probability that the number of secondary users increases by one within a frame
$P_{k_s}^{dec}$	Probability that the number of secondary users decreases by one within a frame
$Case1$	Event where $k_s > k_{pi}$
$Case2$	Event where $k_s \leq k_{pi}$
$1_{k_s>k_{pi}}$	$\equiv 1$ if $k_s > k_{pi}$, else 0
$1_{k_s\leq k_{pi}}$	$\equiv 1$ if $k_s \leq k_{pi}$, else 0
C_{sp}	Average power constraint for SP users
C_{ss}	Average power constraint for SS users
$\sigma_{ss}^{opt}(k_{ss})$	OLPC optimum SNR-target for SS users
σ_{sp}^{opt}	OLPC optimum SNR-target for SP users
$E[\gamma_{sp}]$	Average received SNR of SP users with total channel inversion
$E[\gamma_{ss}]$	Average received SNR of SS users with total channel inversion
$E[\frac{1}{\gamma_{sp}}]$	Average inverted received SNR of SP users with total channel inversion
$E[\frac{1}{\gamma_{ss}}]$	Average inverted received SNR of SS users with total channel inversion
$E[\gamma_{sp}]_{\gamma_{sp}^{trunc}}$	Average received SNR of SP users with truncated channel inversion
$E[\gamma_{ss}]_{\gamma_{ss}^{trunc}}$	Average received SNR of SS users with truncated channel inversion
$E[\frac{1}{\gamma_{sp}}]_{\gamma_{sp}^{trunc}}$	Average inverted received SNR of SP users with truncated channel inversion
$E[\frac{1}{\gamma_{ss}}]_{\gamma_{ss}^{trunc}}$	Average inverted received SNR of SS users with truncated channel inversion
m'	Nakagami fading parameter

The core of science is not a mathematical modeling--it is intellectual honesty. It is a willingness to have our certainties about the world constrained by good evidence and good argument.

Sam Harris

Chapter 5

Conclusions and Future Research Proposals

5.1 Conclusions

The explosive growth in access and demand for diverse wireless applications supplicate intelligent systems capable of expertly adapting parameters across different network layers to link variations. Radio resource management is of eminent importance in design of effective and efficient wireless communication systems. The need for achieving high data rates whilst accommodating multiple classes of traffic with distinct QoS requirements, under limited radio resources and adverse characteristics of wireless channels, heightens the significance of this concept.

The long familiar and widely referred OSI model has been central to the success and proliferation of today's telecommunication networks. However, with the rapid evolution of wireless networks and rising demand for QoS satisfaction, the traditional layered architecture has proved to be inefficient to solve the problems associated with modern wireless networks. To this end, cross-layer design and optimization has enormous potential to obtain global optimal performance and to guarantee the QoS demands in all layers of the protocol stack.

In the last decade, a great deal of attention has been paid to improvement and development in all layers of the communication network, except possibly the physical layer. In fact, further enhancements in PHY-layer capacity, have proved to be very

challenging. Cognitive radio is a prominent candidate to be the next step towards improving capacity. Further, cognitive radio is considered as an effective tool to solve the problem of spectrum shortage, through intelligent and efficient utilization of the available radio spectrum.

In addition, co-operation among cellular mobile networks that incorporate different radio access technologies is significantly important to utilize the shared resources more effectively and to support high network capacity. In this sense, there is still large room for improving the current third generation of cellular mobile systems as such networks are expected to co-exist with the emerging fourth generation technologies for years to come. Similar trend has been experienced in the past, with second generation technologies still in operation today many years after the emergence of 3G networks. During the transition period of upgrading the existing 3G networks to 4G, it is believed that service providers will accommodate 3G and 4G services simultaneously. Hence, further enhancements in current 3G networks would be particularly valuable in future heterogeneous wireless networks.

Code division multiple access is the dominant air interface technology in current 3G universal mobile telecommunication systems. Adaptive resource allocation strategies are essential for achieving desirable performance in CDMA networks. In particular dynamic power control is a necessity towards tackling multiple access interference and near-far effect. In UMTS standards, the uplink power control within CDMA networks consists of outer-loop power control and inner-loop power control: the former provides the required transmission quality by setting the SNR-target and the latter aims to attain the transmission quality by increasing/decreasing the transmit power. In practice, pre-defined look up tables select the transmission quality in terms of SNR-target based on the received BER. However, without exploiting the optimum OLPC SNR-target, maximum throughput is not achieved.

Inspired by these challenges, this thesis focused on cross-layer design and optimization in heterogeneous cellular mobile networks, involving the parameters from physical layer and data link layer, with the goal of maximizing the total deliverable throughput. With regards to radio resource management in PHY-layer, this thesis developed optimized schemes for power control and rate control. In particular,

closed-form expressions for optimal closed-loop power control mechanism and the corresponding optimal variable spreading factors were derived. Truncated automatic repeat request mechanism at the DLL, together with linear block codes, were integrated in the design for error control. With regards to cognitive radio, a dynamic spectrum sharing algorithm integrated with a cross-layer design, was proposed in the context of cognitive heterogeneous OFDM/CDMA networks. Frequency -flat and -selective fading channels, using Nakagami-m fading, in single- and multi- service scenarios were considered. The performances of the proposed cross-layer schemes were compared to non-optimized systems, and other state-of-the-art resource allocation algorithms for throughput maximization in multi-user systems. The achievable gain in performance was accomplished in the presence of transmission power constraints, as well as QoS requirements.

In Chapter 1, a survey on fundamental concepts of current and emerging cellular mobile networks was conducted. Following a brief history on wireless communication, an overview of cellular mobile systems and the layered network architecture was given. Radio access technologies, with single- and multi- carrier transmission modulation schemes, were studied. Particular emphasis was placed on functionalities and associated challenges of 3G UMTS and 4G-LTE networks. Performance evaluation measures of mobile communication systems over fading channels were discussed in detail. Furthermore, radio resource management, cross-layer design and spectrum sharing concepts were discussed.

In Chapter 2, a novel cross-layer design was developed, facilitating joint optimization of closed-loop power control and rate control in the physical layer with truncated-ARQ in the data link layer. The focus was on the uplink of a single-cell multi-user conventional cellular DS-CDMA communication system. Frequency-flat fading channels and conventional matched-filter detector in the receiver were considered. The number of active users in the cell was modeled with a one-dimensional discrete Markov chain. Given an ARQ delay limit, and for a prescribed maximum target packet loss rate in the DLL, closed-form expressions for the optimum OLPC SNR-target and the corresponding adaptive spreading factors in the PHY-layer were analytically derived, as functions of the Normally-distributed MAI in the cell. Due

to the significance of near-far effect in CDMA systems, the inner-loop power control was employed so that the users' received SNRs at the base station remain equal. Total and truncated channel inversion power adaptation policies were implemented in the ILPC to attain the optimum OLPC SNR-target. Average transmit power and target packet error rate constraints were imposed on the system. Proof of convexity for the optimization problem under consideration was provided.

Maximum achievable throughput, and improvements achieved relative to a 'constant SNR-target' case, the 'PHY-layer based variable SNR-target' scheme in [84], and the VSF system in [85], all with continuous rate and power adaptation, were demonstrated for various sets of system parameters. A considerable power gain was demonstrated by means of the proposed cross-layer scheme, in comparison to the non-optimized system where OLPC SNR-target was not exploited. The proposed scheme produced better gains under more severe fading conditions, particularly at low received SNRs, $5 - 25$ dB. For higher received SNRs (> 25 dB), the attainable gain gradually diminished. Moreover, it was observed that the choice of cut-off SNR threshold for truncated channel inversion power adaptation policy greatly affects the achievable throughput. In particular at low SNRs, a high cut-off SNR threshold can effectively suspend any transmissions.

Imposing more stringent QoS requirements on the system, considerably reduced the sum-throughput performance, as a large percentage of the available resources are exploited towards preserving a low received PER. However, the optimized scheme yielded higher gains under more strict target packet error rates. The effective throughput performance was analysed for different upper-limit ARQ truncation levels. Increasing the maximum number of retransmissions amplified the realizable throughput. However, the throughput improvement progressively receded for higher truncation levels, due to the extra induced delay. In fact, the maximum gain, i.e. best trade-off between throughput and delay, was achieved with one ARQ-retransmission. The impact of different traffic load scenarios on the optimal achievable throughput was also studied. Generally a greater traffic load constitutes to higher MAI, therefore lower spreading factors were adopted which reduced the effective throughput.

The proposed cross-layer optimized technique outperformed the 'optimized PHY-layer only' scheme in [84], even without the aid of ARQ retransmissions. The improvement was particularly significant for lower average SNRs with ARQ-assistance, for instance, at $E[\gamma] = 25$ dB, the cross-layer scheme with $\eta = 1$, achieved a 34.3% gain in throughput compared to the 'optimized PHY-layer only' case. Moreover, the optimized throughput performance was compared to the 'optimized VSF scheme' in [85]. It was observed that the cross-layer scheme yields higher gains compared to the 'optimized VSF scheme', particularly with ARQ retransmissions. In all of the above cases, continuous-rate spreading factor adaptation was considered, thus, results should be regarded as upper-bounds for practical discrete spreading factors.

The cross-layer design framework implemented in Chapter 2 was extended and analysed for frequency-selective channels with MRC coherent RAKE receiver in Chapter 3. I relax the assumption about the arrival time for new users. Specifically, random arrival time for a new user within a frame is considered. A closed-form expression for the optimum outer-loop SNR-target is derived, with the goal of maximizing total DLL throughput of a frequency-selective L_p-path channel with a maximum ratio combining RAKE receiver. It was shown that the OLPC SNR-target does not depend on the received number of paths, and neither is dependent on the Uniformly-distributed arrival time for new users.

The optimized system results were compared to those of a non-optimized system with VSF and truncated-ARQ where the OLPC SNR-target was not optimally selected. The achievable gain through our optimization scheme, under multipath fading and random arrival time for new users, were demonstrated for various settings of system parameters. Given a fixed packet error rate target, increasing the number of paths required higher spreading factors and consequently reduced sum-throughput. Further, an increase in the number of paths lowered the achievable gain in sum-throughput through our optimization approach. Practical feasibility of the optimized scheme was also studied through simulation results with discrete-rate spreading factor adaptation under a practical Nakagami-m shadowed environment. Comparison of theoretical and simulation results indicated a performance gap, due to the fact that in the simulation orthogonal Walsh-Hadamard discrete-rate spreading

codes were implemented, whereas for the theoretical results continuous-rate spreading factors were employed which provide an upper-bound for the attainable throughput. The degradation in simulation performance due to composite fading/shadowing channel conditions was also acknowledged.

In Chapter 4, firstly, the proposed cross-layer design and optimization technique was extended and evaluated for a multi-service network of heterogeneous data classes. According to different service specifications of the classes, distinct closed-form expressions for the optimum OLPC SNR/SINR-targets and hence optimal spreading factors, as functions of the number of active users in the two classes, were derived. A multi-dimensional discrete Markov chain was used to model the number of data/voice users in the cell. LU decomposition was employed to solve the global balance equation for the steady-state probabilities. To incorporate the higher QoS demand and delay sensitivity of voice-transmission over data communication, lower target packet loss rates and lower ARQ truncation levels were imposed on the voice users. Moreover, to emphasize on the higher terminal priority of voice users over data users, higher traffic loads were assigned for the voice service in our results. The achievable power gain through our optimization method, relative to the non-optimized case, was demonstrated with theoretical and simulation for various sets of system parameters. In particular, sum-throughput simulation of the optimized and non-optimized multi-service schemes with truncated channel inversion policy over practical Rayleigh shadowed channels was carried out.

Next in Chapter 4, a dynamic spectrum sharing algorithm was integrated with the proposed cross-layer design strategy in the context of heterogeneous OFDM/CDMA networks. AL-OSA was employed to exploit the inactive parts of the primary OFDM spectrum, without any intervention to the primary service operation. Based on randomly-varying number of users in the cells, each secondary CDMA user was dynamically assigned to either an idle primary sub-channel or the secondary spectrum, for transmission of data. Using this dynamic spectrum sharing algorithm, the cognitive users experienced no MAI, and therefore achieved near-optimal capacity performance. Consequently, exploiting the idle primary sub-channels minimized the MAI in the secondary spectrum, hence, secondary-secondary

users gained significant throughput improvements. To achieve optimal performance, a cross-layer design strategy, for jointing optimizing the PHY-layer and DLL parameters, was integrated in the shared-spectrum algorithm. Total deliverable secondary throughput in the optimized AL-OSA system, and improvements achieved relative to the non-shared-spectrum case, were illustrated for various settings of the systems parameters. In particular, the impacts of different primary users' activity factors and number of available primary sub-channels on the achievable performance, were investigated. Due to multipath fading conditions, the CDMA users in the non-shared-spectrum system experienced high levels of MAI, and therefore their sum-throughput performance was severely degraded. Hence, using the optimized cross-layer AL-OSA scheme realized significant improvements in secondary sum-throughput performance, even with high primary users' activity factor and low number of idle primary sub-channels. Perfect sensing and perfect CSI availability were assumed. Hence, the results served as upper-bounds for practical cases with imperfect sensing and non/partial CSI.

5.2 Future Work

In this section, additional research suggestions for promoting future work are highlighted. In particular, several potential enhancements to the proposed algorithms are suggested.

An immediate extension to the work proposed in Chapter 2 is to incorporate the maximum number of ARQ retransmissions in the optimization problem, to achieve a better control over the throughput-delay trade-off. It would also be relevant to analyse the performance using Hybrid Automatic Repeat Request (HARQ) error control mechanism. In particular, adaptive HARQ, supported in HSPA, provides increased throughput in packet retransmission. Moreover, it would be beneficial to derive the cross-layer analysis using convolutional coding, with the aim of minimizing the design complexity.

Throughout this work, to simplify the analysis, the probability of packet loss as a result of packet drop in buffer queue was assumed to be zero, i.e. transmit buffer

had infinite length. However, in practical systems with finite length buffers, queuing delay is a crucial QoS parameter affecting the achievable performance. Hence, taking queuing delay into consideration would be an interesting research undertaking.

To improve the practical feasibility of the proposed cross-layer algorithms, analysis can be extended for a multiple-cell scenario. Inter-cell interference must be taken into account, particularly in the power control mechanism. For example, users farthest from the base stations, i.e. located near cell boundaries, experience higher inter-cell interference, and therefore should be given more power. On the other hand, the problem of cell membership needs to be considered. To achieve optimal performance, the base station that generates the maximum power at the reference user equipment must be selected.

It would be also be beneficial to extend and analyse the proposed cross-layer framework in the downlink. Generally, downlink power control is not as crucial as uplink power control, particularly for analysis on a single-cell network. This is mainly due to less severe near-far effect in downlink scenarios. Nevertheless, downlink power control mechanism must effectively and efficiently adjust its transmit power in real-time to the user equipments, with the goal of maintaining a target link quality. Obtaining a closed-form expression for the optimal target link quality, in the presence of MAI and near-far effect, could therefore be an exciting research undertaking.

The maximal ratio diversity combining technique employed in Chapter 3, provides the maximum throughput improvement compared to other diversity combining methods. The achieved upper-bound performance can be relaxed by incorporating other path diversity schemes, such as selection combining. Moreover the assumption of Uniformly-distributed users can be loosened by considering path loss. Nakagami-m block fading model was used throughout this work, implying that the fading is generated independently according to the probability density function at slot level. Hence, the time-correlated nature of fading according to Doppler velocity can also be investigated as a potential future work.

It would be beneficial to examine the performance of the proposed framework using multi-user decorrelating detectors. Unlike matched-filter detection, where the

interfering users' signals are treated as noise, the decorrelating detector distinguishes each user's signal separately and in theory achieves perfect demodulation in the absence of noise. Multi-user detection surpasses the cross-correlation matrix of the signature waveforms which quantifies MAI. In practice, decorrelating detectors can achieve higher gains by taking the cross-correlation matrix into consideration. However, in presence of severe fading conditions, a higher probability of error is induced by the decorrelating detection, through amplified noise levels.

The analysis for for the dual-service of voice/data classes in Chapter 4, can be extended to a multi-class scenario with video transmission. This would be particularly beneficial in the emerging heterogeneous wireless systems, where video streaming co-exist with data and voice services. Exigent service specifications of video communication, such as high delay- and loss- sensitivity, must be adopted in the design.

To enhance the spectrum sharing analysis carried out in Chapter 4, probabilities of miss-detection and false-alarm can be included in the analysis as proactive measures for imperfect sensing. Further, interference-limited opportunistic spectrum access in heterogeneous OFDM/CDMA networks can be an exciting research undertaking. On the other hand, devising spectrum sharing strategies for heterogeneous networks with primary CDMA and secondary OFDM can be very beneficial. In addition, the proposed spectrum sharing algorithm can be extended to a shared-spectrum environment across multiple adjacent cells.

References

[1] D. Bertsekas and R. Gallager, *Data networks.* Prentice-Hall, 1987. 1.3.1, 1.3.1.2, 2.3.1, 3.2.3, 4.2.2

[2] D. Spohn, *Data network design*, ser. McGraw-Hill series on computer communications. McGraw-Hill, 1993. 1.3.1

[3] B. Forouzan, *Data Communications and Networking*, ser. McGraw-Hill Forouzan Networking Series. McGraw-Hill, 2003. 1.3.1, 1.3.1.2, 3.4

[4] J. Marcus, *Designing Wide Area Networks and Internetworks: A Practical Guide.* Addison-Wesley, 1999. 1.3.1

[5] P. Roshan and J. Leary, *802.11 Wireless Lan Fundamentals*, ser. Fundamentals Series. Cisco Press, 2004. 1.3.1

[6] D. Tse and P. Viswanath, *Fundamentals of wireless communication.* Cambridge University Press, 2005. 1.3.1.1

[7] T. Rappaport, *Wireless Communications: Principles and Practice.* Prentice Hall PTR, 2001. 1.3.1.1, 1.3.3.3

[8] J. Day and H. Zimmermann, "The osi reference model," *Proceedings of the IEEE*, vol. 71, no. 12, pp. 1334–1340, dec. 1983. 1.3.1.2

[9] J. R. Aschenbrenner, "Open systems interconnection," *IBM Systems Journal*, vol. 25, no. 3.4, pp. 369–379, 1986. 1.3.1.2

[10] P. Bartoli, "The application layer of the reference model of open systems interconnection," *Proceedings of the IEEE*, vol. 71, no. 12, pp. 1404–1407, dec. 1983. 1.3.1.2

[11] W. Stevens and G. Wright, *TCP/IP Illustrated: The Protocols*, ser. Addison-Wesley Professional Computing Series. Addison-Wesley Publishing Company, 1994, no. v. 1. 1.3.1.2

[12] D. Comer, *Internetworking with TCP/IP: Principles, protocols, and architecture*, ser. Internetworking with TCP/IP. Pearson Prentice Hall, 2006. 1.3.1.2

[13] J. Proakis, *Digital Communications*, 4th ed. McGraw-Hill, 2000. 1.3.2.1, 1.3.3.4, 2.3.1

[14] A. Goldsmith, *Wireless communications*. Cambridge Univ Pr, 2005. 1.3.2.1, 1.3.3.2, 1.3.3.2, 1.3.3.2, 1.3.3.2

[15] K. Fazel and S. Kaiser, *Multi-Carrier and Spread Spectrum Systems: From Ofdm and MC-Cdma to Lte and Wimax*. John Wiley & Sons, 2009. 1.3.2.1

[16] M. Pursley, "Performance evaluation for phase-coded spread-spectrum multiple-access communication–part i: System analysis," *Communications, IEEE Transactions on*, vol. 25, no. 8, pp. 795–799, aug. 1977. 1.3.2.1, 2.3.1, 4.2.2

[17] M. Pursley and D. Sarwate, "Performance evaluation for phase-coded spread-spectrum multiple-access communication–part ii: Code sequence analysis," *Communications, IEEE Transactions on*, vol. 25, no. 8, pp. 800–803, aug. 1977. 1.3.2.1

[18] R. Pickholtz, D. Schilling, and L. Milstein, "Theory of spread-spectrum communications–a tutorial," *Communications, IEEE Transactions on*, vol. 30, no. 5, pp. 855–884, may 1982. 1.3.2.1

[19] H. Holma and A. Toskala, *WCDMA for UMTS: HSPA Evolution and LTE*. John Wiley & Sons, Inc., 2007. 1.3.2.1, 1.4.2, 1.4.3, 1, 2.1, 2.2, 3.1, 3.3

[20] H. Holma and A. Toskala, Eds., *WCDMA for UMTS: Radio Access for Third Generation Mobile Communications*. John Wiley & Sons, Inc., 2001. 1.3.2.1, 1.3.3.2, 1.4.2, 1.4.3

[21] H. Liu and G. Li, *OFDM-Based Broadband Wireless Networks: Design And Optimization*. Wiley-Interscience, 2005. 1.3.2.2, 1.4.2

[22] S. Glisic, *Advanced Wireless Communications: 4G Technologies*. John Wiley & Sons, 2006. 1.3.2.2

[23] H. Holma and A. Toskala, *Lte for Umts - Ofdma and Sc-fdma Based Radio Access*. John Wiley & Sons, 2009. 1.3.2.2

[24] Y. Kim and R. Prasad, *4G Roadmap and Emerging Communication Technologies*. Artech House, 2006. 1.3.2.2

[25] L. Hanzo, *OFDM and MC-CDMA for Broadband Multi-user Communications, WLANs, and Broadcasting*. J. Wiley, 2003. 1.3.2.2

[26] G. Orfanos, *Development and Performance Evaluation of an Adaptive MAC Protocol for MC-CDMA Wireless LANs with QoS Support*. Mainz, 2006. 1.3.2.2

[27] M. Ergen, *Mobile Broadband: Including WiMAX and LTE*. Springer, 2009. 1.3.3.1, 1.4.2

[28] M. Simon and M. Alouini, *Digital Communication Over Fading Channels*. Wiley-Interscience, 2005. 1.3.3.1, 1.3.3.2, 1.3.3.2, 1.3.3.4, 2.4, 3.2.2

[29] D. MacKay, *Information Theory, Inference, and Learning Algorithms.* Cambridge University Press, 2003. 1.3.3.2

[30] L. Li, N. Jindal, and A. Goldsmith, "Outage capacities and optimal power allocation for fading multiple-access channels," *Information Theory, IEEE Transactions on*, vol. 51, no. 4, pp. 1326–1347, apr. 2005. 1.3.3.2

[31] A. Goldsmith and P. Varaiya, "Capacity of fading channels with channel side information," *Information Theory, IEEE Transactions on*, vol. 43, no. 6, pp. 1986–1992, nov. 1997. 1.3.3.2, 2.1, 2.2, 1

[32] G. Caire and S. Shamai, "On the capacity of some channels with channel state information," *Information Theory, IEEE Transactions on*, vol. 45, no. 6, pp. 2007–2019, sep. 1999. 1.3.3.2

[33] H. Chen, *The Next Generation CDMA Technologies*, ser. IEEE journal on selected areas in communications. John Wiley, 2007. 1.3.3.2, 2.2

[34] M.-S. Alouini and A. Goldsmith, "Capacity of rayleigh fading channels under different adaptive transmission and diversity-combining techniques," *Vehicular Technology, IEEE Transactions on*, vol. 48, no. 4, pp. 1165–1181, jul. 1999. 1.3.3.2

[35] M. Yavuz, F. Meshkati, S. Nanda, A. Pokhariyal, N. Johnson, B. Raghothaman, and A. Richardson, "Interference management and performance analysis of umts/hspa+ femtocells," *Communications Magazine, IEEE*, vol. 47, no. 9, pp. 102–109, sep. 2009. 1.3.3.2

[36] S. W. Kim and A. Goldsmith, "Truncated power control in code division multiple access communications," in *Global Telecommunications Conference, 1997. GLOBECOM '97., IEEE*, vol. 3, nov. 1997, pp. 1488–1493 vol.3. 1.3.3.2

[37] M. Dörpinghaus, *On the Achievable Rate of Stationary Fading Channels.* Springer, 2011. 1.3.3.2

[38] R. Bernhardt, "Macroscopic diversity in frequency reuse radio systems," *Selected Areas in Communications, IEEE Journal on*, vol. 5, no. 5, pp. 862–870, jun. 1987. 1.3.3.3

[39] R. H. Clarke, "A statistical theory of mobile-radio reception," *Bell Systems Technical Journal*, vol. 47, no. 5, pp. 957–1000, 1968. 1.3.3.3

[40] S. Fischer, S. Kudras, V. Kuhn, and K. Kammeyer, "Analysis of diversity effects for satellite communication systems," in *Global Telecommunications Conference, 2001. GLOBECOM '01. IEEE*, vol. 4, 2001, pp. 2759–2763 vol.4. 1.3.3.3

[41] G. Sugar, "Some fading characteristics of regular vhf ionospheric propagation," *Proceedings of the IRE*, vol. 43, no. 10, pp. 1432–1436, oct. 1955. 1.3.3.3

[42] H. Janes and P. Wells, "Some tropospheric scatter propagation measurements near the radio horizon," *Proceedings of the IRE*, vol. 43, no. 10, pp. 1336–1340, oct. 1955. 1.3.3.3

[43] A. Coulson, A. Williamson, and R. Vaughan, "A statistical basis for lognormal shadowing effects in multipath fading channels," *Communications, IEEE Transactions on*, vol. 46, no. 4, pp. 494–502, apr. 1998. 1.3.3.3

[44] J. Salo, L. Vuokko, H. M. El-Sallabi, and P. Vainikainen, "An additive model as a physical basis for shadow fading," *Vehicular Technology, IEEE Transactions on*, vol. 56, no. 1, pp. 13–26, jan. 2007. 1.3.3.3

[45] I. Abou-Faycal, M. Trott, and S. Shamai, "The capacity of discrete-time memoryless rayleigh-fading channels," *Information Theory, IEEE Transactions on*, vol. 47, no. 4, pp. 1290–1301, may 2001. 1.3.3.3

[46] A. Saleh and R. Valenzuela, "A statistical model for indoor multipath propagation," *Selected Areas in Communications, IEEE Journal on*, vol. 5, no. 2, pp. 128–137, feb. 1987. 1.3.3.3

[47] L. Greenstein, D. Michelson, and V. Erceg, "Moment-method estimation of the ricean k-factor," *Communications Letters, IEEE*, vol. 3, no. 6, pp. 175–176, jun. 1999. 1.3.3.3

[48] C. Tepedelenlioglu, A. Abdi, and G. Giannakis, "The ricean k factor: estimation and performance analysis," *Wireless Communications, IEEE Transactions on*, vol. 2, no. 4, pp. 799–810, jul. 2003. 1.3.3.3

[49] R. Bultitude, S. Mahmoud, and W. Sullivan, "A comparison of indoor radio propagation characteristics at 910 mhz and 1.75 ghz," *Selected Areas in Communications, IEEE Journal on*, vol. 7, no. 1, pp. 20–30, jan. 1989. 1.3.3.3

[50] P. Shaft, "On the relationship between scintillation index and rician fading," *Communications, IEEE Transactions on*, vol. 22, no. 5, pp. 731–732, may 1974. 1.3.3.3

[51] A. Abu-Dayya and N. Beaulieu, "Switched diversity on microcellular ricean channels," *Vehicular Technology, IEEE Transactions on*, vol. 43, no. 4, pp. 970–976, nov. 1994. 1.3.3.3

[52] M. Nakagami, "The m-distribution- a general formula of intensity distribution of rapid fading," in *Statistical Methods in Radio Wave Propagation.* OXFORD, UK.: Pergamon Press, 1960, pp. 3–36. 1.3.3.3, 1.3.3.3

[53] L.-L. Yang and L. Hanzo, "Performance of generalized multicarrier ds-cdma over nakagami-m fading channels," *Communications, IEEE Transactions on*, vol. 50, no. 6, pp. 956–966, jun. 2002. 1.3.3.3, 3.6

[54] T. Eng and L. Milstein, "Coherent ds-cdma performance in nakagami multipath fading," *Communications, IEEE Transactions on*, vol. 43, no. 234, pp. 1134–1143, apr. 1995. 1.3.3.3, 1.3.3.4, 2.2, 3.3, 3.3, 3.6, 4.3.1, 4.3.2

[55] M.-S. Alouini and A. J. Goldsmith, "Adaptive modulation over nakagami fading channels," *Wireless Personal Communications*, vol. 13, pp. 119–143, 2000. 1.3.3.3

[56] U. Charash, "Reception through nakagami fading multipath channels with random delays," *Communications, IEEE Transactions on*, vol. 27, no. 4, pp. 657–670, apr. 1979. 1.3.3.3

[57] S. Abbas and A. Sheikh, "A geometric theory of nakagami fading multipath mobile radio channel with physical interpretations," in *Vehicular Technology Conference, 1996. Mobile Technology for the Human Race., IEEE 46th*, vol. 2, apr.-may 1996, pp. 637–641 vol. 2. 1.3.3.3

[58] M. Ibnkahla, *Signal Processing for Mobile Communications Handbook*. CRC Press, 2004. 1.3.3.4

[59] G. Turin, F. Clapp, T. Johnston, S. Fine, and D. Lavry, "A statistical model of urban multipath propagation," *Vehicular Technology, IEEE Transactions on*, vol. 21, no. 1, pp. 1–9, feb. 1972. 1.3.3.4

[60] T. Rappaport, S. Seidel, and K. Takamizawa, "Statistical channel impulse response models for factory and open plan building radio communicate system design," *Communications, IEEE Transactions on*, vol. 39, no. 5, pp. 794–807, may 1991. 1.3.3.4

[61] D. Brennan, "Linear diversity combining techniques," *Proceedings of the IEEE*, vol. 91, no. 2, pp. 331–356, feb. 2003. 1.3.3.4

[62] L. Kleinrock, *Queueing systems: Computer applications*, ser. Wiley-Interscience Publication. John Wiley & Sons, 1976, no. v. 2. 1.3.3.5

[63] A. Papoulis and S. Pillai, *Probability, random variables, and stochastic processes*, ser. McGraw-Hill electrical and electronic engineering series. McGraw-Hill, 2002. 1.3.3.5, 2.2, 3.3

[64] J. Hayes, "Adaptive feedback communications," *Communication Technology, IEEE Transactions on*, vol. 16, no. 1, pp. 29–34, feb. 1968. 1.4.1

[65] J. Pérez-Romero, *Radio resource management strategies in UMTS*. John Wiley & Sons, 2005. 1.4.2, 1.4.3

[66] C. Johnson, *Radio Access Networks for UMTS: Principles and Practice*. Wiley, 2011. 1.4.2, 1.4.3

[67] R. Patachaianand, *Adaptive Power Control for UMTS*. University of Technology, Sydney, 2007. 1.4.2

[68] D. Kivanc, G. Li, and H. Liu, "Computationally efficient bandwidth allocation and power control for ofdma," *Wireless Communications, IEEE Transactions on*, vol. 2, no. 6, pp. 1150 –1158, nov. 2003. 1.4.2

[69] G. Song and Y. Li, "Cross-layer optimization for ofdm wireless networks-part i: theoretical framework," *Wireless Communications, IEEE Transactions on*, vol. 4, no. 2, pp. 614–624, mar. 2005. 1.4.2

[70] B. Krongold, K. Ramchandran, and D. Jones, "Computationally efficient optimal power allocation algorithms for multicarrier communication systems," *Communications, IEEE Transactions on*, vol. 48, no. 1, pp. 23–27, jan. 2000. 1.4.2

[71] K. Nehra and M. Shikh-Bahaei, "Spectral efficiency of adaptive mqam/ofdm systems with cfo over fading channels," *Vehicular Technology, IEEE Transactions on*, vol. 60, no. 3, pp. 1240–1247, mar. 2011. 1.4.2

[72] A. Shadmand, R. Dilmaghani, M. Ghavami, and M. Shikh-Bahaei, "Wavelet-based downlink scheduling and resource allocation for long-term evolution cellular systems," *Communications, IET*, vol. 5, no. 14, pp. 2091–2095, 23 2011. 1.4.2

[73] V. Srivastava and M. Motani, "Cross-layer design: a survey and the road ahead," *Communications Magazine, IEEE*, vol. 43, no. 12, pp. 112–119, dec. 2005. 1.5

[74] M. Chiang, S. Low, A. Calderbank, and J. Doyle, "Layering as optimization decomposition: A mathematical theory of network architectures," *Proceedings of the IEEE*, vol. 95, no. 1, pp. 255–312, jan. 2007. 1.5

[75] Q. Liu, S. Zhou, and G. Giannakis, "Cross-layer combining of adaptive modulation and coding with truncated arq over wireless links," *Wireless Communications, IEEE Transactions on*, vol. 3, no. 5, pp. 1746–1755, sep. 2004. 1.5, 2.1, 2.2

[76] E. Malkamaki and H. Leib, "Performance of truncated type-ii hybrid arq schemes with noisy feedback over block fading channels," *Communications, IEEE Transactions on*, vol. 48, no. 9, pp. 1477–1487, sep. 2000. 1.5, 2.1, 2.2

[77] I. Mitola, J. and J. Maguire, G.Q., "Cognitive radio: making software radios more personal," *Personal Communications, IEEE*, vol. 6, no. 4, pp. 13–18, aug. 1999. 1.6

[78] T. Yucek and H. Arslan, "A survey of spectrum sensing algorithms for cognitive radio applications," *Communications Surveys Tutorials, IEEE*, vol. 11, no. 1, pp. 116 –130, quarter 2009. 1.6

[79] I. F. Akyildiz, W.-Y. Lee, M. C. Vuran, and S. Mohanty, "Next generation/dynamic spectrum access/cognitive radio wireless networks: A survey," *COMPUTER NETWORKS JOURNAL (ELSEVIER*, vol. 50, pp. 2127–2159, 2006. 1.6

[80] Y.-C. Liang, Y. Zeng, E. Peh, and A. T. Hoang, "Sensing-throughput tradeoff for cognitive radio networks," *Wireless Communications, IEEE Transactions on*, vol. 7, no. 4, pp. 1326–1337, apr. 2008. 1.6

[81] Z. Han, R. Fan, and H. Jiang, "Replacement of spectrum sensing in cognitive radio," *Wireless Communications, IEEE Transactions on*, vol. 8, no. 6, pp. 2819–2826, jun. 2009. 1.6

[82] S. Srinivasa and S. Jafar, "How much spectrum sharing is optimal in cognitive radio networks?" *Wireless Communications, IEEE Transactions on*, vol. 7, no. 10, pp. 4010–4018, oct. 2008. 1.6, 4.1, 4.3.1

[83] A. Ghasemi and E. Sousa, "Interference aggregation in spectrum-sensing cognitive wireless networks," *Selected Topics in Signal Processing, IEEE Journal of*, vol. 2, no. 1, pp. 41 –56, feb. 2008. 1.6, 4.3.1

[84] F. Zarringhalam, B. Seyfe, M. Shikh-Bahaei, G. Charbit, and H. Aghvami, "Jointly optimized rate and outer loop power control with single- and multi-user detection," *Wireless Communications, IEEE Transactions on*, vol. 8, no. 1, pp. 186–195, jan. 2009. 1.7, 2.1, 2.4, 2.12, 2.4, 2.5, 5.1

[85] L.-L. Yang and L. Hanzo, "Adaptive rate ds-cdma systems using variable spreading factors," *Vehicular Technology, IEEE Transactions on*, vol. 53, no. 1, pp. 72–81, jan. 2004. 1.7, 2.1, 2.4, 2.4, 2.13, 2.5, 2.7.1, 5.1

[86] A. Shojaeifard, F. Zarringhalam, and M. Shikh-Bahaei, "Joint physical layer and data link layer optimization of cdma-based networks," *Wireless Communications, IEEE Transactions on*, vol. 10, no. 10, pp. 3278–3287, oct. 2011. 1.7

[87] A. Shojaeifard, F. Zarringhalam, and M. Shikh-Bahaei, "Packet error rate(per)-based cross-layer optimization of cdma networks," in *Global Telecommunications Conference (GLOBECOM 2011), 2011 IEEE*, dec. 2011, pp. 1–6. 1.7

[88] A. Shojaeifard and M. Shikh-Bahaei, "Cross-layer design and optimization of cdma networks in frequency-selective fading channels," *Wireless Communications Letters, IEEE*, vol. 1, no. 6, pp. 605–608, dec. 2012. 1.7

[89] A. Shojaeifard, F. Zarringhalam, and M. Shikh-Bahaei, "Throughput-optimal cross-layer resource allocation in ds-cdma systems with nakagami multipath fading," in *Personal Indoor and Mobile Radio Communications (PIMRC), 2011 IEEE 22nd International Symposium on*, sep. 2011, pp. 1526–1530. 1.7

[90] A. Shojaeifard and M. Shikh-Bahaei, "Joint physical layer and data link layer optimization of multi-service networks," *Wireless Communications Letters, IEEE, submission under 2nd round of review*, pp. 1–4, Sep. 2012. 1.7

[91] A. Shojaeifard and M. Shikh-Bahaei, "Cross-layer design and optimization of multi-service cdma networks," in *VTC, 2013 IEEE, submission under review*, Aug. 2012, pp. 1–7. 1.7

[92] A. Shojaeifard, M. M. Mahyari, and M. Shikh-Bahaei, "Cross-layer design with dynamic resource allocation in heterogeneous cognitive radio networks," in *ICC, 2013 IEEE, submission under review*, Sep. 2012, pp. 1–5. 1.7

[93] A. Shojaeifard and M. Shikh-Bahaei, "Cross-layer design and optimization of shared-spectrum heterogeneous networks," *Wireless Communications, IEEE Transactions on, to be submitted in Jan. 2013.* 1.7

[94] M. M. Mahyari, A. Shojaeifard, and M. Shikh-Bahaei, "Adaptive transmission in cognitive radio networks with cooperative spectrum sensing," *Wireless Communications Letters, IEEE, submission under review*, pp. 1–4, jan. 2013. 1.7

[95] V. Chandrasekhar and J. Andrews, "Uplink capacity and interference avoidance for two-tier femtocell networks," *Wireless Communications, IEEE Transactions on*, vol. 8, no. 7, pp. 3498–3509, jul. 2009. 2.1

[96] M. Yavuz, F. Meshkati, S. Nanda, A. Pokhariyal, N. Johnson, B. Raghothaman, and A. Richardson, "Interference management and performance analysis of umts/hspa+ femtocells," *Communications Magazine, IEEE*, vol. 47, no. 9, pp. 102–109, sep. 2009. 2.1

[97] N. Arulselvan, V. Ramachandran, S. Kalyanasundaram, and G. Han, "Distributed power control mechanisms for hsdpa femtocells," in *Vehicular Technology Conference, 2009. VTC Spring 2009. IEEE 69th*, apr. 2009, pp. 1–5. 2.1

[98] S. ping Yeh, S. Talwar, S. choon Lee, and H. Kim, "Wimax femtocells: a perspective on network architecture, capacity, and coverage," *Communications Magazine, IEEE*, vol. 46, no. 10, pp. 58–65, oct. 2008. 2.1

[99] S. Jafar and A. Goldsmith, "Adaptive multirate cdma for uplink throughput maximization," *Wireless Communications, IEEE Transactions on*, vol. 2, no. 2, pp. 218–228, mar. 2003. 2.1

[100] F. Adachi, M. Sawahashi, and H. Suda, "Wideband ds-cdma for next-generation mobile communications systems," *Communications Magazine, IEEE*, vol. 36, no. 9, pp. 56–69, sep. 1998. 2.1

[101] S. Shamai and S. Verdu, "The impact of frequency-flat fading on the spectral efficiency of cdma," *Information Theory, IEEE Transactions on*, vol. 47, no. 4, pp. 1302–1327, may 2001. 2.1

[102] M. Rintamaki, H. Koivo, and I. Hartimo, "Adaptive closed-loop power control algorithms for cdma cellular communication systems," *Vehicular Technology, IEEE Transactions on*, vol. 53, no. 6, pp. 1756–1768, nov. 2004. 2.1

[103] M. Chen and D. Tse, "An upper bound on the convergence rate of uplink power control in ds-cdma systems," *Communications Letters, IEEE*, vol. 10, no. 4, pp. 231–233, apr. 2006. 2.1

[104] S. W. Kim and A. Goldsmith, "Truncated power control in code-division multiple-access communications," *Vehicular Technology, IEEE Transactions on*, vol. 49, no. 3, pp. 965–972, may 2000. 2.1, 2.2, 2.4

[105] S. T. Chung and A. Goldsmith, "Degrees of freedom in adaptive modulation: a unified view," *Communications, IEEE Transactions on*, vol. 49, no. 9, pp. 1561–1571, sep. 2001. 2.1

[106] X. Qiu and K. Chawla, "On the performance of adaptive modulation in cellular systems," *Communications, IEEE Transactions on*, vol. 47, no. 6, pp. 884–895, jun. 1999. 2.1

[107] V. Lau and S. Maric, "Variable rate adaptive modulation for ds-cdma," *Communications, IEEE Transactions on*, vol. 47, no. 4, pp. 577–589, apr. 1999. 2.1

[108] M. Shikh-Bahaei, "Joint optimization of transmission rate and outer-loop snr target adaptation over fading channels," *Communications, IEEE Transactions on*, vol. 55, no. 3, pp. 398–403, mar. 2007. 2.1

[109] B. Vucetic, "An adaptive coding scheme for time-varying channels," *Communications, IEEE Transactions on*, vol. 39, no. 5, pp. 653–663, may 1991. 2.1

[110] M. Honig and M. Tsatsanis, "Adaptive techniques for multiuser cdma receivers," *Signal Processing Magazine, IEEE*, vol. 17, no. 3, pp. 49–61, may 2000. 2.1

[111] A. Goldsmith, "Joint source/channel coding for wireless channels," in *Vehicular Technology Conference, 1995 IEEE 45th*, vol. 2, jul. 1995, pp. 614–618 vol.2. 2.1

[112] H. Minn, M. Zeng, and V. Bhargava, "On arq scheme with adaptive error control," *Vehicular Technology, IEEE Transactions on*, vol. 50, no. 6, pp. 1426–1436, nov. 2001. 2.1

[113] S. Ulukus and L. Greenstein, "Throughput maximization in cdma uplinks using adaptive spreading and power control," in *Spread Spectrum Techniques and Applications, 2000 IEEE Sixth International Symposium on*, vol. 2, 2000, pp. 565–569 vol.2. 2.1

[114] K. Choi, S. K. Shin, and K. Cheun, "Adaptive processing gain cdma networks over poisson traffic channel," *Communications Letters, IEEE*, vol. 6, no. 7, pp. 273–275, jul. 2002. 2.1

[115] R. Vannithamby and E. Sousa, "Performance of multi-rate data traffic using variable spreading gain in the reverse link under wideband cdma," in *Vehicular Technology Conference Proceedings, 2000. VTC 2000-Spring Tokyo. 2000 IEEE 51st*, vol. 2, 2000, pp. 1155–1159 vol.2. 2.1

[116] A. Goldsmith and S.-G. Chua, "Variable-rate variable-power mqam for fading channels," *Communications, IEEE Transactions on*, vol. 45, no. 10, pp. 1218–1230, oct. 1997. 2.1, 2.3.1

[117] C. Fischione and M. Butussi, "Power and rate control outage based in cdma wireless networks under mai and heterogeneous traffic sources," in *Communications, 2007. ICC '07. IEEE International Conference on*, jun. 2007, pp. 5856–5861. 2.1

[118] F. Yu, V. Krishnamurthy, and V. Leung, "Cross-layer optimal connection admission control for variable bit rate multimedia traffic in packet wireless cdma networks," *Signal Processing, IEEE Transactions on*, vol. 54, no. 2, pp. 542–555, feb. 2006. 2.1

[119] S. Buzzi, V. Massaro, and H. Poor, "Energy-efficient resource allocation in multipath cdma channels with band-limited waveforms," *Signal Processing, IEEE Transactions on*, vol. 57, no. 4, pp. 1494–1510, apr. 2009. 2.1

[120] H. Jiang, W. Zhuang, and X. Shen, "Cross-layer design for resource allocation in 3g wireless networks and beyond," *Communications Magazine, IEEE*, vol. 43, no. 12, pp. 120–126, dec. 2005. 2.1

[121] K. Gilhousen, I. Jacobs, R. Padovani, A. Viterbi, J. Weaver, L.A., and I. Wheatley, C.E., "On the capacity of a cellular cdma system," *Vehicular Technology, IEEE Transactions on*, vol. 40, no. 2, pp. 303–312, may 1991. 2.1

[122] A. Viterbi and R. Padovani, "Implications of mobile cellular cdma," *Communications Magazine, IEEE*, vol. 30, no. 12, pp. 38–41, dec. 1992. 2.1

[123] M. Soleimanipour and G. Freeman, "A realistic approach to the capacity of cellular cdma systems," in *Vehicular Technology Conference, 1996. 'Mobile Technology for the Human Race'., IEEE 46th*, vol. 2, may 1996, pp. 1125–1129 vol.2. 2.1

[124] H. Holma and J. Laakso, "Uplink admission control and soft capacity with mud in cdma," in *Vehicular Technology Conference, 1999. VTC 1999 - Fall. IEEE VTS 50th*, vol. 1, 1999, pp. 431–435 vol.1. 2.1

[125] M. Shikh-Bahaei and A. Aghvami, "Joint planning of soft-capacity and soft-coverage for 3g wcdma systems," in *3G Mobile Communication Technologies, 2001. Second International Conference on (Conf. Publ. No. 477)*, 2001, pp. 78–81. 2.1

[126] F. Gunnarsson, E. Geijer-Lundin, G. Bark, and N. Wiberg, "Uplink admission control in wcdma based on relative load estimates," in *Communications, 2002. ICC 2002. IEEE International Conference on*, vol. 5, 2002, pp. 3091–3095 vol.5. 2.1

[127] L. Song, N. Mandayam, and Z. Gajic, "Analysis of an up/down power control algorithm for the cdma reverse link under fading," *Selected Areas in Communications, IEEE Journal on*, vol. 19, no. 2, pp. 277–286, feb. 2001. 2.1

[128] Q. Wu, "Optimum transmitter power control in cellular systems with heterogeneous sir thresholds," *Vehicular Technology, IEEE Transactions on*, vol. 49, no. 4, pp. 1424–1429, jul. 2000. 2.1

[129] J. Tang and X. Zhang, "Quality-of-service driven power and rate adaptation over wireless links," *Wireless Communications, IEEE Transactions on*, vol. 6, no. 8, pp. 3058–3068, aug. 2007. 2.1

[130] L. Ding and J. Lehnert, "An uplink power control based on truncated channel inversion for data traffic in a cellular cdma system," *Vehicular Technology, IEEE Transactions on*, vol. 50, no. 3, pp. 854–866, may 2001. 2.1

[131] S. Ramakrishna and J. Holtzman, "A scheme for throughput maximization in a dual-class cdma system," *Selected Areas in Communications, IEEE Journal on*, vol. 16, no. 6, pp. 830 –844, aug. 1998. 2.1

[132] H. Kawai, H. Suda, and F. Adachi, "Outer-loop control of target sir for fast transmit power control in turbo-coded w-cdma mobile radio," *Electronics Letters*, vol. 35, no. 9, pp. 699–701, apr. 1999. 2.1

[133] M. Shikh-Bahaei, M. Mouna-Kingue, and G. Nokia, "Joint optimisation of outer-loop power control and rate adaptation over fading channels," in *Vehicular Technology Conference, 2004. VTC2004-Fall. 2004 IEEE 60th*, vol. 3, sep. 2004, pp. 2205–2209 Vol. 3. 2.1

[134] T. Chulajata and H. Kwon, "Combinations of power controls for cdma2000 wireless communications system," in *Vehicular Technology Conference, 2000. IEEE VTS-Fall VTC 2000. 52nd*, vol. 2, 2000, pp. 638–645 vol.2. 2.1

[135] C.-S. Koo, S.-H. Shin, R. DiFazio, D. Grieco, and A. Zeira, "Outer loop power control using channel-adaptive processing for 3g wcdma," in *Vehicular Technology Conference, 2003. VTC 2003-Spring. The 57th IEEE Semiannual*, vol. 1, apr. 2003, pp. 490–494 vol.1. 2.1

[136] G. Mingxiang, G. Qing, and L. Xing, "Ds-cdma system outer loop power control and improvement for multi-service," *Systems Engineering and Electronics, Journal of*, vol. 19, no. 3, pp. 453–460, jun. 2008. 2.1

[137] S. Niida, T. Suzuki, and Y. Takeuchi, "Experimental results of outer-loop transmission power control using wideband-cdma for imt-2000," in *Vehicular Technology Conference Proceedings, 2000. VTC 2000-Spring Tokyo. 2000 IEEE 51st*, vol. 2, 2000, pp. 775–779 vol.2. 2.1

[138] L. T. Ong, M. Shikh-Bahaei, and J. Chambers, "Variable rate and variable power mqam system based on bayesian bit error rate and channel estimation techniques," *Communications, IEEE Transactions on*, vol. 56, no. 2, pp. 177–182, feb. 2008. 2.1

[139] X. Wang, Q. Liu, and G. Giannakis, "Analyzing and optimizing adaptive modulation coding jointly with arq for qos-guaranteed traffic," *Vehicular Technology, IEEE Transactions on*, vol. 56, no. 2, pp. 710–720, mar. 2007. 2.1

[140] S. Pack, X. Shen, and J. Mark, "Optimizing truncated arq scheme over wireless fading channels," *Vehicular Technology, IEEE Transactions on*, vol. 57, no. 2, pp. 1302–1305, mar. 2008. 2.1

[141] J. Lehnert and M. Pursley, "Error probabilities for binary direct-sequence spread-spectrum communications with random signature sequences," *Communications, IEEE Transactions on*, vol. 35, no. 1, pp. 87–98, jan. 1987. 2.2

[142] E. Geraniotis, "Direct-sequence spread-spectrum multiple-access communications over nonselective and frequency-selective rician fading channels," *Communications, IEEE Transactions on*, vol. 34, no. 8, pp. 756–764, aug. 1986. 2.2

[143] S. Verdú, *Multiuser Detection*. Cambridge University Press, 1998. 2.2

[144] R. Buehrer and R. Mahajan, "On the usefulness of outer-loop power control with successive interference cancellation," *Communications, IEEE Transactions on*, vol. 51, no. 12, pp. 2091–2102, dec. 2003. 2.2

[145] J. Yun and M. Kavehrad, "Markov error structure for throughput analysis of adaptive modulation systems combined with arq over correlated fading channels," *Vehicular Technology, IEEE Transactions on*, vol. 54, no. 1, pp. 235–245, jan. 2005. 2.3.1

[146] A. Kobravi and M. Shikh-Bahaei, "Cross-layer adaptive arq and modulation tradeoffs," in *Personal, Indoor and Mobile Radio Communications, 2007. PIMRC 2007. IEEE 18th International Symposium on*, sep. 2007, pp. 1–5. 2.3.1

[147] E. Biglieri, G. Caire, G. Taricco, and E. Viterbo, "How fading affects cdma: an asymptotic analysis with linear receivers," *Selected Areas in Communications, IEEE Journal on*, vol. 19, no. 2, pp. 191–201, feb. 2001. 2.3.1, 2.4

[148] D. Bertsekas, *Constrained Optimization and Lagrange Multiplier Methods*, ser. Computer Science and Applied Mathematics. Academic Press, 1982. 2.3.4

[149] W. Press, S. Teukolsky, W. Vetterling, and B. Flannery, *Numerical Recipes in C++: The Art of Scientific Computing*. Cambridge University Press, 2002. 2.3.4, 4.2.2

[150] J. Nonnenmacher, E. Biersack, and D. Towsley, "Parity-based loss recovery for reliable multicast transmission," *Networking, IEEE/ACM Transactions on*, vol. 6, no. 4, pp. 349–361, aug. 1998. 2.4

[151] M.-J. Ho and G. Stuber, "Co-channel interference of microcellular systems on shadowed nakagami fading channels," in *Vehicular Technology Conference, 1993., 43rd IEEE*, May 1993, pp. 568–571. 2.4, 3.6.2

[152] A. Köpsel and A. Wolisz, "Voice transmission in an ieee 802.11 wlan based access network," in *Proceedings of the 4th ACM international workshop on Wireless mobile multimedia*, ser. WOWMOM '01. New York, NY, USA: ACM, 2001, pp. 23–32. 4.1

[153] K. Balachandran, C. Demetrescu, R. Ejzak, S. Nanda, and H. Xie, "System for statistically multiplexing real-time and non-real-time voice and data traffic in a wireless system," Nov. 8 2005, uS Patent 6,963,544. 4.1

[154] I. Koo, S. Bahng, and K. Kim, "Qos-sensitive admission policy for non-real-time data packets in voice/data integrated cdma systems," in *Global Telecommunications Conference, 2001. GLOBECOM '01. IEEE*, vol. 4, 2001, pp. 2611 –2616 vol.4. 4.1

[155] A. Ghasemi and E. S. Sousa, "Fundamental limits of spectrum-sharing in fading environments," *Wireless Communications, IEEE Transactions on*, vol. 6, no. 2, pp. 649–658, feb. 2007. 4.1

[156] X. Kang, Y.-C. Liang, A. Nallanathan, H. Garg, and R. Zhang, "Optimal power allocation for fading channels in cognitive radio networks: Ergodic capacity and outage capacity," *Wireless Communications, IEEE Transactions on*, vol. 8, no. 2, pp. 940–950, feb. 2009. 4.1

[157] L. Musavian and S. Aissa, "Capacity and power allocation for spectrum-sharing communications in fading channels," *Wireless Communications, IEEE Transactions on*, vol. 8, no. 1, pp. 148–156, jan. 2009. 4.1

[158] M. Khoshkholgh, K. Navaie, and H. Yanikomeroglu, "On the impact of the primary network activity on the achievable capacity of spectrum sharing over fading channels," *Wireless Communications, IEEE Transactions on*, vol. 8, no. 4, pp. 2100–2111, apr. 2009. 4.1

[159] M. Mahyari and M. Shikh-Bahaei, "Joint optimization of rate and outer loop power control for cdma-based cognitive radio networks," in *Computing, Networking and Communications (ICNC), 2012 International Conference on*, feb. 2012, pp. 392–396. 4.1

[160] L. Hanzo, H. Haas, S. Imre, D. O'Brien, M. Rupp, and L. Gyongyosi, "Wireless myths, realities, and futures: From 3g/4g to optical and quantum wireless," *Proceedings of the IEEE*, vol. 100, no. Special Centennial Issue, pp. 1853 –1888, 13 2012. 4.1